Investigations of the mechanism of retention of electrochemically modulated liquid chromatography

by

Gloria Fe M. Pimienta

A dissertation submitted to the graduate faculty

in partial fulfillment of the requirements for the degree of

DOCTOR OF PHILOSOPHY

Major: Analytical Chemistry

Program of Study Committee:
Marc D. Porter, Major Professor
Robert Houk, Major Professor
Keith Woo
Javier Vela-Becerra
Ning Fang

Iowa State University

Ames, Iowa

2010

TABLE OF CONTENTS

ACKNOWLEDGMENTS

I am a success today because I had a friend who believed in me and I didn't have the heart to let him down... *- Abraham Lincoln*

I am fortunate to have several people believing in me, and never doubted my capabilities, even in times when I myself did. I would like to express my sincerest gratitude to these people. Thank you…

To my major professor, Dr. Marc Porter, for guiding me during my Ph. D. journey. It is a great pleasure working with you and learning from you. I very much appreciate the work attitude that you impart to the group.

To my committee members, for sharing their time and expertise to help me improve my research.

To all members of the Porter group, for their suggestions, insights and companionship.

To the staff of the Chemistry Graduate Office of Iowa State University and University of Utah for all the assistance they have given me.

To my friends and VFF's, for providing an outlet especially during stressful times.

To my family – my parents, my siblings, and my in-laws, for their support.

To my husband Ian, for being so patient with me and for being helpful in easing some of my Chemistry confusion (and household responsibilities). Thank you for the calculations. You might have not realized that you have been through three theses with me.

To my son Angelo, my inspiration, my pride and joy.

The support of the US Department of Energy - Ames Laboratory and the Utah Science and Technology Research Institute are greatly acknowledged. The Ames Laboratory is operated for the US Department of Energy by Iowa State University under Contract No. DE-AC0207CH11358.

ABSTRACT

Electrochemically modulated liquid chromatography is a technique which uses a column that is configured as a three-electrode electrochemical cell. The packing is a conductive material, serving both as a stationary phase and as a working electrode. Chromatographic retention is manipulated through changes in the potential applied to the stationary phase (E_{app}) which alters interfacial properties such as surface charge and double layer structure. The stationary phase can thus be viewed as a compositionally tunable packing, with retention properties that can be adjusted to enhance separation efficiency. EMLC separations have been carried out to a wide variety of analyte mixtures, including aromatic sulfonates, monosubstituted benzenes and corticosteroids. EMLC can also be used as a tool for investigating electrosorption processes. The main goal of this dissertation is advance insights into the retention mechanism for EMLC.

Previous works with charged analytes demonstrated the impact of ionic solute-stationary phase interactions in EMLC retention. The potential-dependent retention of neutral solutes implies a mechanism beyond electrostatics. Simple, neutral aromatic solutes are employed as test solutes to examine this fundamental issue. Benzene and a series of alkylbenzenes, and di- and tri- methylbenzenes are chosen in particular to probe EMLC-based retention with respect to solute structure and properties. Retention is monitored at porous graphitic carbon (PGC) stationary phase as a function of E_{app}. The results are then interpreted based on the changes on the strength of solute-stationary

phase interactions, including electron donor-acceptor, solvophobic interactions, and competitive adsorption from supporting electrolyte ions.

In addition, various factors that influence EMLC retention of alkylbenzenes and methylbenzenes are investigated. Retention data for chromatographic runs carried out at various mobile phase composition-E_{app} and supporting electrolyte-E_{app} combinations are analyzed to understand the roles of the mobile phase and supporting electrolyte in EMLC. Temperature-controlled EMLC is used to study the thermodynamic aspect of electrosorption of these solutes on PGC.

CHAPTER 1. GENERAL INTRODUCTION

BACKGROUND INFORMATION

Development of Electrochemically Modulated Liquid Chromatography

High performance liquid chromatography (HPLC) is an invaluable analytical technique. Chromatographic retention, and thus separations, relies on the partitioning of an analyte species between a mobile phase and stationary phase. The equilibrium is mathematically expressed by the distribution coefficient (K_d), which is the ratio of concentrations of an analyte sorbed on the stationary phase (C_{SP}) and dissolved in the mobile phase (C_{MP}):

$$K_d = \frac{C_{SP}}{C_{MP}} \qquad [1]$$

Manipulation of a separation can be achieved through alterations in K_d brought about by controlling the properties of the components of the LC system – the stationary phase, the mobile phase and the analyte. This is most commonly accomplished through changes in the mobile phase composition by addition of an organic modifier or through employment of different stationary phases. In electrochemically modulated liquid chromatography (EMLC), the column is configured as an electrochemical cell and a conducting packing material serves both as a stationary phase and a working electrode. Variations in the potential applied, E_{app}, to the packing influence the properties of the noted components, and thus analyte retention.

Early EMLC studies utilized controlled-potential electrolysis leading to quantitative deposition of metals onto a large-surface area working electrode in the form

of a column in a flow-through system. Voorhies and Davies[1] used carbon black at a controlled E_{app} for the adsorption followed by electrolysis of organic compounds and inorganic anions from a sample solution. This approach thus changes the physico-chemical properties of the analyte, but suffers from poor selectivity for samples with multiple components. All compounds that have a standard reduction potential, E^0, more positive than E_{app} are exhaustively deposited onto the column, and all ions that have E^0 more negative than E_{app} co-elute without retention. Examples of approaches to overcome this problem include carefully selecting and controlling potentials for deposition and stripping,[2-4] dividing the column into sections and applying different potentials to each section,[5] and using a long column electrode through which a gradient potential can be applied.[6]

The imposition of E_{app} can be used to change the bulk chemical composition of the mobile phase through oxidation or reduction of the components. For example, the oxidation or reduction of water can be used to increase or decrease the acidity of the mobile phase. This concept has been used to explore the pH-dependent binding of metal ions to chelates adsorbed on the stationary phase.[7]

Another approach uses a stationary phase composed of an electroactive material such as polypyrrole that has properties that can be altered by oxidation and reduction.[8, 9] This process can be depicted by the following equation for a coating (C) that involves cations as counterions:

$$C^+A^- + e^- \rightleftharpoons C^0 + A^- \qquad [2]$$

The coating can be switched between its oxidized and reduced forms to expel or uptake anions (A^-). The charge density of the ion-exchange sites can be altered by controlling the E_{app}.

The most used retention format in EMLC utilizes E_{app} to influence the acceptor-donor properties and double layer structure of the surface of uncoated carbon-based stationary phases. This approach is discussed in a later section and research aimed at investigating the mechanisms of retention at these materials is detailed.

The challenge in achieving good chromatographic efficiencies curtailed the early development and utility of EMLC. The two methods have conflicting requirements in order to achieve optimum performance. For chromatography, the ratio of the column dead volume to the surface area of the stationary phase must be small to attain the column capacity needed for high resolution separations. However, the small voids between the particles and within the particle pores of the stationary phase translate to a highly resistive pathway, a disadvantage for the column which is part of an electrical circuit in EMLC. More time is needed to charge the electrical double layer at the surface of the stationary phase. As a consequence, column equilibration between changes in applied potential can be unreasonably long. Thus, a large ratio of the column dead volume to the surface area of the stationary phase is electrochemically favorable.

Configuring the column as an electrochemical cell poses additional complications.[10] The column design should not only meet the requirements of conventional LC but should also include additional electrochemical components. The placement of a reference electrode and high surface area auxiliary electrode must be

incorporated into the design. The former is required to precisely control the potential applied to the stationary phase/working electrode and the latter is needed to collect the current that flows from the high surface area working electrode. The components of the column must be electrochemically and chemically inert and an inert supporting electrolyte must be added to the mobile phase to achieve the required solution conductivity. This modification is necessary to minimize the solution resistance of the mobile phase and to effectively control the potential applied to the stationary phase.

Figure 1 is a schematic diagram of our EMLC column design[11] that incorporates the aforementioned key components and requirements. The column is constructed by first inserting a tubular Nafion® ion-exchange membrane into a porous stainless steel cylinder. The column is then packed with high surface area carbonaceous particles like porous graphitic carbon (PGC) which serves the dual purpose as a stationary phase and as a working electrode. The stainless steel cylinder functions as a container that can withstand the high pressures generated during column packing and chromatographic flow and that structurally and mechanically defines the dimensions of the column. It also acts as a high surface area auxiliary electrode to carry the large current flow generated at the high surface area working electrode. The function of the ion-exchange membrane is threefold. It: (1) electrically isolates the stationary phase from the auxiliary electrode; (2) acts as a salt bridge and connects the circuit between the stationary phase and the two other working electrodes; and (3) serves as a barrier to minimize loss of the analyte through the porous stainless steel cylinder and to reduce possible contamination of the stationary phase by any electrolysis products formed at the auxiliary electrode.

Electrical contact is made with the stationary phase/working electrode at the bottom of the column through a stainless steel frit. The column is fitted with an electrolyte-filled reservoir that surrounds the stainless steel cylinder/auxiliary electrode. The electrical circuit is completed by placing a reference electrode (Ag/AgCl saturated NaCl) inside the reservoir. The EMLC column employs the same type of endfittings used for conventional columns which simplifies connection to conventional HPLC hardware. A standard high-power potentiostat is used to control the E_{app}.

This column design successfully overcomes the challenges posed by EMLC, rivaling many aspects of conventional chromatographic columns. The column equilibration time between changes in E_{app} is ~20 min, which is comparable to that needed for conditioning conventional columns in between changes in mobile phase composition. Chromatographic efficiencies are also high (~15,000 plates/m). Separation reproducibility is satisfactory provided the column is periodically flushed with a strongly eluting solvent such as acetonitrile. Columns can function effectively for as long as 6 months with careful maintenance.[11]

Stationary Phases

The stationary phase material for EMLC must be conductive and must satisfy the requirements of conventional HPLC (i.e., small and monodisperse spherical particles of sufficient porosity with a narrow pore size distribution, homogenous surface with large surface area, adequate mechanical strength, chemical stability, and ease and reproducibility in manufacturing). A variety of materials has been used as EMLC

stationary phase, such as metals and metal-coated glass particles, graphitic particles and carbonaceous materials coated with conducting polymeric stationary phases.

The first uses of carbonaceous HPLC stationary phase materials were reported in the mid-1970s. Yashin and co-workers employed pyrolytic carbon-coated silica gel particles,[12, 13] while Guiochon and co-workers used pyrolytic carbon-coated carbon black particles.[14-16] Thin carbon coatings are not suitable as EMLC stationary phase materials because they lack the required electrical conductivity across and between particles. Blaedel and Strohl[17] published the first work on the application of a potential to a carbonaceous stationary phase, specifically, crushed graphite particles. Several reviews on carbon-based packing materials for liquid chromatography are available in literature.[18-21]

Attempts at the synthesis of the ideal carbon stationary phase revealed issues such as poor particle stability, surface inhomogeneity and high retentiveness.[22-24] Porous glassy carbon introduced by Knox and Gilbert[25] showed improved chromatographic performance but it required the use of mobile phase additives. They later improved the manufacturing process, producing porous graphitic carbon (PGC), which demonstrated good mechanical stability and satisfactory chromatographic performance. The role of PGC as a stationary phase in HPLC has been reviewed in several articles.[26-29]

Porous Graphitic Carbon

A high porosity HPLC silica gel is used as template for manufacturing PGC. It is impregnated with a phenol-hexamine mixture then heated to 80-160 °C to polymerize

within the pores of the silica. The resulting resin is polymerized at 1000 °C in high-purity nitrogen, and then the silica template is dissolved out with alkali. Graphitization is achieved through thermal treatment at about 2000 °C in high-purity argon. This process eliminates surface functional groups and closes the micropores. The product is PGC, which is now commercialized by Thermo Scientific under the trade name Hypercarb® and is available in 3, 5 and 7-μm grades. The porosity of PGC is about 75% and pore diameter is around 250 Å. The surface area is ~120 m^2/g.[19, 29]

PGC consists of intertwined graphitic ribbons in which each ribbon is made up of some 30 sheets.[30] This ribbon structure accounts for the high mechanical strength of PGC. The graphitic sheets consist of hexagonally-arranged sp^2-hybridized carbon. The carbon atoms within the sheets are about 1.40 Å apart and are bound together via covalent forces. The sheets are spaced about 3.44 Å and are held together by van der Waals interactions. Graphite can conduct electricity due to the freely moving electrons delocalized within the carbon layers.[19]

Liquid chromatographic retention reflects a combination of interactions between the solute and the stationary phase, the solute and the mobile phase, and the mobile and stationary phases. Thorough reviews on retention models for the adsorption of solutes from the mobile phase to carbonaceous stationary phases are found in literature.[19, 26, 31-36] Early works showed the primary interactions of molecules with graphite were dispersive and that retention increased with increasing hydrophobicity of the solute. Thus, initially, graphite was thought of as an ideal hydrophobic reverse-phase packing material.[32, 37, 38] Kaliszan's group observed behavior in contrast to what might be expected of an ideal

reverse-phase packing. Graphite exhibits a stronger retention for polar solutes compared to their nonpolar homologs, a property termed the polar retention effect by graphite (PREG).[39, 40] Mockel[41] and Tanaka[42] suggested the importance of polarizability and geometric factors to the strength of solute-stationary phase interactions. These investigations demonstrated that retention on PGC is a complex mixing of dispersion, solvophobic, and donor-acceptor interactions.[19]

The dispersive interactions are non-specific interactions between the solute and polarizable graphitic stationary phase, resulting from charge fluctuations on the molecules. This type of interaction accounts for the increase in retention with increasing number of carbons along a homologous series of small aromatic solutes, as described by Equation 3:[36]

$$\log k' = \log k'_0 + \alpha n \qquad [3]$$

where k' is the retention factor of the solute with n carbons in the aliphatic side chain, k'_0 is the theoretical retention factor for benzene and α is the measure of the change in retention with increasing alkyl chain length. Kriz and co-workers showed that the dependence of ln k' with carbon number for alkylbenzenes and methylbenzenes is stronger in graphite compared to traditional reversed phase stationary phases.[36]

Solvophobic effects arise from the solvation of the analyte by the mobile phase and increase the retention of hydrophobic molecules when hydrophilic mobile phases are used. In mixed aqueous-organic solvent systems, the retention for small aromatic molecules typically decreases with increasing organic modifier content in the mobile phase according to Equation 4:[34]

$$\log k' = \log k_w - S\varphi \qquad [4]$$

where φ is the volume fraction of the organic modifier in the mobile phase, k_w is the retention factor extrapolated to 100% water as mobile phase ($\varphi = 0$), and S denotes the sensitivity of solute retention to φ and is a constant for a given analyte and a given reversed phase system. The value of S has been found to correlate with solute polarity.

Donor-acceptor or charge-induced interactions occur between the n- or π-electrons of an analyte and the delocalized π-system at the surface of graphite and promote the retention of polar molecules, i.e., PREG. Two explanations have been offered for this phenomenon. One is that the delocalized electrons in the large graphite ribbons impart a high polarizability to the PGC surface in which a mirror charge is induced in the presence of polar or charged solutes.[26] Another explanation is based on the presence of two types of interaction sites, and follows Hanai's model[33] of graphite as a large polynuclear aromatic hydrocarbon. In this model, the center of the graphite planes are electron-deficient, with a low positive charge (close to neutral) accounting for interactions with nonpolar solutes, while the edge carbons are negatively-charged and thus provide sites for interaction with polar solutes.

Graphite possesses additional unique retention properties. First, graphite exhibits stereochemical selectivity, owing to differences in the ability of structural isomers to interact with the planar surface based on geometric factors. This property also applies to PGC, where the possible curvature of the graphite ribbons can apparently be neglected at the molecular level.[43] The retention of an isomer is influenced by its ability to align with the flat surface. In addition, retention of polar compounds is dependent on the degree in

which the polar group can interact with the surface. For isomeric polar solutes, retention is increases as the steric hindrance around the polar group decreases.[35]

It is also important to note that graphite is not completely devoid of adventitious functional groups. X-ray photoelectron spectroscopy (XPS) showed a 0.14 atomic % oxygen content from phenol, carbonyl, carboxylic acid, lactone and quinone groups.[44] These edge defects serve as adsorption sites for polar and for charged solutes.[45-47] The changes in the amount and structure of chemisorbed oxygen therefore can also alter retention.

EMLC Retention Mechanism

EMLC research efforts in our group focus on using E_{app} to alter stationary phase properties such as donor-acceptor character, surface charge, oxidation state and electrical double layer structure, which in turn manipulates solute retention. The stationary phase is thus compositionally tunable, with retention behavior that can be controlled to enhance separation efficiency.[48, 49] This approach has been utilized in the analysis of a wide range of analytes, including aromatic sulfonates,[50, 51] monosubstituted benzenes,[52] costicosteroids,[53] benzodiazepines,[54] enantiomers of hexobarbital and mephenytoin,[55] and inorganic anions.[56] Experiments have been carried out at elevated temperatures for high speed separations.[57] The possibility of employing boron-doped diamond particles (BDDP) as stationary phase due to its compositional and microstructural stability has also been studied.[58] With these applications presenting the potential of EMLC as a separation

technique, investigations of the retention mechanism are therefore fundamentally and technically valuable.

The utility of EMLC as a tool in studying electrosorption phenomena has been demonstrated. Ting and Porter[52] used monosubstituted benzenes as solutes to show the potential value of EMLC as a tool for studying the fundamentals of the adsorption of organic compounds on electrode surfaces. The dependence of retention on E_{app} was found to be correlated to the submolecular polarity parameter (δ) and the energy for the highest occupied molecular orbital (E_{HOMO}). An extensive work utilizing EMLC to examine electrified interfaces and investigate electrosorption processes with mono- and divalent ions as test solutes has also been presented.[59] In this case, the retention data were analyzed in terms of the Gibbs adsorption equation and the Lippmann equation to determine interfacial excesses (Γ), changes in interfacial tension ($d\gamma$), the charge of the electrode (q^E), and the potential of zero charge (PZC) for various solute-supporting electrolyte combinations.

There are two prominent theories for retention in LC – partition[60] and adsorption.[61] In the partition model, the solute distributes itself between the mobile phase and the layer of solvent and coating material on the stationary phase. On the other hand, in the adsorption model, the stationary phase has discrete adsorption sites and the solute molecules displace mobile phase molecules adsorbed on the surface. The mechanism of retention is generally considered to be a combination of partition and displacement.[62-65]

The retention process in EMLC is controlled by the formation of an electrical double layer as charged and dipolar species arrange at the electrode-solution interface.[66-71] The

electrical double layer theory attempts to account for solvent adsorption and orientation, the specific and non-specific adsorption of both ions and neutrals, and the electronic properties and composition of the electrode.[66, 67, 71] The solution side of electrode-solution interfaces consists of two layers - the compact layer and the diffuse layer. The solid phase (i.e., the working electrode) may have an excess or deficit of electrons resulting in a net electrical surface charge.

The compact layer consists of the inner Helmholtz plane (IHP) and the outer Helmholtz plane (OHP). The IHP is composed of highly ordered solvent molecules and specifically adsorbed solutes while the OHP is composed of solvated ions and solvent molecules. The diffuse layer is a region between the OHP and bulk solution that contains any remaining charge in order to ensure the electroneutrality of the interface. The potential drop is linear with distance from the electrode through the compact layer, followed by an exponential decay through the diffuse layer to the potential of the bulk solution. The electrical double layer is used to model the EMLC system components, specifically the structure and distribution of charge at the electrode-solution interface. In the context of EMLC, these charges could be solute or electrolyte molecules in the mobile phase or excess charge on the stationary phase.

At the PZC, the interactions between the analyte and stationary phase are based on inherent retention properties of carbonaceous materials as discussed above (i.e., donor-acceptor, dispersion and hydrophobic). The application of a potential influences these interactions thus manipulating retention. A simplified model for the effect of E_{app} on the retention at a carbonaceous stationary phase is shown in Figure 2. This model

takes into account the potential-induced changes in the donor-acceptor character of the stationary phase and the double layer structure at the electrode-surface interface. When E_{app} is negative of the PZC, the packing has a net negative surface charge and a compact electrical double layer forms. This leads to an enhancement of the donor-acceptor interactions of the stationary phase with positively-charged and acceptor species in solution. When E_{app} is positive of the PZC, the stationary phase acquires a net positive charge and its interactions with negatively-charged and donor species are enhanced. Retention can thus be controlled and separations fine tuned through manipulations in E_{app}.

Solute retention is governed by interactions occurring in the LC column. Table 1 serves as a reference for the definitions of interactions pertinent to this dissertation. Also included are specific examples found in EMLC. The next section discusses our past research efforts aimed at understanding how E_{app} influences these interactions and thus retention in EMLC.

EMLC Mechanistic Studies

For ionic analytes, the dependence of k' on E_{app} can be roughly described in terms of the influence of an electric field on the Boltzmann distribution of ions.[48, 72] Although this perspective takes into account only the effect of E_{app} on electrostatic interactions, it provides a useful, simplistic starting point for the analysis of the EMLC retention data for charged solutes. The relationship predicts that the slope of a plot for log k' as a function of E_{app} for cations would be negative whereas that for anions would be positive. In

addition, plots for doubly charged ions would have slopes twice as large as those for singly charged ions.

Several works have shown that changes in retention with E_{app} are consistent with expectations based on ion-ion interactions.[50, 51, 73, 74] Keller and co-workers[74] studied the retention of mono- and divalent ions and found the trends generally consistent with the predictions based on the ion distribution law. Due to the decreased thickness of the diffuse region of the double layer with high supporting electrolyte concentration in the mobile phase, charged solutes in the bulk solution are more effectively shielded from the charged stationary phase, resulting to weaker electrostatic interactions, thus influencing retention. While these results showed electrostatic interactions have a strong impact on the dependence of retention on E_{app}, the studies also indicated that several other factors need to be considered. First, ions with the same valency showed differences in sensitivity, indicating the importance of non-electrostatic interactions. In addition, the slopes for monovalent anions were larger than those of monovalent cations, pointing to contributions of the donor-acceptor interactions between the π-systems of the analytes and those of PGC, which work in concert with electrostatic interactions for anions and in opposition for cations. Lastly, the eluotropic order of the supporting electrolytes correlates to the strengths of specific adsorption of the electrolyte anions.

Furthermore, if a neutral analyte exhibits a potential dependent retention or if the relationship between ln k' and E_{app} for a charged analyte is non-linear, the purely electrostatic model fails and must be revised.[75-77] Ting and Porter[52] used neutral monosubstituted benzenes as solutes in EMLC and found linear relationship between

ln k' and E_{app}. The sensitivity (i.e., the slope of the plot of ln k' vs. E_{app}) correlated to the submolecular polarity parameter and the energy for the highest occupied molecular orbital of the solutes. The retention of neutral, structurally-similar benzodiazepine compounds show varying dependencies on the E_{app}, such as linear with positive slope, linear with negative slope and quadratic.[54] Nikitas[78] used an adsorption molecular theory to model EMLC, and some combinations of solute-solvent types resulted to anomalous or irregular behavior.

Research Motivation

The goal of the research herein is to refine the EMLC model to account for the effect of E_{app} on the non-electrostatic interactions during the retention process, and thus build on the current mechanistic picture. To achieve this goal, small, neutral aromatic molecules were chosen as test solutes. Benzene, alkylbenzenes and di- and tri-methylbenzenes are suitable analytes for these investigations. Retention can be analyzed based on molecular structure and properties such as hydrophobicity, polarization and steric effects.

The retention of alkylbenzenes and methylbenzenes on PGC has been examined mainly to compare the properties of PGC to other stationary phases such as silica, alumina, octadecylsilica and phenylsilica.[36, 41] Zhang and McGuffin[79] investigated the thermodynamics and kinetics of the retention of alkylbenzenes and methylbenzenes on PGC. The change in molar entropy ($\Delta H°$) and change in molar volume ($\Delta V°$) for the retention process were determined using the dependence of retention on temperature and

pressure, respectively. Kaliszan's group[39] used quantitative structure-retention relationships (QSRR)[80] to analyze the retention mechanism of simple aromatic derivatives including benzene, toluene and dimethylbenzenes. In this method, experimentally-determined retention factors are quantitatively related to structural information extracted from structural descriptors of solutes. Jackson and co-workers[81] used linear solvation energy relationships (LSER) to correlate retention of carbon media, including PGC, to descriptors of dispersion, dipolarity/polarizability, and hydrogen bond basicity for several benzene derivatives, including alkylbenzenes. This dissertation draws on these insights to further the development of the retention mechanism of EMLC.

DISSERTATION ORGANIZATION

Chapter 2 presents chromatographic experiments and results for the retention of benzene, methylbenzenes and alkylbenzenes on a PGC-packed EMLC column. The potential-induced changes in retention are related to alterations in the strength of donor-acceptor, solvophobic and dispersion interactions. In Chapter 3, the role of the supporting electrolyte in EMLC retention is examined. Chapter 4 describes retention as a function of the mobile phase composition, and sensitivity as a function of E_{app} to investigate the role of the mobile phase in the retention process. Chapter 5 discusses EMLC studies carried out at different temperatures to study the thermodynamics of adsorption of the test solutes on the PGC surface. General conclusions are presented in Chapter 6.

REFERENCES

(1) Voorhies, J. D.; Davis, S. M. *Anal. Chem.* **1959**, *31*, 1855.

(2) Blaedel, U. J.; Strohl, J. H. *Anal. Chem.* **1964**, *36*, 1245.

(3) Roe, D. K. *Anal. Chem.* **1964**, *36*, 2371.

(4) Blaedel, U. J.; Strohl, J. H. *Anal. Chem.* **1965**, *37*, 64.

(5) Fujinaga, T.; Nagai, T.; Takagi, C.; Okazaki, S. *Nippon Kagaku Zasshi*, **1963**, *84*, 941.

(6) Fujinaga, T.; Kihara, S. *CRC Crit. Rev. Anal. Chem.* **1977**, *6*, 223.

(7) Hern, J. L.; Strohl, J. H. *Anal. Chem.* **1978**, *50*, 1955.

(8) Ghatak-Roy, A. R.; Martin, C. R. *Anal. Chem.* **1986**, *58*, 1574.

(9) Ge, H.; Wallace, G. G. *Anal. Chem.* **1989**, *61*, 2391.

(10) Ge, H.; Teasdale, P. R.; Wallace, G. G. *J. Chromatogr.* **1991**, *544*, 305.

(11) Ting, E.-Y.; Porter, M. D. *Anal. Chem.* **1998**, *70*, 94.

(12) Bebris, N. K.; Vorobieva, R. G.; Kiselev, A. V.; Nikitin, Y. S.; Tarasova, L. V.; Frolov, I. I.; Yashin, Y. I. *J. Chromatogr.* **1976**, *117*, 257.

(13) Bebris, N. K.; Kiselev, A. V.; Nikitin, Y. S.; Frolov, I. I.; Tarasova, L. V.; Yashin, Y. I. *Chromatographia*, **1978**, *11*, 206.

(14) Colin, H.; Guiochon, G. *J. Chromatogr.* **1976**, *126*, 43.

(15) Colin, H.; Eon, C.; Guiochon, G. *J. Chromatogr.* **1976**, *122*, 223.

(16) Colin, H.; Eon, C.; Guiochon, G. *J. Chromatogr.* **1976**, *119*, 41.

(17) Blaedel, W. J.; Strohl, J. H. *Anal. Chem.* **1964**, *36*, 1245.

(18) Knox, J. H.; Unger, K. K.; Mueller, H. *J. Liq. Chromatogr.* **1983**, *6*, 1.

(19) Knox, J. H.; Ross, P. In *Advances in Chromatography*; Brown, P. R., Grushka, E., Eds.; Marcel Dekker Inc: New York, 1997; Vol. 37.

(20) Knox, J. H.; Kaur, B. In *High Performance Liquid Chromatography Chemical Analysis*; Brown, P. R., Ed.; John Wiley & Sons, 1989; Vol. 98.

(21) Unger, K. K. *Anal. Chem.* **1983**, *55*, 361A.

(22) Plzak, Z.; Dousek, J.; Jansa, J. *J. Chromatogr.* **1978**, *147*, 137.

(23) Unger, K.; Roumeliotis, H.; Mueller, H.; Goetz, J. *J. Chromatogr.* **1980**, *202*, 3.

(24) Ciccioli, P.; Tappa, R.; di Corcia, A.; Liberti, A. *J. Chromatogr.* **1981**, *206*, 35.

(25) Knox, J. H.; Gilbert, M. T.: US Patent 4263268, 1979.

(26) Ross, P. *LC GC North America*, **2000**, *18*, 14.

(27) Bassler, B. J.; Hartwick, R. A. *J. Chromatogr. Sci.* **1989**, *27*, 162.

(28) Hennion, M.-C. In *Encyclopedia of Separation Science* Cooke, M., Poole, C. F., Eds.; Academic Press: San Diego, 2000; Vol. 8.

(29) West, C.; Elkafir, C.; Lafosse, M. *J. Chromatogr. A*, **2010**, *1217*, 3201.

(30) Knox, J. H.; Kaur, B.; Millward, G. R. *J. Chromatogr.* **1986**, *352*, 3.

(31) Leboda, R.; Lodyga, A.; Charmas, B. *Mater. Chem. Phys.* **1998**, *55*, 1.

(32) Knox, J. H.; Kaur, B.; Millward, G. R. *J. Chromatogr.* **1986**, *352*, 3.

(33) Hanai, T. *J. Chromatogr. A*, **2003**, *989*, 183.

(34) Forgacs, E. *J. Chromatogr. A*, **2002**, *975*, 229.

(35) Lepont, C.; Gunatillaka, A. D.; Poole, C. F. *Analyst*, **2001**, *126*, 1318.

(36) Kriz, J.; Adamcova, E.; Knox, J. H.; Hora, J. *J. Chromatogr. A*, **1994**, *663*, 151.

(37) Gilbert, M. T.; Knox, J. H.; Kaur, B. *Chromatographia*, **1982**, *16*, 138.

(38) Kaur, B. *LC GC Int.* **1989**, *3*, 41.

(39) Kaliszan, R.; Osmialowski, K.; Bassler, B. J.; Hartwick, R. A. *J. Chromatogr.* **1990**, *499*, 333.

(40) Bassler, B. J.; Kaliszan, R.; Hartwick, R. A. *J. Chromatogr.* **1989**, *461*, 139.

(41) Mockel, H. J.; Braedikow, A.; Melzer, H.; Aced, G. *J. Liq. Chromatogr.* **1991**, *14*, 2477.

(42) Tanaka, N.; Kimata, K.; Hosoya, K.; Miyanishi, H.; Araki, T. *J. Chromatogr. A*, **1993**, *656*, 265.

(43) Burg, P.; Abraham, M. H.; Cagniant, D. *Carbon*, **2003**, *41*, 867.

(44) Kinoshita, K. *Carbon: Electrochemical and Physicochemical Properties*; John Wiley & Sons: New York, 1988.

(45) McDermott, M. T.; McCreery, R. L. *Langmuir*, **1994**, *10*, 4307.

(46) Ray, K.; McCreery, R. L. *Anal. Chem.* **1997**, *69*, 4680.

(47) Xu, J.; Chen, Q.; Swain, G. M. *Anal. Chem.* **1998**, *70*, 3146.

(48) Harnisch, J. A.; Porter, M. D. *Analyst*, **2001**, *126*, 1841.

(49) Porter, M. D.; Takano, H. In *Encyclopedia of Separation Science*; Wilson, I. D., Adlar, E. R., Cooke, M., Poole, C. F., Eds.; Academic Press: London, 2000.

(50) Deinhammer, R. S.; Ting, E.-Y.; Porter, M. D. *J. Electroanal. Chem.* **1993**, *362*, 295.

(51) Deinhammer, R. S.; Ting, E.-Y.; Porter, M. D. *Anal. Chem.* **1995**, *67*, 237.

(52) Ting, E.-Y.; Porter, M. D. *J. Electroanal. Chem.* **1998**, *443*, 180.

(53) Ting, E.-Y.; Porter, M. D. *Anal. Chem.* **1997**, *69*, 675.

(54) Ting, E.-Y.; Porter, M. D. *J. Chromatogr. A*, **1998**, *793*, 204.

(55) Ho, M. K.; Wang, S. J.; Porter, M. D. *Anal. Chem.* **1998**, *70*, 4314.

(56) Ponton, L. M.; Porter, M. D. *J. Chromatogr. A*, **2004**, *1059*, 103.

(57) Ponton, L. M.; Porter, M. D. *Anal. Chem.* **2004**, *76*, 5823.

(58) Muna, G. W.; Swope, V. M.; Swain, G. M.; Porter, M. D. *J. Chromatogr. A*, **2008**, *1210*, 154.

(59) Keller, D. W.; Porter, M. D. *Anal. Chem.* **2005**, *77*, 7399.

(60) Martin, A. J. P.; Synge, R. L. M. *Biochem. J.* **1941**, *35*, 1358.

(61) Snyder, L. R. *Principles of Adsorption Chromatography*; Marcel Dekker Inc.: New York, 1968.

(62) Lough, W. J.; Wainer, I. W. *High Performance Liquid Chromatography*; Blackie Academic & Professional: New York, 1995.

(63) Jaroniec, M. *J. Chromatogr. A,* **1992**, *656*, 37.

(64) Robards, K.; Haddad, P. R.; Jackson, P. E. *Principles and Practice of Modern Chromatographic Methods*; Academic Press: Boston, 1994.

(65) Neue, U. *HPLC Columns: Theory, Technology and Practice*; Wiley-VCH: New York, 1997.

(66) Bockris, J. O. M.; Reddy, A. K. N. *Modern Electrochemistry, an Introduction to an Interdisciplinary Areas*; Macdonald: London, 1970.

(67) Bard, A. J.; Faulkner, L. R. *Electrochemical Methods: Fundamentals and Applications*; John Wiley & Sons, Inc.: New York, 2001.

(68) Chattoraj, D. K.; Birdi, K. S. *Adsorption and the Gibbs Surface Excess*; Plenum Press: New York, 1984.

(69) Conway, B. E. In *Encyclopedia of Surface and Colloid Science*; Somasundaran, P., Ed.; Marcel Dekker Inc.: New York, 2002.

(70) Lyklema, J. *Fundamentals of Interface and Colloid Science: Liquid Solid Interfaces*; Academic Press: London, 1995.

(71) Mattson, J. S.; Mark, H. B. *Activated Carbon: Surface Chemistry and Adsorption from Solution*; Marcel Dekker Inc.: New York, 1971.

(72) Adamson, W. *Physical Chemistry of Surfaces*; Wiley Interscience: New York, 1990.

(73) Ting, E.-Y.; Porter, M. D. *Anal. Chem.* **1998**, *70*, 94.

(74) Keller, D. W.; Ponton, L. M.; Porter, M. D. *J. Chromatogr. A*, **2005**, *1089*, 72.

(75) Deinhammer, R. S.; Ting, E.-Y.; Porter, M. D. *Anal. Chem.* **1995**, *67*, 237-246.

(76) Ting, E.-Y.; Porter, M. D. *J. Electroanal. Chem.* **1998**, *443*, 180-185.

(77) Takano, H.; Porter, M. D. *Proc. Electrochem. Soc.* **1999**, *99-5*, 50-60.

(78) Nikitas, P. *J. Electroanal. Chem.* **2000**, *484*, 137.

(79) Zhang, Y.; McGuffin, V. L. *J. Liq. Chrom. Relat. Tech.* **2007**, *30*, 1551.

(80) Kaliszan, R. *Chem. Rev.* **2007**, *107*, 3212.

(81) Jackson, P. T.; Schure, M. R.; Weber, T. P.; Carr, P. W. *Anal. Chem.* **1997**, *69*, 416.

(82) Morokuma, K. *Acc. Chem. Res.* **1977**, *10*, 294-300.

(83) Wan, Q.-H.; Ramaley, L.; Guy, R. *Chromatographia*, **1998**, *48*, 523.

(84) Hunter, C. A.; Sanders, J. K. M. *J. Am. Chem. Soc.* **1990**, *112*, 5525.

(85) Chipot, C.; Jaffe, R.; Maigret, B.; Pearlman, D. A.; Kollman, P. A. *J. Am. Chem. Soc.* **1996**, *118*, 11217.

(86) Moore, W. J. *Physical Chemistry*, 4th ed.; Prentice-Hall: Englewood-Cliffs, 1972.

(87) Melander, W.; Campbell, D. E.; Horvath, C. *J. Chromatogr.* **1978**, *158*, 215.

(88) Garau, C.; Frontera, A.; Quinonero, D.; Ballester, P.; Costa, A.; Deya, P. M. *J. Phys. Chem. A*, **2004**, *108*, 9423.

(89) Clements, A.; Lewis, M. *J. Phys. Chem. A*, **2006**, *110*, 12705.

(90) Quinonero, D.; Garau, C.; Frontera, A.; Ballester, P.; Costa, A.; Deya, P. M. *Chem. Phys. Lett.* **2002**, *359*, 486.

(91) Kim, D.; Tarakeshwar, P.; Kim, K. S. *J. Phys. Chem. A*, **2004**, *108*, 1250.

FIGURES AND TABLE

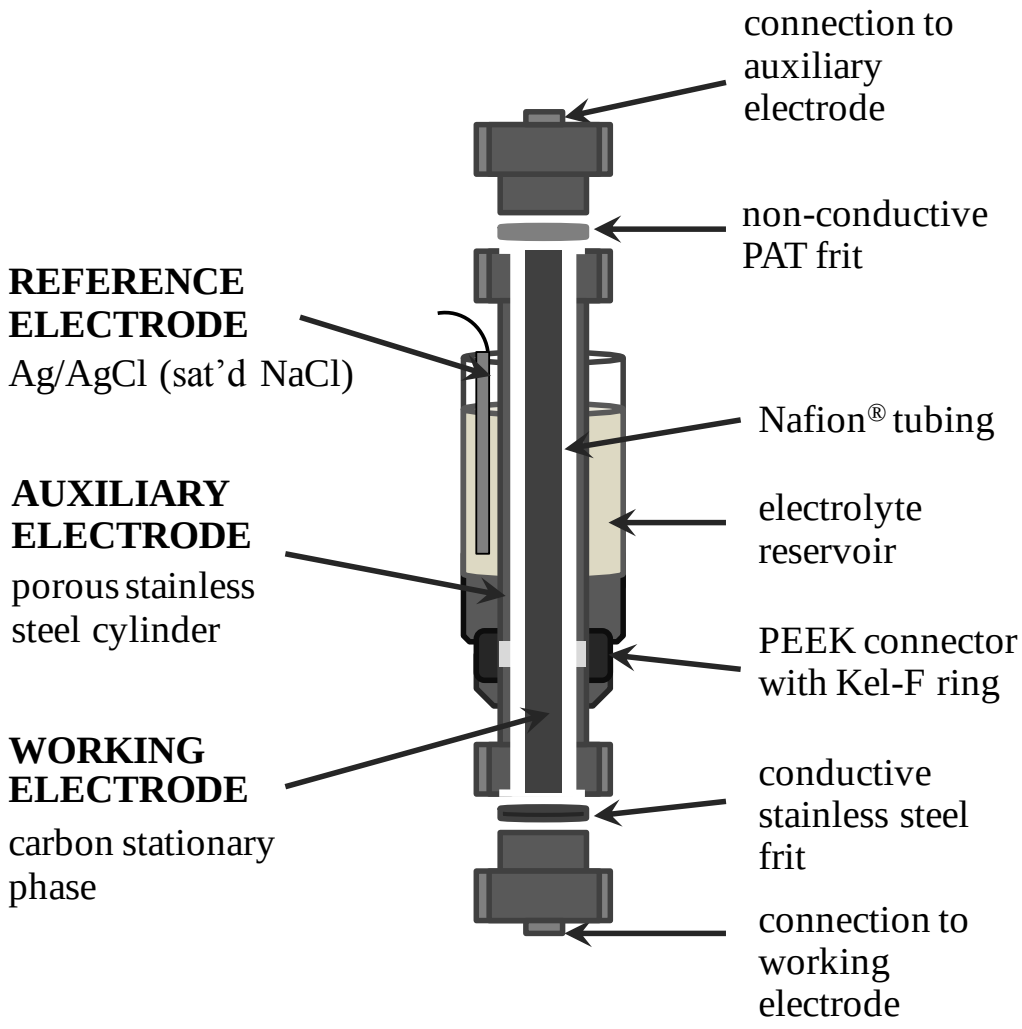

Figure 1. Schematic representation of the EMLC column.

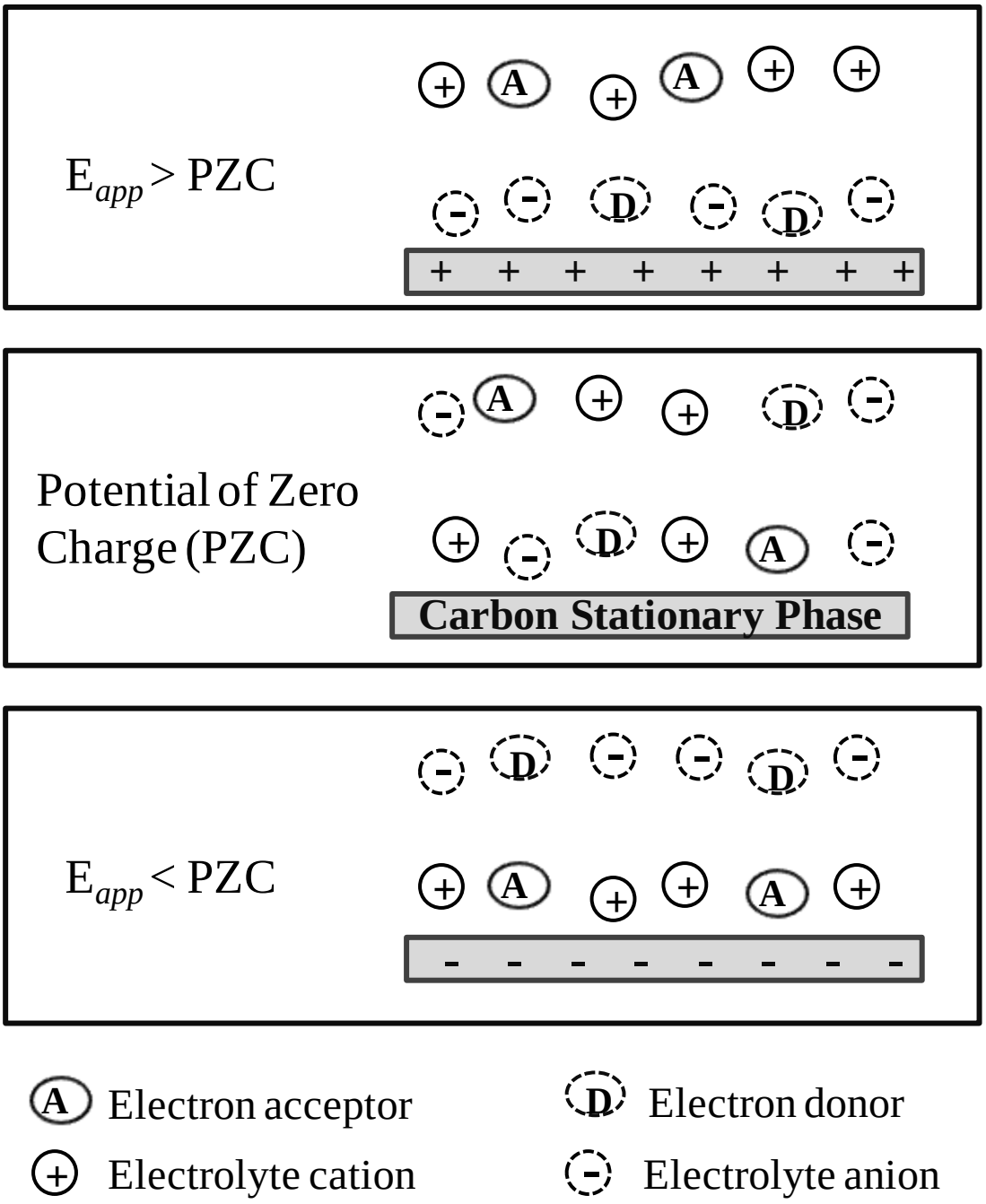

Figure 2. Schematic representation of how E_{app} influences analyte retention.

Table 1. Definitions and examples of interactions of the solute with the stationary phase, mobile phase and supporting electrolyte discussed in this dissertation.

Interaction	**Definition**	**Additional Information**	**Example in EMLC**	**Ref.**
<u>Solute-Stationary Phase</u> PGC(+) = PGC stationary phase at E_{app} > PZC (positive net surface excess charge) PGC(-) = PGC stationary phase at E_{app} < PZC (negative net surface excess charge) PGC(0) = PGC stationary phase at E_{app} = PZC (zero net surface excess charge)				
Electron donor-acceptor interactions - Partial or complete transfer of an electron from a donor to an acceptor				82, 83
Ion-ion/ Electro-static	Interaction between **A** and **B** that contain net permanent charges (ionic).	Long-range interactions with strength varying with r^{-1} (r = molecular distance).	A = PGC(+) B = benzene sulfonate; or A = PGC(-) B = pyridinium	
Ion-dipole	Interaction between an ion **A** and a polar molecule **B**.	Strength varies with r^{-2}.	A = PGC(+) B = phenol	
Ion-induced dipole	Interaction that results from the approach of an ion **A** that induces distortion in the electron distribution, thus forming a dipole in a nonpolar molecule **B**.	Strength varies with r^{-4}.	A = PGC(+) B = benzene; or A = benzene sulfonate B = PGC(0)	
Dipole-induced dipole	Interaction that results from the approach of a polar molecule **A** that induces distortion in the electron distribution, thus forming a dipole in a nonpolar molecule **B**.	Strength varies with r^{-6}.	A = Phenol B = PGC(0)	

Table 1. (Continued)

Interaction	Definition	Additional Information	Example in EMLC	Ref.
π-π	Strong attractive interactions between π-systems of molecules **A** and **B**.	Actually due to π-σ interaction; Favorable geometries are T-shaped and offset π-stacked.	A = PGC π-system B = benzene ring of the solute	84, 85
Dispersion interactions	Arise from instantaneous changes in electron distribution of nonpolar molecules **A** and **B**. A temporary dipole in one molecule induces a dipole in the other molecule.	Typically very weak; Strength varies with r^{-6}; Strength increases as the molecule becomes larger.	A = PGC(0) B = benzene	86
Solvophobic effects	Tendency of the solute to associate with the stationary phase when more hydrophilic mobile phases are used.	Governed by the relative affinity of the solute to the stationary and mobile phases	More water in the mobile phase increases solute retention	87
<u>Solute-Mobile Phase</u>				
Solvophobic effects	Decrease in the affinity of the solute with the mobile phase when more hydrophilic mobile phases are used.	Governed by the relative affinity of the solute to the stationary and mobile phases	More water in the mobile phase increases solute retention	87
<u>Solute-Supporting Electrolyte</u>				
Anion-π interactions	Interactions between an anion **A** and the π-system of the benzene ring of a molecule **B**.		A = supporting electrolyte anion B = benzene	88-91

CHAPTER 2. MECHANISTIC FACTORS IN THE RETENTION OF ALKYLBENZENES AND METHYLBENZENES IN ELECTROCHEMICALLY MODULATED LIQUID CHROMATOGRAPHY

A paper to be submitted to the *Journal of Chromatography A*

Gloria Fe M. Pimienta,[a,b] and Marc D. Porter[b,*]

[a]Department of Chemistry, Iowa State University, Ames, Iowa 50011

[b]Departments of Chemistry, Chemical Engineering, and Bioengineering, University of Utah, Salt Lake City, UT 84108

ABSTRACT

The retention mechanism of electrochemically modulated liquid chromatography (EMLC) is studied using neutral aromatic solutes – benzene, alkylbenzenes and di-and tri- methylbenzenes. EMLC is a separation technique that manipulates retention through changes in the potential applied (E_{app}) to a conductive stationary phase like porous graphitic carbon (PGC). Herein, retention dependence with respect to E_{app} is examined based on the structure (i.e., alkyl chain length and number and position of methyl substituents) and properties (i.e., hydrophobicity and polarity) of the analytes.

The dependence of retention of these neutral analytes on E_{app} can be attributed to the interplay of donor-acceptor and solvophobic interactions between the solute and PGC

---

*Corresponding author:

email: marc.porter@utah.edu

phone: 801-587-1505

and of the competitive adsorption of the supporting electrolyte. The shapes of the plots of ln k' vs. E_{app} for the solutes provide insights on the importance of the contributions of these factors on the mechanism of retention for this class of solutes.

INTRODUCTION

Electrochemically modulated liquid chromatography (EMLC) is a unique combination of electrochemistry and chromatography.[1, 2] In this technique, a column is configured as a three-electrode electrochemical cell by using a conductive packing material, like porous graphitic carbon (PGC), as both the stationary phase and the working electrode. The potential applied (E_{app}) to the conductive stationary phase therefore serves as a means to affect the efficiency of a separation in a manner similar to changing the mobile phase composition in conventional LC. With EMLC, retention is manipulated due to changes in the interfacial properties (e.g., surface charge, double layer structure, and oxidation state) of the stationary phase brought about by manipulation of the E_{app}.

EMLC has been used to separate a wide variety of analyte mixtures, including aromatic sulfonates,[3, 4] monosubstituted benzenes,[5] corticosteroids,[6] benzodiazepines,[7] enantiomers of hexobarbital and mephenytoin,[8] and inorganic anions.[9] High-speed EMLC has been demonstrated by carrying out separations at elevated temperatures to reduce elution times.[10] The possibility of employing boron-doped diamond particles (BDDP) as stationary phase has also been explored.[11]

Studies have shown that the retention factor, k', on carbonaceous materials reflects a complex mixing of several interactions - donor-acceptor, dispersion, and

solvophobic - between the analyte and the stationary phase surface. In investigations of the influence of E_{app} on the retention of aromatic sulfonates, it was found that electrostatic interactions play a major role in how the retention behavior of this class of anionic was manipulated by changes in E_{app}.[12, 13] Generally, ln *k′* showed a linear dependence with E_{app}, as would be predicted by the influence of an electric field on a Boltzmann distribution of ions. As the E_{app} is poised at more positive values with respect to the potential of zero charge (PZC), the stationary phase acquires a net positive surface excess charge, resulting in an increase in retention of these negatively-charged analytes. On the other hand, retention decreased at values of E_{app} negative of the PZC, owing to the negative surface excess charge on the stationary phase. The observed dependencies strongly correlated with analyte charge in that the slope of ln *k′* vs. E_{app} plots were similar for analytes with like charges, and those for divalent anions were about twice those for monovalent anions. Other interactions (e.g., dispersive, hydrophobic and ion-induced dipole) between the stationary phase surface and analyte also take part in the manipulation of retention, as revealed by small differences in the slopes of analytes with like charges but different substituents and by the ability to affect retention when E_{app} is negative of the PZC. The combined weight of these works showed that EMLC is not only an intriguing addition to the many variants in the LC separations toolbox, but also a valuable new methodology for examining the mechanistic underpinnings of electrosorption phenomena.

The goal of the research work detailed herein is to investigate the influence of E_{app} on uncharged analytes in an attempt to more fully gain an understanding of how other interactions (i.e., non-electrostatic) influence retention on PGC. The analytes

chosen for these studies include benzene, a series of alkylbenzenes, and di- and tri-methylbenzenes. Retention behavior is analyzed with respect to their geometric structure and various other properties (e.g., molar polarization and hydrophobicity). The observed changes in the retention of these analytes due to changes in E_{app} provide important insights into the role of non-electrostatic interactions with respect to adsorption on PGC.

EXPERIMENTAL SECTION

The EMLC Column

The design and construction of the EMLC column has been detailed elsewhere.[14] Briefly, Nafion tubing (Perma Pure, Toms River, NJ, USA) is inserted into a porous stainless steel cylinder (Mott Metallurgical, Farmington, CT, USA). The column is slurry packed with PGC (Thermo Scientific, Waltham, MA, USA), which serves as a stationary phase and as a working electrode. A Ag/AgCl (saturated NaCl) reference electrode (Bioanalytical Systems, West Lafayette, IN, USA) is placed inside the external electrolyte reservoir that surrounds the stainless steel cylinder; all values of E_{app} are reported with respect to this electrode.

The experiments employed 5-μm diameter PGC particles as the packing material. PGC is devoid of detectable oxygen-containing surface groups, as judged by X-ray photoelectron spectroscopy (detection limit ~0.2 atomic %).[4] The manufacturer specifies a nominal pore diameter of ~250 Å, and a porosity of ~80%.[15] The surface area of PGC packed in the column is ca. 30 m^2, based on BET measurements (120 m^2/g)[16] and the amount of PGC loaded in the column (~0.25 g).

Instrumentation

Chromatographic experiments were performed using an Agilent 1200 Series module equipped with a solvent cabinet, autosampler, quaternary pumping system, and UV/Vis diode array detector. The module was interfaced to a Pentium IV 600 MHz computer. ChemStation software controls the pump and injector parameters, set-up of sequences, and signal acquisition; it was also used for data processing. The potential of the electrode was controlled using a potentiostat/galvanostat model 263A (EG&G Princeton Applied Research, Oak Ridge, TN, USA).

Chemicals and Reagents

The analytes benzene (EMD, Gibbstown, NJ, USA), toluene (Sigma-Aldrich, St. Louis, MO, USA), ethylbenzene (Alfa Aesar, Ward Hill, MA, USA), *n*-propylbenzene (Alfa Aesar), *n*-butylbenzene (Alfa Aesar), 1,2-dimethylbenzene (Fluka, St. Louis, MO, USA), 1,3-dimethylbenzene (Alfa Aesar), 1,4-dimethylbenzene (Alfa Aesar), 1,3,5-trimethylbenzene (TCI America, Portland, OR, USA), 1,2,4-trimethylbenzene (Fluka), and 1,2,3-trimethylbenzene (TCI America) were used as received. Lithium perchlorate was purchased from Sigma-Aldrich. Water and acetonitrile were high purity solvents from EMD.

Mode of Operation

The mobile phase, which is a water/acetonitrile solution (40:60 *v:v*) containing 0.10 M lithium perchlorate as the supporting electrolyte, flowed at 0.40 mL/min. After a change in E_{app}, the system was allowed to reach a steady state for 30 min. In cases when

more time is needed, the column conditioning is carried on until the baseline remains stable for 10 min.

All analytes were prepared at 100 μM concentrations using acetonitrile as sovent which also served as the nonretained marker used for the determination of the dead time, t_0. Injection volumes were set at 5.00 μL and all runs of the mixtures were repeated three times at each value of E_{app}. Individual injections of each analyte were also performed in triplicate for identification of all elution bands. The wavelength for detection was 214 nm. All experiments were performed at room temperature. To compensate for peak tailing, retention times, t_r, were determined from the first statistical moment analysis of all chromatographic peaks. The retention factor, k', was calculated according to the equation:

$$k' = (t_r - t_0)/t_0 .$$

RESULTS AND DISCUSSION

Approach

The analytes used in this work are benzene, alkylbenzenes, and di- and tri-methylbenzenes. Their structures and designations are shown in Figure 1. Abbreviations are used for benzene, toluene and the rest of the alkylbenzenes. The positions of the methyl groups on the benzene ring are used for the di- and tri- methylbenzenes.

As noted, the adsorption of solutes on a PGC stationary phase spans a range of interactions (i.e., electron donor-acceptor, dispersion, and hydrophobic). Electron-donor acceptor interactions, which include electrostatic and dipole-induced dipole interactions, occur largely between the n- and/or π- electrons of the solute and the delocalized π-

electron system of PGC. Dispersion interactions have a non-specific nature and typically track with the molecular weight of the solute. Solvophobic interactions are reflected by the solubility of the analyte in the mobile phase. Competition from the electrosorption of the supporting electrolyte and mobile phase additives can also prove important.[17, 18] Interpretations of the retention data herein are based on the strength of these interactions, and how each interaction is manipulated by variations in E_{app}. As part of the basis for relating retention behavior to molecular structure, values of the logarithm of the octanol-water distribution coefficient,[19] log D_{ow}, and the molar polarization,[20] P, of the analytes are shown in Table 1. D_{ow} is defined as the quotient of the equilibrium concentration of a solute in the octanol-rich phase to that in the water-rich phase and is thus a measure of the hydrophobicity of the substance and can be related to solvophobic interactions. P-values represent the total electric dipole per mole and are an indicator of solute polarity and a correlator for the strength of the dipole induced on the solute.

Chromatographic Results

Chromatographic experiments were performed at different values of E_{app} (-0.250 to +0.350 V vs. Ag/AgCl sat'd NaCl). This potential window reflects limitations set by the oxidation of the stationary phase and the reduction of the mobile phase. Typical chromatograms for the separation of the 11-component mixture are shown in Figure 2. While there are subtle, but intriguing changes in retention, the order of elution is the same at all values of E_{app}. This subsection examines the factors central to determining the elution order within each of the structural subsets.

BZ and the homologous series of alkylbenzenes (TO, EB, PB, and BB) generally elute in the earlier portion of the chromatogram. The elution order (BZ < TO < EB < BB) is consistent with an increase in the dispersion interactions with the stationary phase upon the incremental addition of a methylene group.[21, 22] It also follows considerations based on the log D_{ow} and on *P*-values in Table 1. These measures of molecular interactions, however, do not predict the trends across the complete set of solutes, pointing to the importance of other mechanistic factors.

For BZ, TO, and di- and tri- methylbenzenes, retention time increases with the number of methyl groups on the aromatic ring. The ordering reflects an increase in dispersion forces with the addition of methyl groups. The strength of electron donor-acceptor interactions are also amplified due to an increase in the electron density of the aromatic ring as the number of electron-donating methyl groups increases.

The order of elution of the three positional isomers of dimethylbenzene on PGC is consistent with published results.[15, 22-24] When using conventional bonded phases, the *meta* (1,3) isomer is retained more strongly than the *para* (1,4) and *ortho* (1,2) isomers and is separated easily by isocratic elution.[25] At PGC, a reversal in elution order is observed. The *meta* isomer is eluted first because it has the lowest π-electron density among the isomers.[22] The unsymmetric π-electron distribution on the aromatic ring of the *ortho* isomer, which can induce a greater dipole on the PGC surface may contribute to its extended retention.[26, 27]

The elution order of the trimethylbenzenes can be explained, as described by Kriz and co-workers[25] using the same reasoning. 1,3,5 which is essentially a "double *meta*" (i.e., the methyl group on C_3 and C_5 positions of the benzene ring are both *meta* to the

methyl substituent at the position C_1) elutes first, followed by 1,2,4, which is an "*ortho-meta*" (the substituent on the C_2 position is ortho to that of the methyl group on the C_1 position, and the substituent on C_3 is meta to that on C_1). Lastly, 1,2,3 is a "double *ortho*" (i.e., the methyl groups on C_1 and C_3 positions are both ortho to that on the C_2 position).

Influence of E_{app} on Retention

As already noted, the elution order of the solutes is unchanged at all values of E_{app}. There are, however, subtle changes in solute retention, which alter the total analysis time, and result in differences in selectivity (i.e., the relative separation between elution bands). More interestingly, some of the analytes (e.g., TO) undergo an increase in retention as E_{app} increases, whereas that of others (e.g., 1,3,5) initially increase and then decrease. This dependence, which has been theoretically predicted,[28] is in sharp contrast to that consistently observed for charged analytes, including a large number of benzene- and naphthalene- sulfonates. The retention of aromatic sulfonates exhibits a linear dependence (ln k' vs. E_{app}) that increases as E_{app} moves to more positive values. Moreover, these changes are a few or more orders of magnitude greater than those in Figure 2. Those works indicated that changes in retention were governed primarily by electrostatic (ion-ion) interactions, and follow the general expectations of an ion-exchange mechanism at values of E_{app} well removed from PZC. For the neutral, relatively non-polar analytes studied herein, the strongest electron donor-acceptor interaction is between an ion (i.e., charged stationary phase) and an induced dipole (i.e.,

the solute), which is not modulated as much by alterations in the E_{app} as an ion-ion electrostatic interaction.

The EMLC-based retention dependence of each solute is summarized by the plots of ln k' vs. E_{app} in Figure 3. Each data point is an average value obtained from triplicate injections, and the error bars for ln k' are roughly the size of the data points. These plots show that the induced changes in retention via E_{app} are small compared to the differences in retention between the solutes. As a result, several intriguing trends in these dependencies are not readily apparent.

To further the analysis of the observed dependencies, five possible pathways by which E_{app} can influence the retention of neutral analytes is summarized in Figure 4. There are three principal mechanisms operative in the EMLC-based manipulation of the retention of neutral analytes: (1) changes in the strength of donor-acceptor interactions via ion-induced dipole and π-π interactions; (2) changes in the interfacial concentration of the supporting electrolyte anions and cations and the organic modifier in the mobile phase; and (3) changes in the solvophobicity of the mobile phase-stationary phase interface.

In donor-acceptor interactions, the electron acceptor character of PGC increases as E_{app} becomes more positive due to an increase in excess positive surface charge density. The solutes in Figure 1, which are π-electron donors, therefore undergo an increase in electron donor-acceptor interactions with PGC. Retention due to donor-acceptor interactions is thus increased as E_{app} moves to more positive values.

Changes in the excess charge density on PGC also alter the interfacial excess of the components of the supporting electrolyte. When the E_{app} is poised positive of the

PZC, more electrolyte anions interact electrostatically with the stationary phase. These interactions can affect retention due to competition between solute and electrolyte anions for adsorption sites, which would then decrease solute retention. In a similar way, at values of E_{app} negative of the PZC, more electrolyte cations compete for adsorption sites, resulting in a decrease in retention. The PZC can be viewed as the potential in which the competition from electrolyte ions would be at its lowest.

The build-up of excess surface charge has one more notable consequence. It causes the hydrophilicity of the stationary phase to increase, which weakens solvophobic interactions with the solute, resulting in decreased retention. Thus, the strength of solvophobic interactions in the electrical double layer for nonpolar solutes (e.g., those in Figure 1) is at a maximum at PZC and decreases with both positive and negative excursions of the E_{app} from the PZC. The next subsections examine the data in Figures 2 and 3 in more detail.

The ability to ascertain the possible contributors to the EMLC-based retention of the nonpolar aromatic compounds is, of course, inherently linked to the location of the PZC. Literature reports[13] place the PZC for carbonaceous materials like PGC between -0.20 and +0.10 V (vs. Ag/AgCl sat'd NaCl). The span in these values reflects the differences in the type of carbon (absence of surface groups such as quinones, phenols, and carboxylic acids). The reported values are also dependent on the technique (e.g., capacitance and surface tension) used for the determination. Indeed, we recently reported on the use of EMLC as a means to determine the PZC for PGC.[16] This approach correlated the retention dependence of a series of aromatic sulfonates with both E_{app} and the identity and concentration of the supporting electrolyte. Thus, the intersection of an

overlay of plots of ln k' vs. E_{app} at different concentrations of supporting electrolytes signifies that the electrostatic driving force for the adsorption is essentially zero (i.e., the PZC corresponds to the potential in which retention is invariant with respect to electrolyte concentration).

That study showed, as expected, that the PZC when using NaF, KCl, and $LiClO_4$ as supporting electrolytes followed the strength of the specific adsorption of the electrolyte anion and the given solute. As such, the PZC for Cl^- was ~0.18 V more negative than that for F^-, but ~0.07 V more positive than that for ClO_4^-. Moreover, the apparent PZC was found to be more positive for solutes like benzenedisulfonate, which can be viewed as interacting with PGC mainly through electrostatics (i.e., nonspecific adsorption) as opposed to chlorobenzenesulfonate which has both nonspecific interactions dictating retention. These factors will also be taken into account in the subsequent mechanistic analysis.

EMLC-Based Retention of Alkylbenzenes

The plots in Figure 5 are taken from those in Figure 3, presented in such a way that aids in the side-by-side comparison of the differences in retention behavior. All the plots have an *x*-axis range from -0.400 to +0.400 V. The *y*-axis range of the plots all spans 0.3 ln k' units, but, as noted in the caption, have absolute values that are different for each solute.

The top panel of Figure 5 shows ln k' vs. E_{app} plots for each of the five alkylbenzenes. As is evident, the dependence of ln k' undergoes an increase in curvature as the length of the alkyl chain increases. BZ and TO exhibit the lowest levels of

curvature. Indeed, the trends for both analytes, along with EB (albeit exhibiting slight curvatures at the positive end of the E_{app}), are consistent with the influence of E_{app} on electron donor-acceptor interactions, in that the dipole-induced dipole interactions of these three solutes with PGC dictate the observed change in retention.

On a broader level, the observed differences in the shapes of these plots (i.e., linear, curved, or parabolic) can be qualitatively understood by considering the possible effects from the competitive adsorption of supporting electrolyte ions and/or changes in interfacial solvophobicity. Based on the discussion of Figure 4, the competitive adsorption of electrolyte ions is a minimum at the PZC and increases with positive and negative excursions from the PZC. Furthermore, the strength of solvophobic interactions is at a maximum at PZC, decreasing as E_{app} deviates from PZC in both positive and negative directions. Both these factors can result in a decrease in retention when the potential applied to the stationary phase moves away from the PZC.

How then to determine which of these processes dictate the observed evolution in the curvature of the plots of ln k' vs. E_{app}? We would expect the impact of competition from specifically and nonspecifically adsorbed electrolyte ions to be present in all five of the plots. That is, competition from the electrolyte cation would appear as a decrease in retention as E_{app} becomes increasingly negative of the PZC, which is in fact, what is observed. However, a similar dependence would then be expected in instances in which the electrolyte anion also competes with analyte retention (i.e., when $E_{app} > PZC$). Both expectations are clearly evident in the plots for PB and BB, but only marginally so (if at all) for BZ and TO. Indeed, one would reasonably expect that the competition from the supporting electrolyte would even be more readily apparent in the ln k' vs. E_{app} plots for

BZ and TO, being the most weakly retained solute among this group. We therefore view the competition of the supporting electrolyte as a contributor to the evolution of the five plots, and need to more fully assess the potential role of changes in the solvophobicity of the electrical double layer.

The contribution from solvophobicity is supported by a qualitative correlation between the extent of curvature and the values of log D_{ow} for this set of solutes, as evident in Table 1. That is, BZ with the least degree of curvature has the smallest value of log D_{ow}. At the other end of the trend, PB and BB have the largest log D_{ow} values and the greatest extent of curvature.

To summarize briefly, the shape of the ln k' vs. E_{app} plots for benzene and the alkylbenzenes demonstrate a mixing of contributions from electron donor-acceptor interactions, supporting electrolyte adsorption, and solvophobic effects with respect to changes in the potential applied to the PGC stationary phase. The analysis of the data in the next subsection attempts to more fully delineate the possible roles of each of these interactions.

Effect of E_{app} on the Retention of Methylbenzenes

Based on the above discussion, the effect of E_{app} on the retention of the di- and tri- methylbenzenes should be dominated by donor-acceptor interactions that can be heavily modulated by supporting electrolyte competition and/or solvophobic interactions at large positive and large negative excursions in E_{app} with respect to the PZC.

As apparent in the middle and bottom panels of Figure 5, plots for the di- and tri-methylbenzenes show varying degrees of curvature, and as is the case for BZ and the

alkylbenzenes, the degree of curvature qualitatively correlates with the log D_{ow} value of the analyte. However, the same arguments used to possibly relegate competition from electrolyte ions as the main contributor to the observed evolution in the ln k' vs. E_{app} plots are countered by these data. In other words, the observation of clearly curved and parabolic plots argues that the dependencies for BZ and TO are more than likely a consequence of the inability to examine the retention at more positive values of E_{app}, which would more fully establish the shape of the profile. It is also important to note that the more strongly retained solutes more effectively compete with electrolyte for adsorption sites, and that the retention maximum is an indicator of the PZC as measured by a given solute.

CONCLUSIONS

This paper has demonstrated the role played by the donor-acceptor and solvophobic interactions, and the competitive adsorption of the supporting electrolyte on the dependence of the retention of benzene, a series of alkylbenzenes, and di- and tri-methylbenzenes on the changes in E_{app} to a PGC stationary phase. Through the studies presented herein, a better understanding of the retention mechanism of EMLC has been achieved. In addition, it is shown that EMLC is an effective tool in studying electrosorption on conductive stationary phases. Further studies will aim at unraveling the influence of the other components of the liquid chromatographic system. Specifically, retention will be investigated as a function of the mobile phase composition, supporting electrolyte concentration and identity, and temperature.

ACKNOWLEDGMENTS

This work was supported by the U.S. Department of Energy - Ames Laboratory and the Utah Science and Technology Research Initiative. The Ames Laboratory is operated for the U.S. Department of Energy by Iowa State University under Contract No. DE-AC0207CH11358.

REFERENCES

(1) Porter, M. D.; Takano, H. In *Encyclopedia of Separation Science*; Wilson, I. D., Adlar, E. R., Cooke, M., Poole, C. F., Eds.; Academic Press: London, 2000.

(2) Harnisch, J. A.; Porter, M. D. *Analyst*, **2001**, *126*, 1841.

(3) Deinhammer, R. S.; Ting, E.-Y.; Porter, M. D. *J. Electroanal. Chem.* **1993**, *362*, 295.

(4) Deinhammer, R. S.; Ting, E.-Y.; Porter, M. D. *Anal. Chem.* **1995**, *67*, 237.

(5) Ting, E.-Y.; Porter, M. D. *J. Electroanal. Chem.* **1998**, *443*, 180.

(6) Ting, E.-Y.; Porter, M. D. *Anal. Chem.* **1997**, *69*, 675.

(7) Ting, E.-Y.; Porter, M. D. *J. Chromatogr. A*, **1998**, *793*, 204.

(8) Ho, M. K.; Wang, S. J.; Porter, M. D. *Anal. Chem.* **1998**, *70*, 4314.

(9) Ponton, L. M.; Porter, M. D. *J. Chromatogr. A*, **2004**, *1059*, 103.

(10) Ponton, L. M.; Porter, M. D. *Anal. Chem.* **2004**, *76*, 5823.

(11) Muna, G. W.; Swope, V. M.; Swain, G. M.; Porter, M. D. *J. Chromatogr. A*, **2008**, *1210*, 154.

(12) Keller, D. W., Iowa State University, Ames, 2005.

(13) Keller, D. W.; Ponton, L. M.; Porter, M. D. *J. Chromatogr. A*, **2005**, *1089*, 72.

(14) Ting, E.-Y.; Porter, M. D. *Anal. Chem.* **1998**, *70*, 94.

(15) Knox, J. H.; Kaur, B.; Millward, G. R. *J. Chromatogr.* **1986**, *352*, 3.

(16) Keller, D. W.; Porter, M. D. *Anal. Chem.* **2005**, *77*, 7399.

(17) Antrim, R. F.; Yacynych, A. M. *Anal. Lett.* **1988**, *21*, 1085.

(18) Baczek, T.; Markuszewski, M.; Kaliszan, R.; van Straten, M. A.; Claessens, H. A. *J. High Resol. Chromatogr.* **2000**, *23*, 667.

(19) *CRC Handbook of Chemistry and Physics*, 89 ed.; CRC Press: Boca Raton, 2009.

(20) Altshuller, A. P. *J. Phys. Chem.* **1954**, *58*, 392.

(21) Knox, J. H.; Ross, P. In *Advances in Chromatography*; Brown, P. R., Grushka, E., Eds.; Marcel Dekker Inc: New York, 1997; Vol. 37.

(22) Zhang, Y.; McGuffin, V. L. *J. Liq. Chrom. Relat. Tech.* **2007**, *30*, 1551.

(23) Gilbert, M. T.; Knox, J. H.; Kaur, B. *Chromatographia*, **1982**, *16*, 138.

(24) Bassler, B. J.; Hartwick, R. A. *J. Chromatogr. Sci.* **1989**, *27*, 162.

(25) Kriz, J.; Adamcova, E.; Knox, J. H.; Hora, J. *J. Chromatogr. A*, **1994**, *663*, 151.

(26) Jackson, P. T.; Carr, P. W. *J. Chromatogr. A*, **2002**, *958*, 121-129.

(27) West, C.; Lesellier, E. *J. Chromatogr. A*, **2005**, *1099*, 175-184.

(28) Nikitas, P. *J. Electroanal. Chem.* **2000**, *484*, 137.

FIGURES AND TABLE

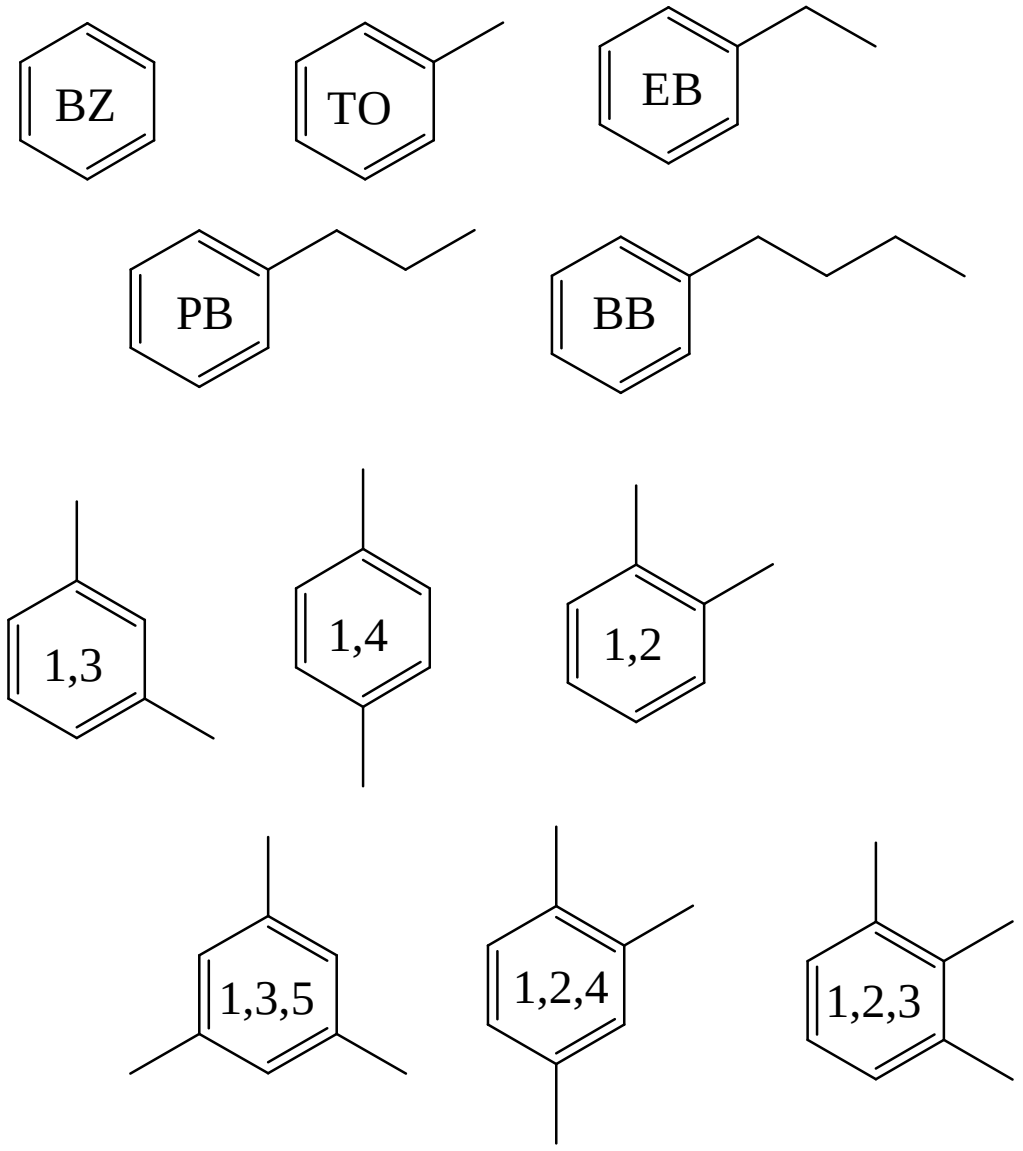

Figure 1. Structures and designations for the analytes used in this work: (BZ) benzene; (TO) toluene; (EB) ethylbenzene; (PB) propylbenzene; (BB) butylbenzene; (1,3), (1,4), and (1,2) dimethylbenzenes; and (1,3,5), (1,2,4), and (1,2,3) trimethylbenzenes.

Table 1. Molecular descriptors of the analyte and related information.

Analyte	Molecular Formula	log D_{ow} [a]	Molar Polarization (cm^3/mol) [b]	Elution Order
BZ	C_6H_6	2.13	26.65	1
TO	C_7H_8	2.73	33.55	2
EB	C_8H_{10}	3.15	39.05	3
PB	C_9H_{12}	3.69	43.75	4
BB	$C_{10}H_{14}$	4.26	48.65	8
1,3	C_8H_{10}	3.20	38.45	5
1,4	C_8H_{10}	3.15	36.65	6
1,2	C_8H_{10}	3.12	41.55	7
1,3,5	C_9H_{12}	3.42	41.55	9
1,2,4	C_9H_{12}	3.60	43.20	10
1,2,3	C_9H_{12}	3.63	47.45	11

[a]From Ref. 19. [b]From Ref. 20.

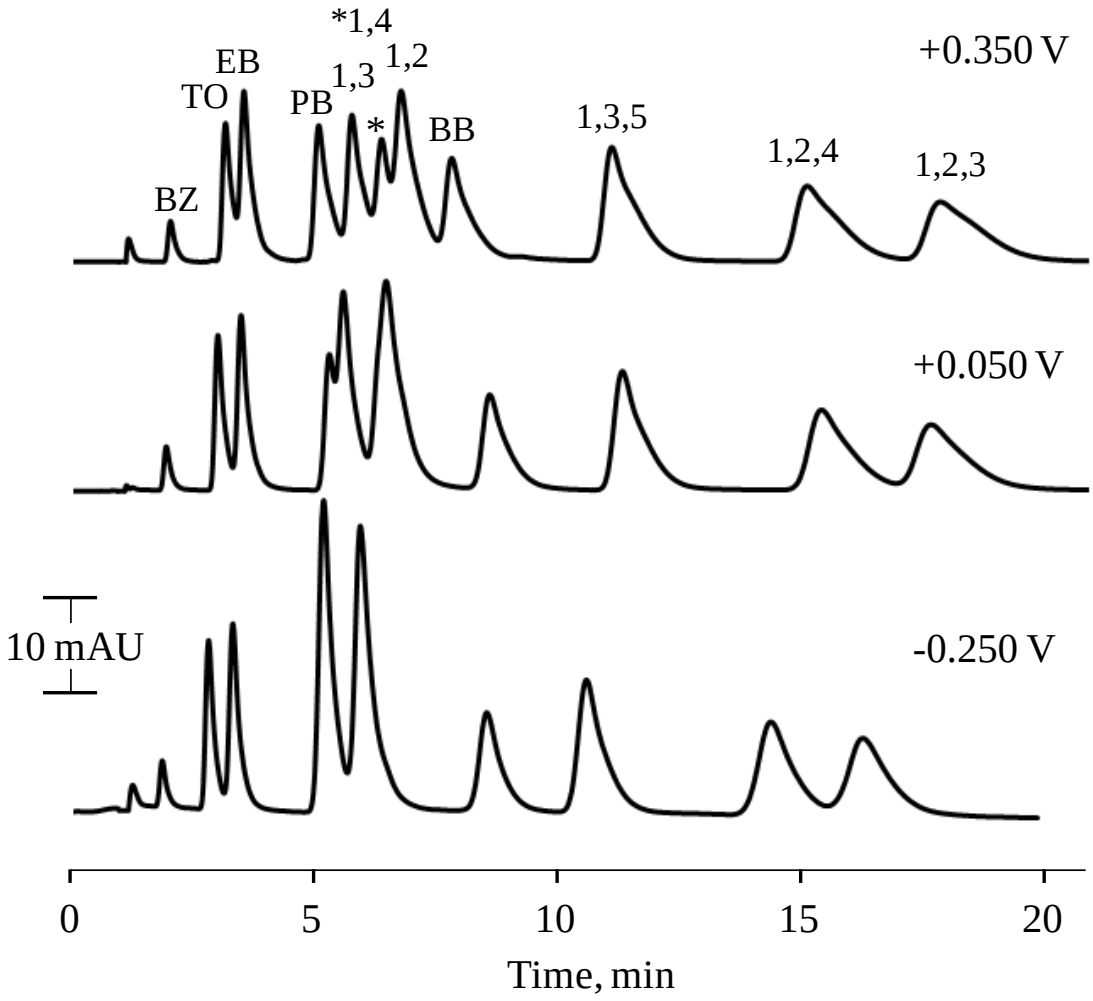

Figure 2. Chromatograms of the analyte mixture at varied E_{app} (vs. Ag/AgCl sat'd NaCl) values. The mobile phase was 40/60 mixture of H_2O/CH_3CN with 0.10 M $LiClO_4$, flowing at 0.40 mL/min. The analytes were prepared in 0.100 mM concentration in CH_3CN. The injection volume was 5.00 μL.

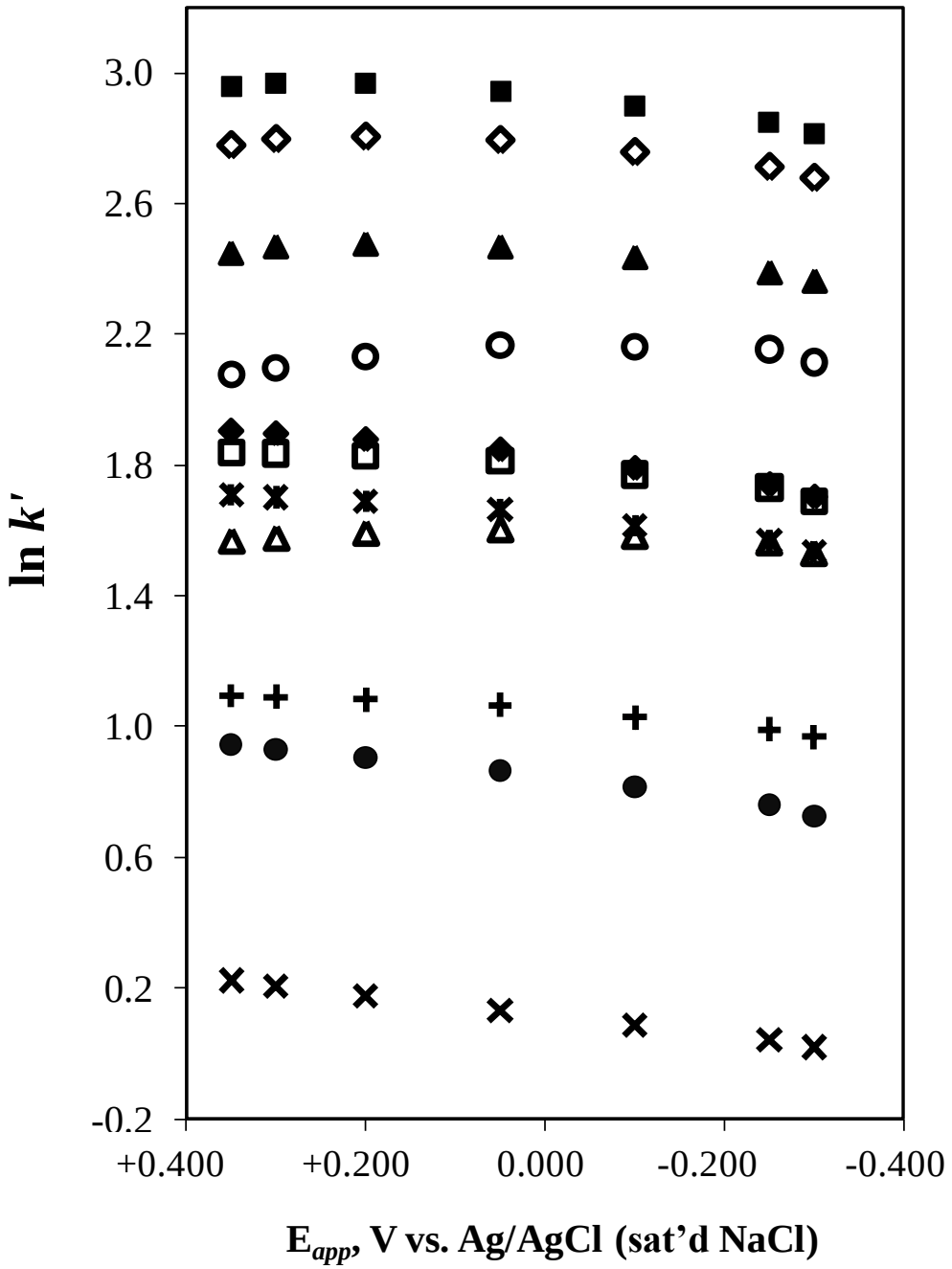

Figure 3. Capacity-potential plots for the analytes. BZ (✖), TO (●), EB (✚), PB(△), 1,3 (✱), 1,4 (□), 1,2 (◆), BB (○), 1,3,5 (▲), 1,2,4 (◇), and 1,2,3 (■). N=3, and error bars are roughly the size of the marker.

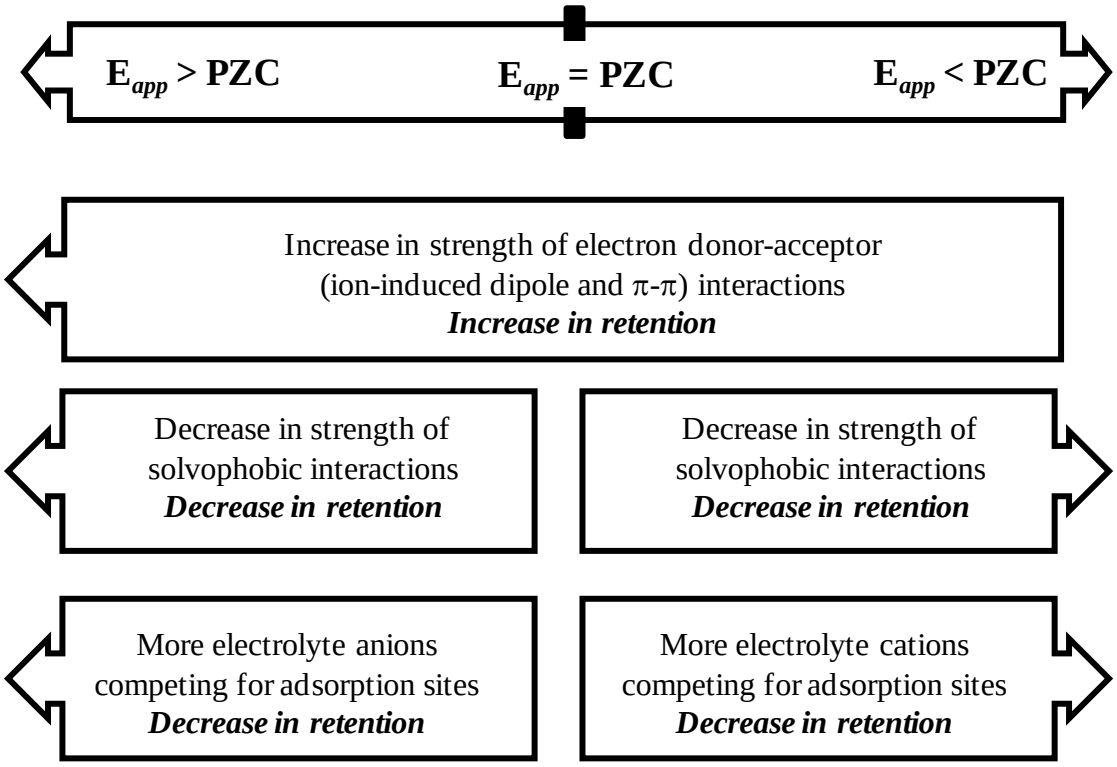

Figure 4. Influence of E_{app} on the retention of neutral analytes.

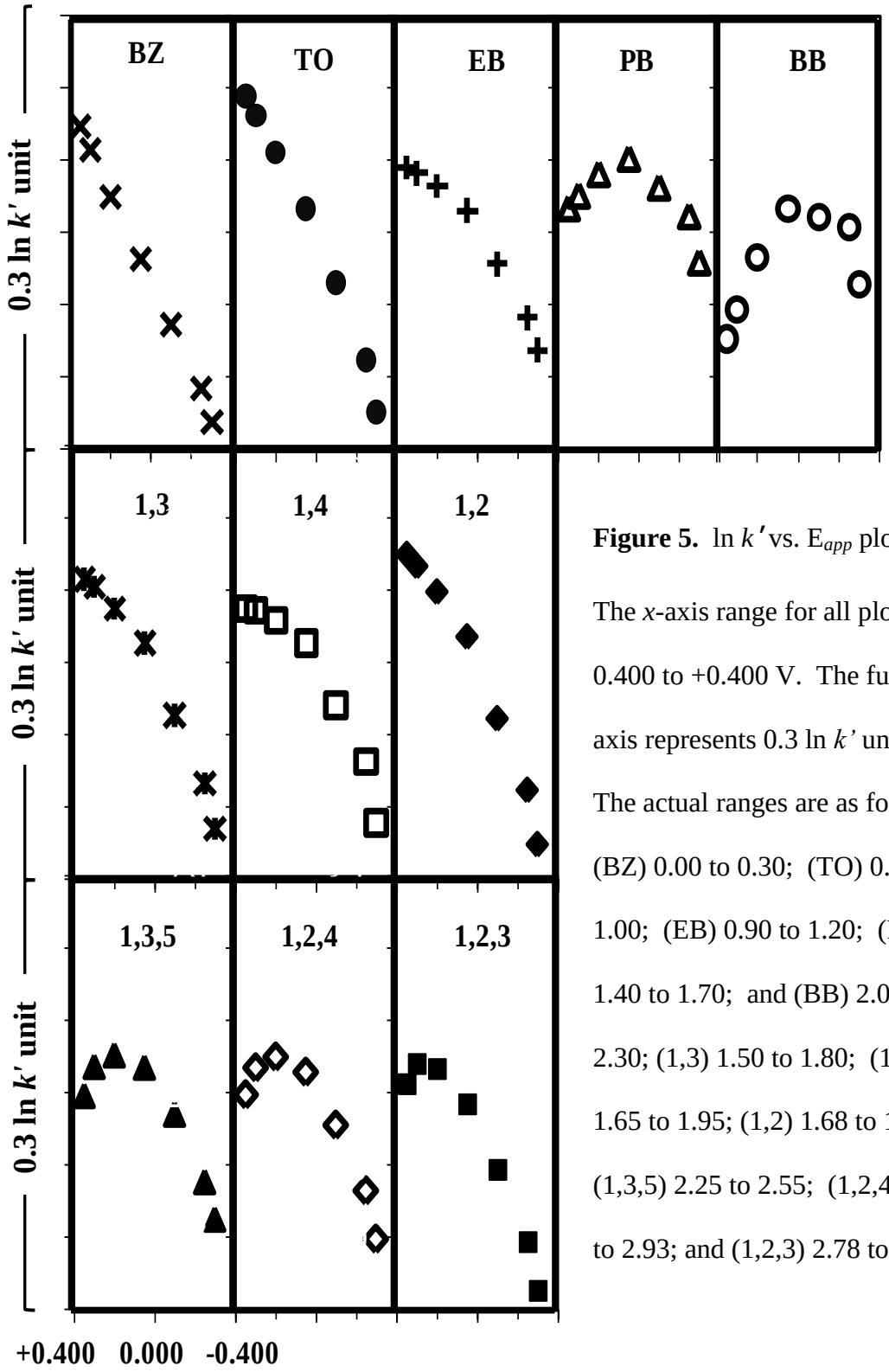

Figure 5. ln k' vs. E_{app} plots. The *x*-axis range for all plots is -0.400 to +0.400 V. The full *y*-axis represents 0.3 ln *k'* units. The actual ranges are as follows: (BZ) 0.00 to 0.30; (TO) 0.70 to 1.00; (EB) 0.90 to 1.20; (PB) 1.40 to 1.70; and (BB) 2.00 to 2.30; (1,3) 1.50 to 1.80; (1,4) 1.65 to 1.95; (1,2) 1.68 to 1.98; (1,3,5) 2.25 to 2.55; (1,2,4) 2.63 to 2.93; and (1,2,3) 2.78 to 3.08.

CHAPTER 3. THE ROLE OF THE SUPPORTING ELECTROLYTE IN ELECTROCHEMICALLY MODULATED LIQUID CHROMATOGRAPHY

A paper to be submitted to *Journal of Electroanalytical Chemistry*

Gloria Fe M. Pimienta[a,b] and Marc D. Porter[b,*]

[a]Department of Chemistry, Iowa State University

[b]Departments of Chemistry, Chemical Engineering, and Bioengineering, University of Utah, Salt Lake City, UT 84108

ABSTRACT

The influence of the supporting electrolyte concentration on the retention of benzene, a series of alkylbenzenes, and a series of di- and tri- methylbenzenes in electrochemically modulated liquid chromatography (EMLC) is reported. In EMLC, retention is manipulated through changes in the potential applied (E_{app}) to a conductive stationary phase like porous graphitic carbon (PGC). The electrochemistry component of this separation technique necessitates that the mobile phase contain a supporting electrolyte, which can influence solute retention. To gain further insight into the role of the supporting electrolyte, the retention behavior of these solutes is examined at various concentrations of lithium perchlorate in a mixed solvent (40/60 *v/v* H_2O/CH_3CN) mobile phase at multiple values of E_{app}. Retention is found to increase with increasing

---

*Corresponding author:

email: marc.porter@utah.edu

phone: 801-587-1505

supporting electrolyte concentration at all values of E_{app} studied. The results are interpreted based on the interactions that occur between the stationary phase, the solutes, and the supporting electrolyte. These results also indicate, interestingly, that retention is governed by the interactions of the π-system of the solute with the supporting electrolyte anion. A mechanism for the role of the supporting electrolyte in the retention of these neutral, aromatic solutes is proposed.

INTRODUCTION

Electrochemically modulated liquid chromatography (EMLC) is a unique combination of HPLC and electrochemistry.[1, 2] In EMLC, retention is manipulated through changes in the potential applied (E_{app}) to a conductive stationary phase like porous graphitic carbon (PGC). The column is configured as an electrochemical cell, with the packing material serving a dual purpose by acting both as stationary phase and working electrode. Variations in E_{app} in effect alter the surface composition of the stationary phase, and thus its adsorptive properties. The utility of EMLC has been demonstrated for the separation of a wide range of analytes, such as aromatic sulfonates,[3, 4] monosubstituted benzenes,[5] corticosteroids,[6] benzodiazepines,[7] and inorganic anions.[8]

Because EMLC uses an applied potential to manipulate retention, a supporting electrolyte must be added to the mobile phase.[9] As such, the supporting electrolyte has three main functions: (1) increase solution conductivity, (2) minimize migration effects, and (3) create a reproducible double layer.[10, 11] Expectedly, the presence of the

supporting electrolyte has a notable impact on solute retention. Keller and co-workers[12] summarized the possible influences of the supporting electrolyte in EMLC (Figure 1), which include the competition between the supporting electrolyte and analyte for adsorption sites on the stationary phase and interactions between the electrolyte ions and analyte in the mobile and stationary phases. Thus, the free energy of adsorption, ΔG_{tot}, is the sum of the free energies of interactions between all the species in the system. The $\Delta G_{a\text{-}lyte}$ term refers to interactions between the stationary phase and analyte (i.e., donor-acceptor and dispersion interactions, and compact layer dielectric effect). The free energies of adsorption of the supporting electrolyte ions are defined by $\Delta G_{\pm e\text{-}lyte}$, and the free energies of interaction between the analyte and the electrolyte ions at the surface and in the bulk solution are given by $\Delta G_{\pm N\text{-}N}$ and $\Delta G_{\pm int}$, respectively. There are other interactions neglected in Figure 1, including the effect of the possible presence of oxygen-containing groups[13-15] on the stationary phase surface and the influence of the mobile phase (e.g., analyte solubility),[16-21] ΔG_{sol}.

The majority of studies on the influence of the supporting electrolyte on EMLC-based retention has focused on charged solutes, mostly benzenesulfonates.[12, 22] The elution strength of monovalent supporting electrolytes was found to relate to the degree of specific adsorption of the electrolyte anion[23] on the stationary phase, signifying the importance of $\Delta G_{-e\text{-}lyte}$. In addition, an increase in $LiClO_4$ concentration in the mobile phase resulted in a decrease in the retention of negatively-charged analytes and an increase in the retention of positively-charged analytes when E_{app} is positive of the potential of zero charge (PZC). Both observations were tentatively attributed to the

decrease in the thickness of the diffuse region of the electrical double layer, resulting to a more effective shielding of the solutes in the bulk solution from the positively charged PGC surface. This shielding leads to a reduced level of electrostatic analyte-stationary phase interactions, which decreases the attraction of negatively-charged analytes to stationary phase and the repulsion of positively-charged solutes.

More recently, neutral analytes, in particular, benzene, alkylbenzenes and methylbenzenes, have been employed to probe the electrosorption mechanism operative in EMLC.[24] The main goal of these investigations, including the work presented herein, is to advance the EMLC mechanistic model by focusing on non-ionic solute-stationary phase interactions. The retention trends of charged analytes in EMLC depend mainly on ion-ion interactions with the stationary phase.[1-4, 12, 25] The non-ionic interactions have lower level of impact on the potential-influenced retention of charged analytes, thus their role in the EMLC process is less understood.

This paper is part of a series of studies focused on the EMLC behavior of these small, neutral analytes. Other mechanistic factors investigated are E_{app}, temperature and mobile phase composition.[24] The emphasis of the work herein is delineation of the role of the supporting electrolyte in the retention of these neutral analytes on PGC.

EXPERIMENTAL SECTION

The EMLC Column

The design and construction of the EMLC column has been detailed elsewhere.[2, 25] Briefly, Nafion tubing (Perma Pure, Toms River, NJ, USA) is inserted

into a porous stainless steel cylinder (Mott Metallurgical, Farmington, CT, USA). The column is slurry packed with PGC (Thermo Scientific, Waltham, MA, USA) which serves as a stationary phase and working electrode. The Ag/AgCl (saturated NaCl) reference electrode (Bioanalytical Systems, West Lafayette, IN, USA) is placed inside the external electrolyte reservoir that surrounds the stainless steel cylinder. All values of E_{app} are reported with respect to this reference electrode.

The experiments employed 5-μm diameter PGC particles as the packing material. PGC is devoid of detectable oxygen-containing surface groups as revealed by x-ray photoelectron spectroscopy (detection limit ~0.2 atomic %). Manufacturer specifies a nominal pore diameter of ~250 Å, and a porosity of ~80%. The surface area of PGC packed in the column is ca. 30 m^2, based on BET measurements (120 m^2/g) and amount of PGC loaded in the column (~0.25 g).

Instrumentation

Chromatographic experiments were performed using an Agilent 1200 Series module equipped with solvent cabinet, autosampler, quaternary pumping system, and UV/Vis diode array detector. The module was interfaced to Pentium IV 600 MHz computer with ChemStation software. The software is used to control the pump and injector parameters, set-up of sequences, and signal acquisition, and to process data. The potential of the electrode was controlled using potentiostat/galvanostat model 263A (EG&G Princeton Applied Research, Oak Ridge, TN, USA).

Chemicals and Reagents

The structures of the analytes and their designations used in this work are shown in Figure 2. Benzene (EMD, Gibbstown, NJ, USA), toluene (Sigma-Aldrich, St. Louis, MO, USA), ethylbenzene (Alfa Aesar, Ward Hill, MA, USA), *n*-propylbenzene (Alfa Aesar), *n*-butylbenzene (Alfa Aesar), 1,2-dimethylbenzene (Fluka, St. Louis, MO, USA), 1,3-dimethylbenzene (Alfa Aesar), 1,4-dimethylbenzene (Alfa Aesar), 1,3,5-trimethylbenzene (TCI America, Portland, OR, USA), 1,2,4-trimethylbenzene (Fluka), and 1,2,3-trimethylbenzene (TCI America) were used as received. Lithium perchlorate was purchased from Sigma-Aldrich. Water and acetonitrile were high purity solvents from EMD.

Mode of Operation

The mobile phase is a 40/60 *v/v* H_2O/ CH_3CN solution containing lithium perchlorate ($LiClO_4$) as the supporting electrolyte at varied concentrations. The mobile phase flow rate was 0.40 mL/min. The analytes were prepared at 0.100 mM concentration using CH_3CN as solvent which also served as the nonretained marker used to determine the dead time, t_0. Various mixtures of analytes were used, ensuring minimal overlapping of the component solute bands. The injection volume was 5.00 μL. The wavelength for detection is 214 nm. The chromatographic runs were performed in triplicates.

The $LiClO_4$ concentrations, [$LiClO_4$], used for this work are 0.04 to 0.20 M, in 0.04 M increments. The potentiostat was set at a constant E_{app}. The system was allowed

to reach a steady state between changes in C_{SE}. This procedure was repeated at potentials from +0.350 to -0.250 V, in 0.150 V increments.

Data Analysis

To compensate for peak tailing, retention times, t_r, were determined from the first statistical moment analysis of all chromatographic peaks. The first moment, M_1, represents the centroid of the peak, and is defined as:

$$M_1 = \frac{\int_{-\infty}^{\infty} t h(t) dt}{\int_{-\infty}^{\infty} h(t) dt} \qquad [1]$$

where h(t) is the height at time t. The retention factor, *k'*, is calculated according to the equation:

$$k' = (t_r - t_0)/t_0 . \qquad [2]$$

RESULTS AND DISCUSSION

Previous Work

Studies by Keller and co-workers[11] showed that the supporting electrolyte has a strong impact on the retention of a charged solute by influencing the structure of the double layer formed at the surface-solution interface when a potential is applied to the conductive stationary phase. A simplified depiction of the formation of the double layer in EMLC is shown in Figure 3. When E_{app} is positive of the PZC, the stationary phase acquires a positive excess charge, which increases the strength of interactions with anionic species (electrolyte anions and negatively-charged solutes) and electron donors.

In contrast, when E_{app} is negative of the PZC, the negative excess charge on the surface enhances the interactions with cationic species (electrolyte cations and positively-charged solutes) and electron acceptors. At the PZC, ions and molecules are retained on the stationary phase through specific interactions, with the presence of adsorbates forming on the compact portion of the electrical double layer (i.e., the diffuse layer is virtually absent).

Gouy-Chapman theory,[11] which predicts that k' is inversely dependent on $C_{SE}^{½}$ (where C_{SE} is the bulk concentration of supporting electrolyte), was used to model the electrostatic contributions of the supporting electrolyte in terms of competition with the solute for adsorption sites. Non-electrostatic effects were analyzed using models for ion-pairing chromatography[26] by Stahlberg[27] and Cantwell.[28] Stahlberg's model takes into account the specific adsorption of the solutes and competing counterions to the stationary phase, and anticipates a linear dependence of log k' vs. log C_{SE}. In Cantwell's model, counterions do not move into the compact layer, but undergo an ion-exchange process with the solute in the diffuse layer. Retention is thus due to the adsorption of solutes in the compact layer and to ion exchange between the solutes and counterions in the diffuse layer, with k' predicted to have a linear dependence on C_{SE}.

Effect of Supporting Electrolyte Concentration on the EMLC retention of Benzene, Alkylbenzenes and Di- and Tri- Methylbenzenes.

Chromatographic separations of mixtures of the 11 solutes were carried out at five values of E_{app} (-0.250 to +0.350 V in 0.150 V increments) for five different

concentrations of the supporting electrolyte $LiClO_4$ (0.04 to 0.20 M in 0.04 M increments) in a 40/60 (*v/v*) H_2O/CH_3CN mobile phase. Figure 4A shows the chromatograms obtained at +0.350 V with the mobile phase containing either 0.04, 0.12, or 0.20 M $LiClO_4$, while Figure 4B presents the results for the same three concentrations of $LiClO_4$ at -0.250 V. In all cases, including the data at the other values of E_{app} and C_{SE} not shown, the elution order remains unchanged. More interestingly, the retention of each analyte undergoes a small but readily observable increase with increasing $LiClO_4$ concentration.

The increase in retention is generally counter to the behavior exhibited by and reported on for ionic solutes.[12] Based on that work, one would predict for neutral solutes that an increase in supporting electrolyte concentration would: (1) have a small effect on electrostatics; and (2) decrease retention due to competition for adsorption sites. The present results correspond to a component of the EMLC retention mechanism not yet explored.

The listing of interactions and their impact on retention shown in Figure 1 can be used as a basis for the analysis of the retention data found for these neutral solutes. The presence of supporting electrolyte ions can decrease retention through competition with the solute for sorption sites (i.e., $\Delta G_{\pm e\text{-}lyte}$), and interactions with the solute in solution (i.e., $\Delta G_{\pm int}$). On the other hand, interactions of the analyte with surface-bound electrolyte ions (i.e. $\Delta G_{\pm N\text{-}N}$) can increase solute retention. Note that the presence or absence of a diffuse layer in the electrical double layer can be reasonably neglected because this set of solutes is neutral and not charged. Moreover, all of the interactions

key to the retention of neutral solutes are sufficiently short-ranged that only the processes in the compact layer of the electrical double layer are important.

Figure 5 summarizes how the $LiClO_4$ concentration, based on the value of E_{app} with respect to the PZC, can influence solute retention. The effects are listed in terms of inducing an increase or decrease or having little to no effect on retention. For example, the compaction of the electrical double layer with higher supporting electrolyte concentration has no effect on retention at the PZC, but may increase or decrease retention depending on the value of the E_{app} and on specific and non-specific solute-stationary phase interactions. Solute complexation with specifically adsorbed electrolyte ion is increased at higher C_{SE} at all E_{app} values since increasing the C_{SE} increases the level of specific adsorption. On the other hand, the change in the amount of non-specifically adsorbed electrolyte anion is exceedingly small (if at all), and will not have an impact on retention when E_{app} is at or negative of PZC.

Competition by an electrolyte anion with the solute for adsorption sites will decrease retention when E_{app} is positive of the PZC but will have little (if any) effect when E_{app} is equal to or more negative than the PZC. The counterargument applies to considerations of the contributions by the electrolyte cation.

The result in Figure 4 shows that retention increases with increased $LiClO_4$ concentration for all analytes at all values of E_{app}. A proposed mechanism consistent with the results is illustrated in Figure 6. This mechanism takes into account several pathways in the retention of an aromatic solute (A) and a supporting electrolyte anion (X^-). Initially, the mobile phase containing X^-_{MP} flows through the column, resulting in

an equilibrium with X^- adsorbed on the stationary phase, X^-_{SP}. When the solute A is introduced into the column, $A_{MP,}$ several processes may take place that involve the adsorption of A_{MP} directly onto PGC as A_{SP}, and the formation of AX^-_{MP} or AX^-_{SP}. If we separate the two pathways as independent processes, the overall retention factor, *k'*, can be written as Equation 3, where k'_{PGC} is the retention factor for A_{MP} sorbing as A_{SP} and k'_{X^-} is that for A_{MP} sorbing as AX^-_{SP}:

$$k' = k'_{PGC} + k'_{X^-} \qquad [3]$$

As shown in the Appendix, an analysis of the equilibria associated with AX-SP shows that a plot of *k'* is expected to be linearly dependent on the initial concentration of X^-, $[X^-]_i$ per Equation 4, where β collects all of the constant terms in the process.

$$k' = k'_{PGC} + \beta[X^-]_i \qquad [4]$$

Retention as a Function of C_{SE} and Sensitivity as a Function of E_{app}

Plots of *k'* vs. $[LiClO_4]$ at E_{app} of +0.350 V and -0.250 V are presented in Figure **7**A and 7B, respectively. In both cases, including other results not shown, the dependence of *k'* on $[LiClO_4]$ for all the analytes is reasonably linear, with R^2 values ranging from 0.92 to 1.00. These data confirm the predictive utility of Equation 4.

The data can be further analyzed by examining the sensitivity of solute retention to the supporting electrolyte concentration (i.e., the slope of the *k'* vs. $[LiClO_4]$ plots, which is defined as $\Delta k'/\Delta[LiClO_4]$). The sensitivities at different E_{app} values are summarized in Table 1, and plotted in Figure 8. At all values of E_{app}, the sensitivities of

more strongly retained solutes are generally greater than those of more weakly retained solutes, thus tracking the strength of solute-stationary phase interactions.

The sensitivity data reveal several intriguing trends. First, the sensitivities of the most strongly retained solutes (i.e., BB; 1,3,5; 1,2,4; and 1,2,3) are greater than that of the more weakly retained solutes (i.e., BZ; TO; EB; PB; 1,3; 1,4; and 1,2). Thus the sensitivity to changes in [ClO_4^-] is clearly correlated with the strength of interactions between the solute and stationary phase. Second, the shapes of the dependencies for these two groupings of solute are markedly different. The plots for the strongly retained solutes show a notable, monotonic increase as E_{app} moves to more negative values, whereas those for the more weakly retained solutes show a more subtle, but observable different, change. The profiles for the set of solutes eluting earlier undergo a small, sometimes barely observable decrease, followed by an increase. These differences are strong indicators of the varied importance of the various processes affecting retention that are overviewed in Figure 6.

To this point, we have considered mainly the impact of possible interactions between the solute and electrolyte anion as related to one of the two contributors to retention (i.e., k'_{X^-}). The dependencies in Figure 8 point to the importance of contributions from interactions directly between A_{MP} and the PGC packing to form A_{SP} (i.e., k'_{PGC}) and the competition of X^-_{SP} with A_{SP} for adsorption sites. As E_{app} moves to more negative values, the amount of X^-_{SP} decreases, which reduces the competition for the formation of A_{SP}. It then follows that the solutes that more strongly interact directly with PGC exhibit larger changes in retention upon changes in ClO_4^- concentration. We

can also conclude that the decrease in electrolyte sensitivity of such solutes as E_{app} becomes more positive reflects an increase in competition from X^-_{SP} which surpasses the contribution of an increase in AX^-_{SP}.

The general dependence for the more weakly retained solutes can be explained by the same set of constructs. In this case, however, the contribution to retention from the formation of AX^-_{SP} is more relatively significant because the adsorption strength of A_{SP} is much lower. The evolution then of the electrolyte sensitivity as E_{app} moves to more negative values suggests that the PZC for this set of experimental conditions is negative of ~0.050 V, and that the subtle increase in sensitivity at more negative values of E_{app} (in comparison to the more strongly retained solutes) reflects the weaker direct interaction with PGC.

Having established the high likelihood of interactions between these nonpolar aromatic solutes, the question then is, "what is the nature of these complexes?" Recent research has revealed that aromatic solutes can strongly interact with ions through cation-π[29-31] and anion-π interactions.[31-33] These quadrupole-ion interactions arise due to the polarizability of aromatic π-electrons.[34] While the formation of Li^+-benzene complex is unlikely because the cation is so strongly solvated,[30] an enhancement of retention may be brought about by the formation of a complex between ClO_4^- and the π-system of the aromatic ring. Thus, retention may become more favorable through the $\Delta G_{\pm N\text{-}N}$ component if it overcomes contributions to $\Delta G_{\pm int}$. If such a process occurs, it points not only to a new intriguing mechanism in EMLC, and more broadly to many other forms of

liquid chromatography, but also the possible use of EMLC as a tool to characterize such interactions.

CONCLUSIONS

In this work, the role of the supporting electrolyte on the retention of benzene, alkylbenzenes and methylbenzenes in EMLC was investigated. The linear relationship between k' and [ClO_4^-] supports a mechanism wherein adsorbed ClO_4^- facilitates retention of the solute through anion-π interactions. The trends in the sensitivity to changes in electrolyte concentration correlate with the strength of solute-stationary phase interactions (i.e., elution order), an implication of the competition of solute with ClO_4^- for adsorption sites on the PGC stationary phase.

ACKNOWLEDGMENTS

This work was supported by the U.S. Department of Energy - Ames Laboratory and the Utah Science and Technology Research Initiative. The Ames Laboratory is operated for the U.S. Department of Energy by Iowa State University under Contract No. DE-AC0207CH11358.

REFERENCES

(1) Porter, M. D.; Takano, H. In *Encyclopedia of Separation Science*; Wilson, I. D., Adlar, E. R., Cooke, M., Poole, C. F., Eds.; Academic Press: London, 2000.

(2) Harnisch, J. A.; Porter, M. D. *Analyst*, **2001**, *126*, 1841.

(3) Deinhammer, R. S.; Ting, E.-Y.; Porter, M. D. *J. Electroanal. Chem.* **1993**, *362*, 295.

(4) Deinhammer, R. S.; Ting, E.-Y.; Porter, M. D. *Anal. Chem.* **1995**, *67*, 237.

(5) Ting, E.-Y.; Porter, M. D. *J. Electroanal. Chem.* **1998**, *443*, 180.

(6) Ting, E.-Y.; Porter, M. D. *Anal. Chem.* **1997**, *69*, 675.

(7) Ting, E.-Y.; Porter, M. D. *J. Chromatogr. A*, **1998**, *793*, 204.

(8) Ponton, L. M.; Porter, M. D. *J. Chromatogr. A*, **2004**, *1059*, 103.

(9) Antrim, R. F.; Yacynych, A. M. *Anal. Lett.* **1988**, *21*, 1085.

(10) Bard, A. J.; Faulkner, L. R. *Electrochemical Methods: Fundamentals and Applications*; John Wiley & Sons, Inc.: New York, 2001.

(11) Bockris, J. O. M.; Reddy, A. K. N. *Modern Electrochemistry, an Introduction to an Interdisciplinary Areas*; Macdonald: London, 1970.

(12) Keller, D. W.; Ponton, L. M.; Porter, M. D. *J. Chromatogr. A*, **2005**, *1089*, 72.

(13) Shibukawa, M.; Unno, A.; Miura, T.; Nagoya, A.; Oguma, K. *Anal. Chem.* **2003**, *75*, 2775.

(14) Shibukawa, M.; Terashima, H.; Nakajima, H.; Saitoh, K. *Analyst*, **2004**, *129*, 623.

(15) Tornkvist, A.; Markides, K. E.; Nyholm, L. *Analyst*, **2003**, *128*, 844.

(16) Balcan, M.; Cserhati, T.; Forgacs, E. *Anal. Lett.* **1997**, *30*, 883.

(17) Coquart, V.; Hennion, M.-C. *J. Chromatogr.* **1992**, *600*, 195.

(18) Hennion, M.-C.; Coquart, V. *J. Chromatogr.* **1993**, *642*, 211.

(19) Tanaka, N.; Tanigawa, T.; Kimata, K.; Hosoya, K.; Araki, T. *J. Chromatogr.* **1991**, *549*, 29.

(20) Ross, P.; Knox, J. H. In *Advances in Chromatography*; Brown, P. R., Grushka, E., Eds.; Marcel Dekker, Inc.: New York, 1997; Vol. 37.

(21) Ross, P. *LC GC North America*, **2000**, *18*, 14.

(22) Keller, D. W.; Porter, M. D. *Anal. Chem.* **2005**, *77*, 7399.

(23) Elkafir, C.; Chaimbault, P.; Dreux, M. *J. Chromatogr. A*, **1998**, *829*, 193.

(24) Pimienta, G. F. M.; Porter, M. D. *in preparation*.

(25) Ting, E.-Y.; Porter, M. D. *Anal. Chem.* **1998**, *70*, 94.

(26) Stahlberg, J. *J. Chromatogr. A*, **1999**, *855*, 3.

(27) Stahlberg, J. *Anal. Chem.* **1994**, *66*, 440.

(28) Cantwell, F. F.; Puon, S. *Anal. Chem.* **1979**, *51*, 623.

(29) Feller, D.; Dixon, D. A.; Nicholas, J. B. *J. Phys. Chem. A*, **2000**, *104*, 11414.

(30) Ma, J. C.; Dougherty, D. A. *Chem. Rev.* **1997**, *97*, 1303.

(31) Garau, C.; Frontera, A.; Quinonero, D.; Ballester, P.; Costa, A.; Deya, P. M. *J. Phys. Chem. A*, **2004**, *108*, 9423.

(32) Kim, D.; Tarakeshwar, P.; Kim, K. S. *J. Phys. Chem. A*, **2004**, *108*, 1250.

(33) Quinonero, D.; Garau, C.; Frontera, A.; Ballester, P.; Costa, A.; Deya, P. M. *Chem. Phys. Lett.* **2002**, *359*, 486.

(34) Clements, A.; Lewis, M. *J. Phys. Chem. A*, **2006**, *110*, 12705.

(35) Yang, X.; Dai, J.; Carr, P. W. *J. Chromatogr. A*, **2003**, *996*, 13.

FIGURES AND TABLE

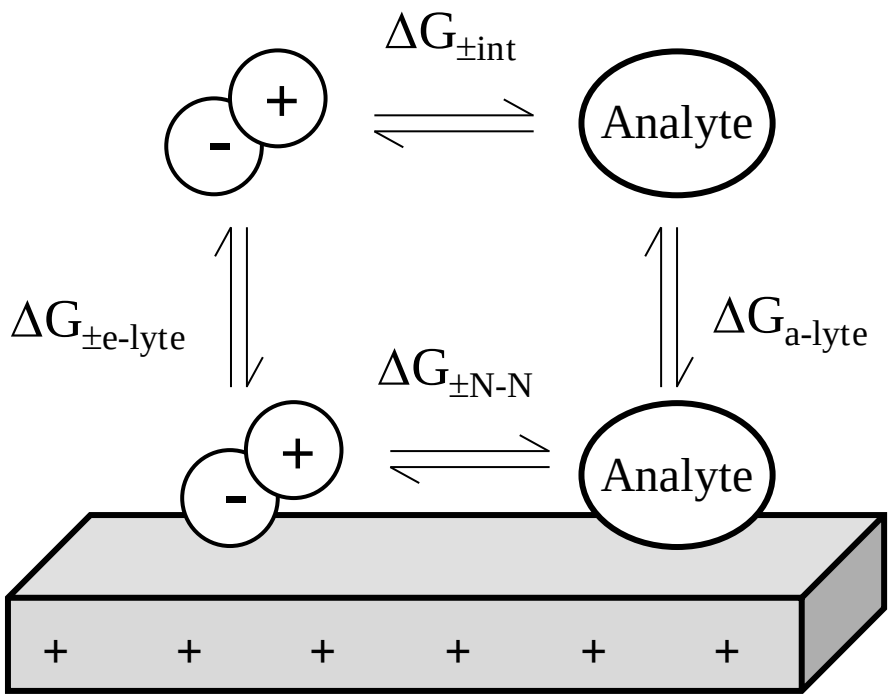

$$\Delta G_{tot} = \Delta G_{a\text{-}lyte} + \Delta G_{\pm N\text{-}N} - \Delta G_{\pm e\text{-}lyte} - \Delta G_{\pm int} + \Delta G_{sol}$$

Figure 1. Scheme for thermodynamic interactions in EMLC showing how the supporting electrolyte influences retention.[12]

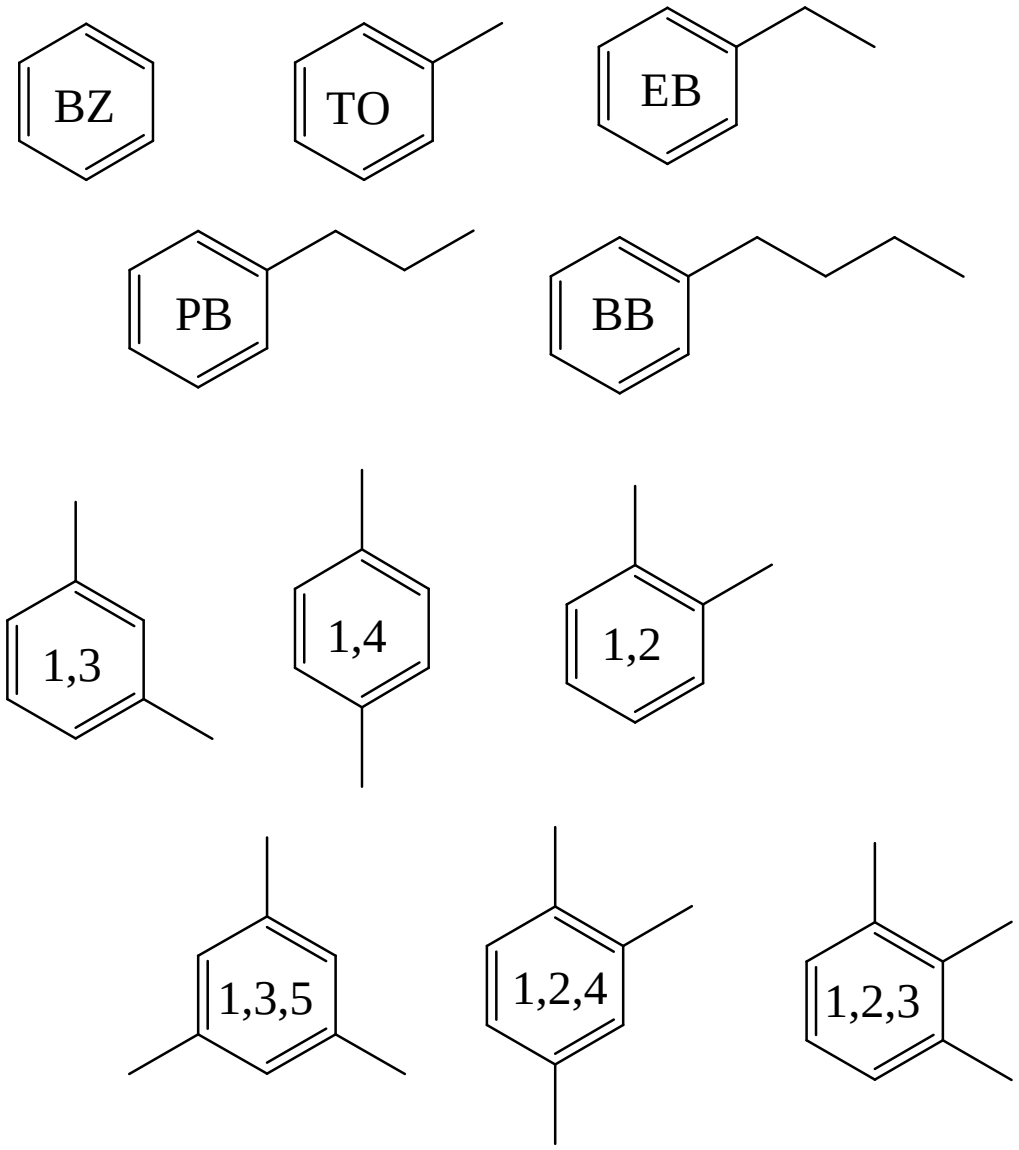

Figure 2. Structures and designations for the analytes used in this work: (BZ) benzene; (TO) toluene; (EB) ethylbenzene; (PB) propylbenzene; (BB) butylbenzene; (1,3), (1,4), and (1,2) dimethylbenzenes; and (1,3,5), (1,2,4), and (1,2,3) trimethylbenzenes.

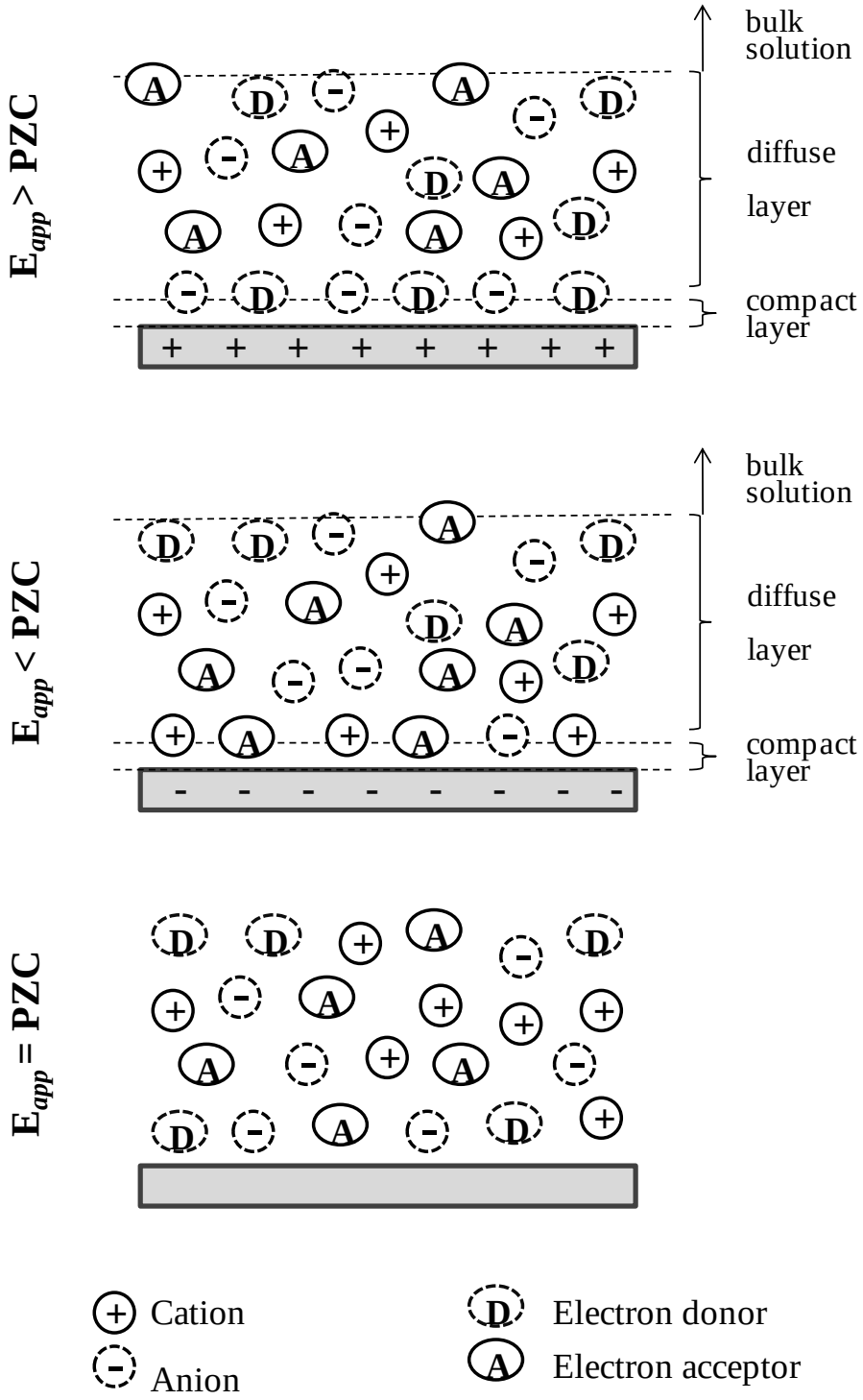

Figure 3. Simplified illustration of the electrode-solution interface in EMLC.

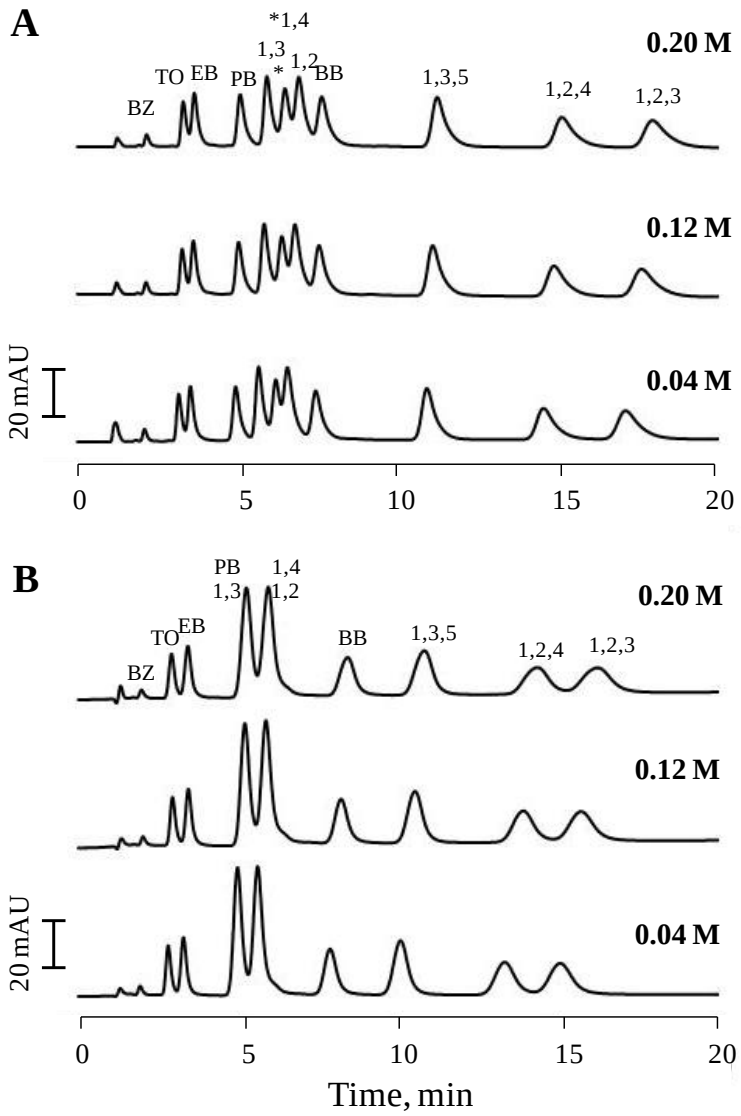

Figure 4. Chromatograms of the analyte mixture at varied supporting electrolyte ($LiClO_4$) concentrations at E_{app} of (A) +0.350 V and (B) -0.250 V vs. Ag/AgCl sat'd NaCl. The mobile phase was 40/60 mixture of H_2O/CH_3CN, flowing at 0.40 mL/min. The analytes were prepared in 0.100 mM concentration in CH_3CN. The injection volume was 5.00 μL.

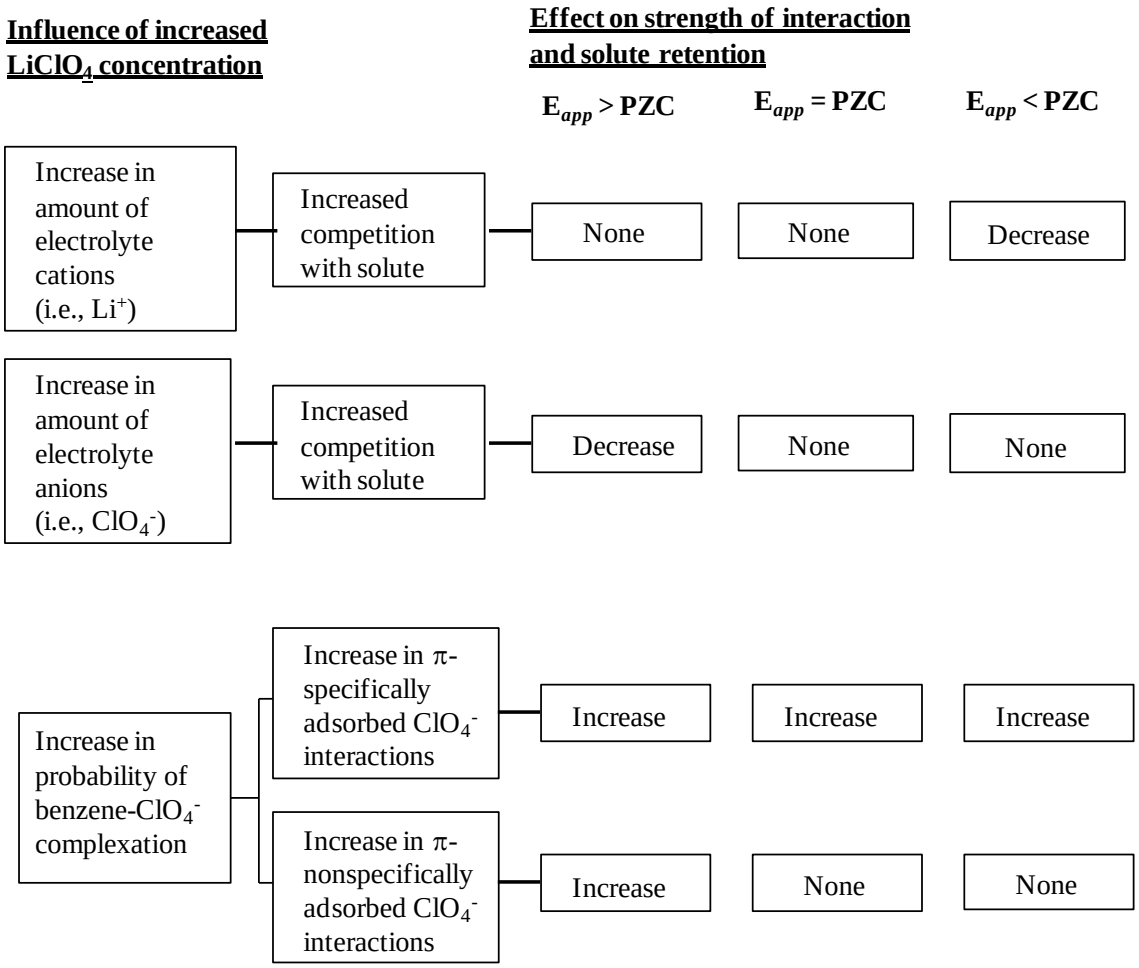

Figure 5. Summary of how [$LiClO_4$] affects the EMLC retention of alkylbenzenes and methylbenzenes on PGC.

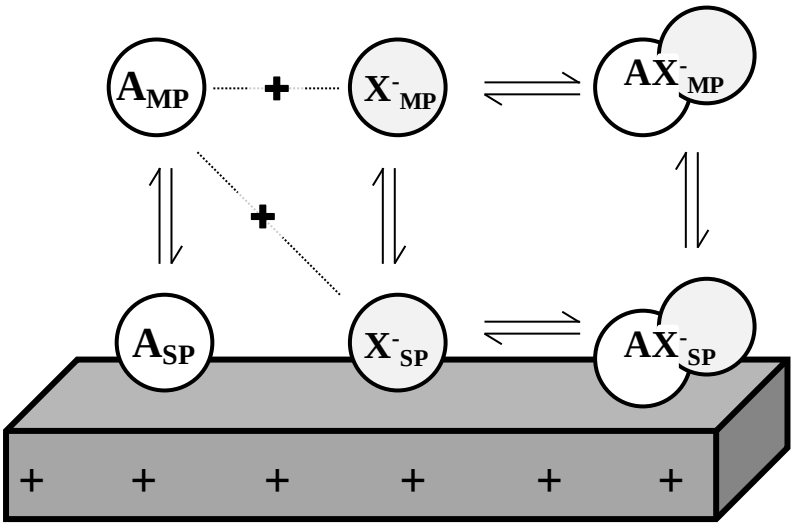

Figure 6. The retention of A_{MP} as A_{SP} and AX^-_{SP}. Legend: A = analyte; X^- = electrolyte anion; AX^- = anion-π complex; M = mobile phase; S = stationary phase.

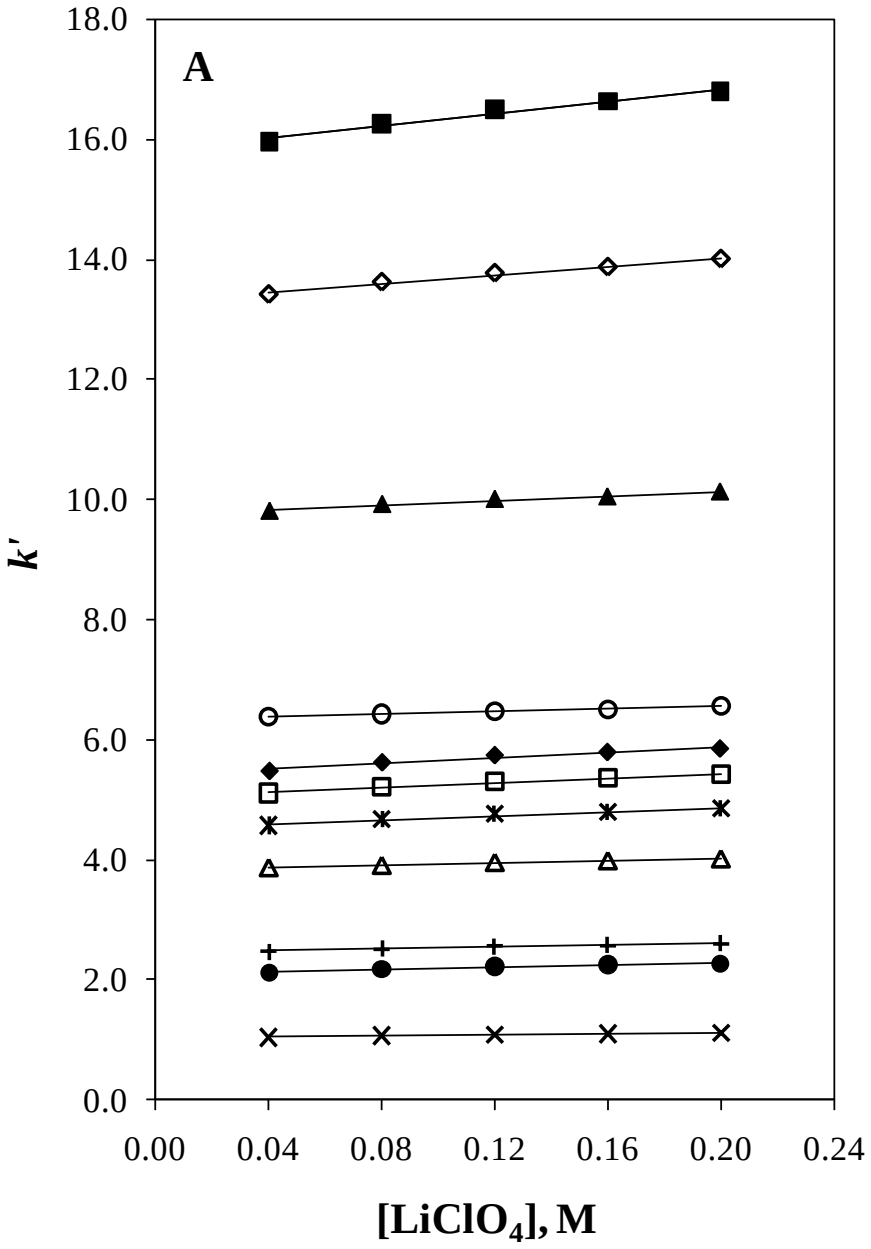

Figure 7A. Dependence of *k'* on $LiClO_4$ concentration at E_{app} of +0.350 V vs. Ag/AgCl sat'd NaCl. Legend: BZ (✖); TO (●); EB (✚); PB (△); 1,3 (✱); 1,4 (□); 1,2 (◆); BB (○); 1,3,5 (▲); 1,2,4 (◇); and 1,2,3 (■). N=3, error bars are roughly the size of the marker.

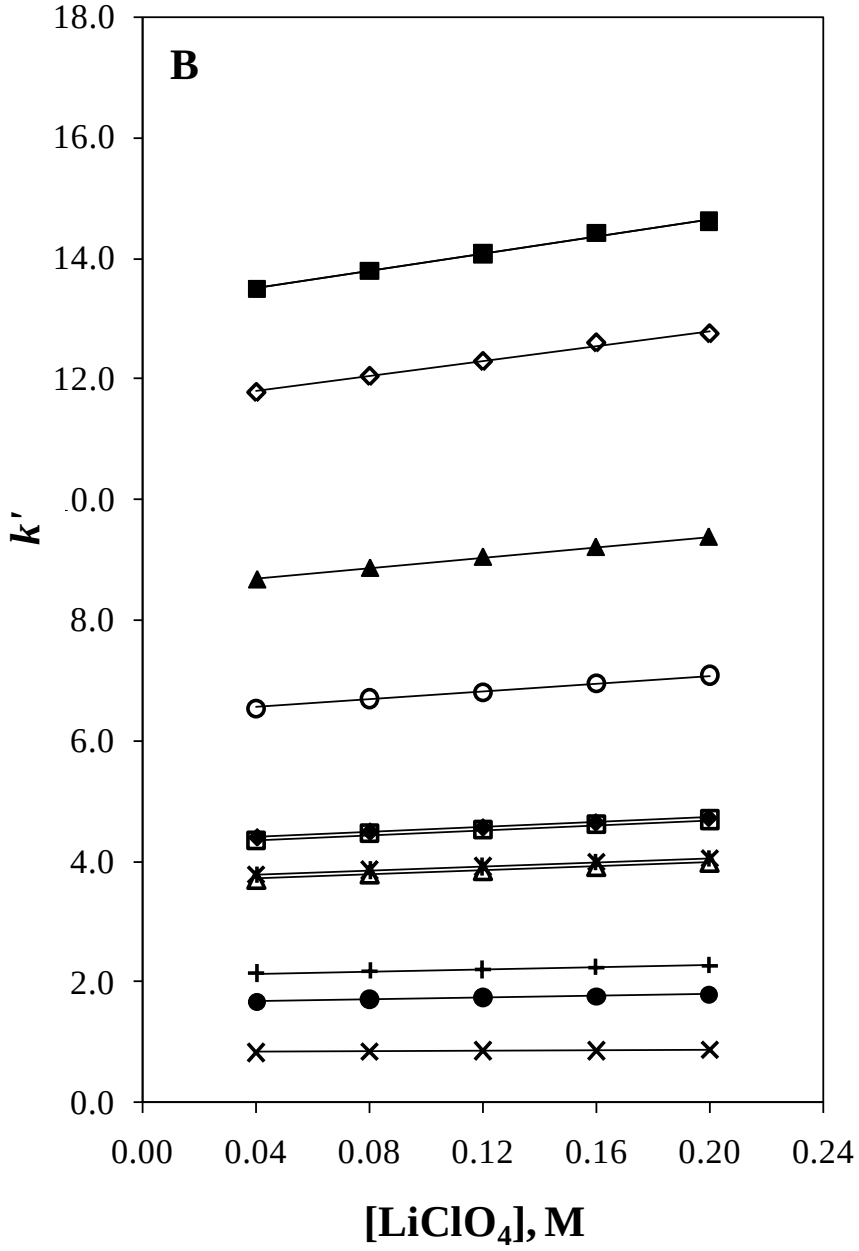

Figure 7B. Dependence of *k′* on $LiClO_4$ concentration at E_{app} of -0.250 V vs. Ag/AgCl sat'd NaCl. Legend: BZ (✖); TO (●); EB (✚); PB (△); 1,3 (✱); 1,4 (□); 1,2 (◆); BB (○); 1,3,5 (▲); 1,2,4 (◇); and 1,2,3 (■). N=3, error bars are roughly the size of the marker.

Table 1. Sensitivity of k' to changes in $[LiClO_4]$.

Analyte	Elution Order	E_{app} (V vs. Ag/AgCl sat'd NaCl)				
		+0.350	**+0.200**	**+0.050**	**-0.100**	**-0.250**
		Sensitivity, $\Delta k'/\Delta[LiClO_4]$ (M^{-1})				
BZ	1	0.47	0.31	0.15	0.35	0.24
TO	2	0.96	0.81	0.61	0.72	0.70
EB	3	0.82	0.70	0.54	0.95	0.84
PB	4	0.95	1.04	1.38	1.24	1.68
1,3	5	1.69	1.68	1.32	1.55	1.67
1,4	6	1.89	1.94	1.77	1.74	2.08
1,2	7	2.26	2.22	1.62	1.97	1.99
BB	8	1.12	1.61	2.68	3.04	3.35
1,3,5	9	1.94	2.89	3.77	4.42	4.40
1,2,4	10	3.59	4.42	5.66	5.49	6.15
1,2,3	11	5.14	5.94	6.91	6.89	7.12

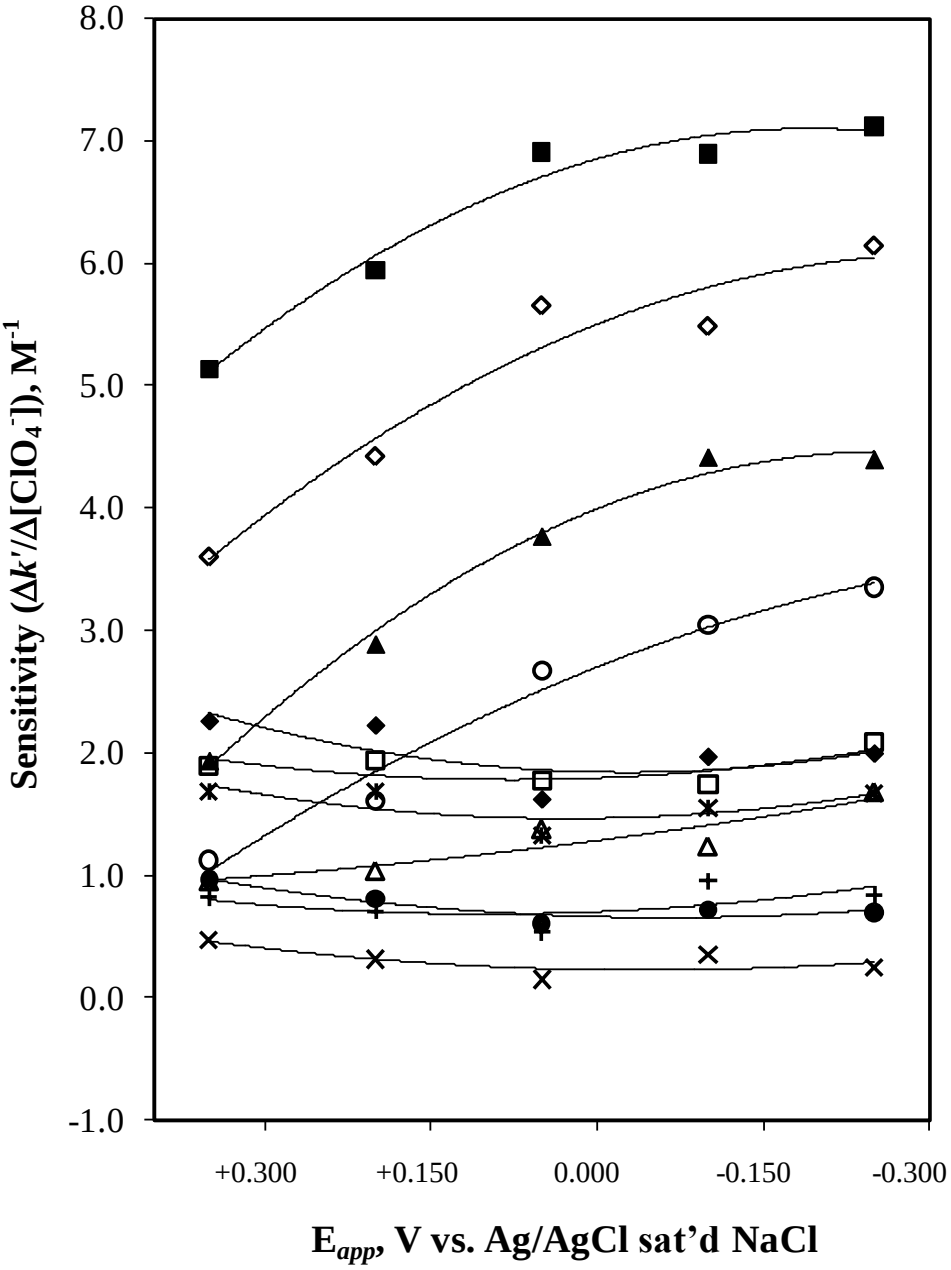

Figure 8. Sensitivity (slope of the plot of k' vs. [$LiClO_4$]) vs. E_{app}. Legend: BZ (✖); TO (●); EB (✚); PB (△); 1,3 (✱); 1,4 (□); 1,2 (◆); BB (○); 1,3,5 (▲); 1,2,4 (◇); and 1,2,3(■). The lines connecting the data points serve only as a guide to the eye.

APPENDIX A: Two-Site Model of Retention

As a basis for modeling the observed effect of ClO_4^- on the retention of the nonpolar, aromatic solutes in Figure 2, a two-site model of mixed mode retention (i.e., electrosorption) is developed that draws, in part, on earlier efforts to gain insights into mechanistic processes in ion-exchange chromatography.[35] As outlined in Figure 6 and further elaborated in Figure A-1, retention can be viewed as occurring at two different, mechanistically independent adsorption sites on the PGC surface. At one site, the solute in the mobile phase, A_{MP}, adsorbs directly onto the surface of PGC as A_{SP} via donor-acceptor and other specific interactions with the packing.

Adsorption at the other site occurs due to the presence of the electrolyte anion (e.g., ClO_4^-) and can follow two different pathways that are thermodynamically indistinguishable. The first path involves the binding of A_{MP} with the electrolyte anion in the mobile phase, X^-_{MP}, to form the soluble complex AX^-_{MP}, with AX^-_{MP} then adsorbing directly onto the PGC surface as AX^-_{SP}. These two steps, along with the corresponding equilibrium expressions, are given by Equations A-1 through A-4:

$$A_{MP} + X^-_{MP} \rightleftharpoons AX^-_{MP} \qquad \text{[A-1]}$$

$$K_1 = \frac{[AX^-]_{MP}}{[A]_{MP}[X^-]_{MP}} \qquad \text{[A-2]}$$

$$AX^-_{MP} \rightleftharpoons AX^-_{MP} \qquad \text{[A-3]}$$

$$K_2 = \frac{[AX^-]_{SP}}{[AX^-]_{MP}} \qquad \text{[A-4]}$$

The second parallel path arises from the complexation of A_{MP} directly with an electrolyte anion that is already adsorbed on the stationary phase, X^-_{SP}. This pathway is summarized by Equations A-5 through A-8:

$$X^-_{MP} \rightleftharpoons X^-_{SP} \qquad \text{[A-5]} \qquad K_3 = \frac{[X^-]_{SP}}{[X^-]_{MP}} \qquad \text{[A-6]}$$

$$A_{MP} + X^-_{SP} \rightleftharpoons AX^-_{SP} \qquad \text{[A-7]} \qquad K_4 = \frac{[AX^-]_{SP}}{[A]_{MP}[X^-]_{MP}} \qquad \text{[A-8]}$$

As expected, $K_1K_2 = K_3K_4$, which corresponds to the overall equilibrium summarized by Equations A-9 and A-10:

$$A_{MP} + X^-_{MP} \rightleftharpoons AX^-_{MP} \qquad \text{[A-9]} \qquad K_t = \frac{[AX^-]_{SP}}{[A]_{MP}[X^-]_{MP}} \qquad \text{[A-10]}$$

where $K_t = K_1K_2 = K_3K_4$.

Since we are considering an independent, two-site model for the observed retention factor, *k'*, can be written as:

$$k' = k'_{PGC} + k'_{X^-} \qquad \text{[A-11]}$$

with k'_{PGC} representing the retention of A_{MP} as A_{SP}, and k'_{X^-} signifying the retention of A_{MP} as AX^-_{SP}.

With respect to k'_{X^-}, it can be further defined by considering the path given, for example, by Equations A-5 and A-7 as:

$$k'_{X^-} = \varphi \frac{[AX^-]_{SP}}{[A]_{MP}} \qquad \text{[A-12]}$$

In Equation A-12, φ is the phrase ratio for the chromatographic system and is defined as:

$$\varphi = \frac{V_{SP}}{V_{MP}} \qquad \text{[A-13]}$$

where V_{SP} and V_{MP} are the respective volumes of the stationary and mobile phases.

Upon combining Equation A-10 with Equation A-12, an expression relating k'_{X^-} to $[X^-]_{MP}$ can be given as:

$$k'_{X^-} = \varphi K_3 K_4 [X^-]_{MP} \qquad \text{[A-14]}$$

Next, $[X^-]_{MP}$ can be formulated in terms of the initial concentration of X^- added to the mobile phase, $[X^-]_i$ by recognizing

$$[X^-]_i = [X^-]_{MP} + [X^-]_{SP} \qquad \text{[A-15]}$$

Equation A-15 can then be used with Equation A-6 to yield

$$[X^-]_{MP} = \frac{[X^-]_i}{K_3 + 1} \qquad \text{[A-16]}$$

Substitution of Equation 16 into Equation 14 produces

$$k'_{X^-} = \frac{\varphi K_3 K_4 [X^-]_i}{K_3 + 1} \qquad \text{[A-17]}$$

Finally, by collecting all of the constants in Equation A-17 as β, we can write:

$$k'_{X^-} = \beta [X^-]_i \qquad \text{[A-18]}$$

which agrees with Equation 4 in the main body of the paper.

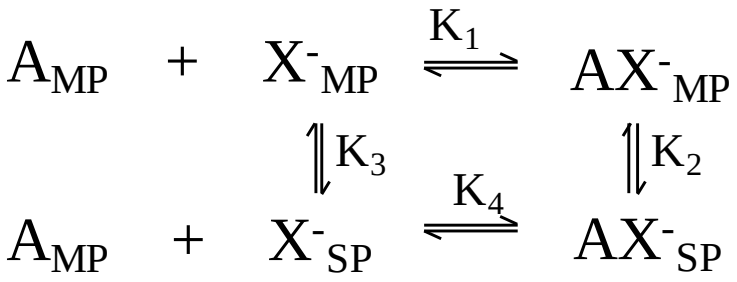

Figure A-1. Representation of the equilibria for retention involving interaction of the solute A with the electrolyte anion X^-.

APPENDIX B: Baseline Studies Using Flowthrough Experiments

Experiment. A 0.010 M aqueous solution of sodium fluoride (NaF) was allowed to flow through the LC line at 0.4 mL/min. The baseline level was studied as a function of E_{app}, at potentials from -0.300 V to +0.300 V, vs. Ag/AgCl sat'd NaCl reference electrode, in 0.075-V increments. The wavelength of detection was 214 nm. The signals were recorded when the baseline level had stabilized for at least 10 min. The experiments were done in triplicate.

Results and Discussion. Sodium fluoride was used in the flowthrough study designed to determine the potential of zero charge (PZC) of the packing. One of the results of these experiments is shown in Figure B-1, as a plot of steady-state baseline signal vs. E_{app} using an aqueous solution of 0.010 M NaF as the mobile phase. The use of this electrolyte in aqueous solutions probes only nonspecific interactions (i.e., electrostatics) with the electrified surface due to the high hydration energy of the small electrolyte anion and cation. As can be seen, the signal decreases as E_{app} moves from -0.300 V to more positive values, reaching rapidly a minimum at -0.075 V, and then undergoes a small increase.

This dependence can be explained from classical descriptions of the electrical double layer. As E_{app} moves negative of the PZC, the electrode/stationary phase has an increasing excess negative charge and thus attracts greater levels of hydrated Na^+ ions

from the mobile phase. While not yet having a clear picture of the origin of the response, we believe that this change in signal is correlated with uptaken/released Na^+ by PGC.

The contrary trend occurs at values increasingly positive of the PZC, which imparts an increasing excess positive charge on the packing surface. In this case, the highly hydrated F^- ions are electrostatically attracted to the surface, resulting in an increase in baseline signal.

These two portions of the baseline signal vs. E_{app} represent two processes. One is for E_{app} > PZC, where the slope is positive and the other is for E_{app} < PZC, where the slope is negative. In Figure B-1, a linear fit to the data has a slope of 4.67 mAU/V (R^2 = 0.99) from +0.150 to +0.300 V. A linear fit through the data from -0.300 to 0.000 V has a slope of -55.5 mAU/V (R^2 = 0.98).

Since the PZC corresponds to zero interfacial excess of nonspecifically adsorbed anions and cations, it follows that the minimum in baseline signal corresponds to the PZC. For the results shown in Figure B-1, the two lines intersect at an E_{app} of +0.010 V. With all three experimental trials taken into consideration, the PZC for this system is determined to be +0.003 ± 0.005 V, which is generally consistent with reports in the literature.

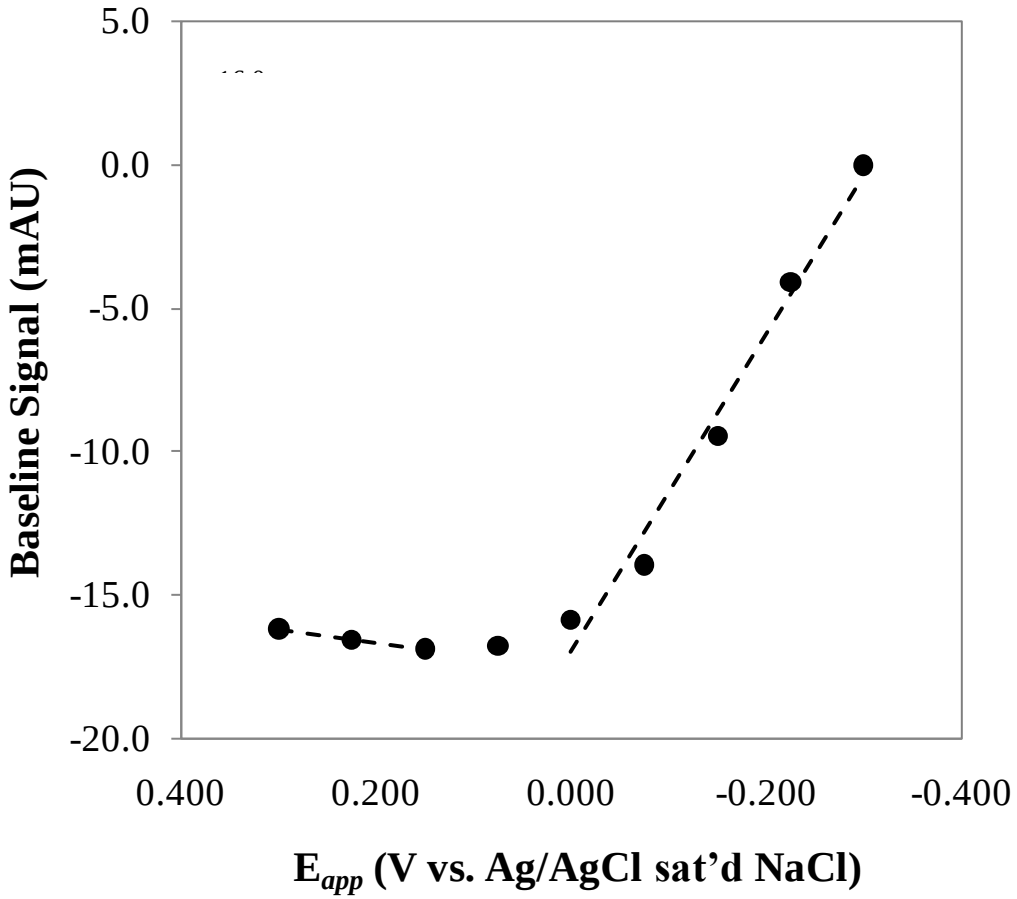

Figure B-1. Baseline level as a function of E_{app} on the EMLC column. An aqueous solution of 0.010 M NaF was allowed to flow through at a rate of 0.4 mL/min. Inset is the zoomed in view of the data points from +0.150 to +0.300 V.

CHAPTER 4. THE ROLE OF THE MOBILE PHASE IN ELECTROCHEMICALLY MODULATED LIQUID CHROMATOGRAPHY

A paper to be submitted to the *Journal of Electroanalytical Chemistry*

Gloria Fe M. Pimienta[a,b] and Marc D. Porter[b,*]

[a]Department of Chemistry, Iowa State University

[b]Departments of Chemistry, Chemical Engineering, and Bioengineering, University of Utah, Salt Lake City, UT 84108

ABSTRACT

The influence of the mobile phase on the retention of benzene and a series of alkylbenzenes and di- and tri- methylbenzenes is investigated using electrochemically modulated liquid chromatography (EMLC) is reported. In EMLC, retention is manipulated through changes in the potential applied to a conductive stationary phase (E_{app}) like porous graphitic carbon (PGC) by using a mixed solvent (e.g., H_2O/CH_3CN) and supporting electrolyte as the mobile phase. This paper examines the role of the mobile phase with respect to its impact on EMLC-based retention. Retention of the analytes is examined as a function of the mobile phase composition. Results show that the relationship is consistent with the Linear Solvent Strength (LSS) model. For all

---

*Corresponding author:

email: marc.porter@utah.edu

phone: 801-587-1505

solute-E_{app} combinations studied, the plot of the logarithm of the retention factor (ln k') vs. fraction (v/v) of CH_3CN in a H_2O/CH_3CN mobile phase (φ) are found to be linear, as in reversed phase liquid chromatography. The slope ($\Delta \ln k'/\Delta\varphi$), which is the sensitivity of retention to changes in the acetonitrile content of the mobile phase, is found to increase with increasing solute hydrophobicity (i.e., increasing alkyl chain length or increasing number of methyl substituents). The y-intercept, log k_w, reflects the strength of hydrophobic interactions between the solute and the stationary phase.

INTRODUCTION

Electrochemically modulated liquid chromatography (EMLC) is a unique separation technique that hybridizes HPLC with electrochemistry.[1, 2] Retention is manipulated through changes in the potential applied (E_{app}) to a conductive stationary phase like porous graphitic carbon (PGC). The column also serves as an electrochemical cell, with the packing material serving a dual purpose: it acts both as a stationary phase and a working electrode. Changes in E_{app} alter the effective surface composition of the stationary phase, and thus its retention properties. The utility of EMLC has been demonstrated for the separation of a wide range of analytes, such as aromatic sulfonates,[3, 4] monosubstituted benzenes,[5] corticosteroids,[6] benzodiazepines,[7] and inorganic anions.[8]

Retention on carbonaceous materials involves a complex mixing of several interactions - donor-acceptor, dispersion, and solvophobic - between the analyte and the stationary phase surface. Indeed, the retention mechanism in EMLC embodies many of

the simultaneous processes that occur in reversed-phase LC (e.g., interactions of the solutes, the mobile phase and any added modifiers, and the alkyl chain packing), but adds pathways due to changes in E_{app} and the presence of the supporting electrolyte. Recent works in our group focused on the mechanism of EMLC by examining how E_{app} influences the strength of these interactions. Studies using aromatic sulfonates as solutes show the key role electrostatic interactions play in the manipulation of retention via E_{app}.[9-11]

Research efforts in our group have focused on advancing the understanding of the retention mechanism of EMLC. The goal of the work presented herein is to investigate the role of the mobile phase in EMLC, by examining the effect of organic modifier concentration on retention at several values of E_{app}. The adsorption[12] and partition[13] mechanisms were used by Nikitas and co-workers,[14, 15] as platforms for modeling the effect of the organic modifier on retention. In the partition model, solute molecules distribute between the stationary and mobile phases, whereas in the adsorption model, solute and modifier molecules co-adsorb on the stationary phase. Gaudin and co-workers[16] investigated several organic solvents and binary mixtures as mobile phase using a PGC column. The eluotropic strength of the mobile phase was found to roughly follow the polarity of the solvent. Other noted factors include geometry and polarizability of the solvent molecules.[17]

In this work, the retention of neutral analytes - benzene, and several alkylbenzenes, and di- and tri- methylbenzenes - is studied at differing compositions of a mixed H_2O-CH_3CN mobile phase, with the PGC packing material poised at various

values of E_{app}. By using the Linear Solvent Strength (LSS) model[18, 19] from reversed phase liquid chromatography, the possible roles of the organic modifier are examined and then incorporated into the existing picture of an EMLC-based retention mechanism.

EXPERIMENTAL SECTION

The EMLC Column

The design and construction of the EMLC column has been detailed elsewhere.[2, 20] Briefly, Nafion tubing (Perma Pure, Toms River, NJ, USA) is inserted into a porous stainless steel cylinder (Mott Metallurgical, Farmington, CT, USA). The column is slurry packed with PGC (Thermo Scientific, Waltham, MA, USA) which serves as a stationary phase and working electrode. The Ag/AgCl (saturated NaCl) reference electrode (Bioanalytical Systems, West Lafayette, IN, USA) is placed inside the external electrolyte reservoir that surrounds the stainless steel cylinder. All values of E_{app} are reported with respect to this reference electrode.

The experiments employed 5-μm diameter PGC particles as the packing material. PGC is devoid of detectable oxygen-containing surface groups as revealed by x-ray photoelectron spectroscopy (detection limit ~0.2 atomic %). The manufacturer specifies a nominal pore diameter of ~250 Å, and a porosity of ~80%. The surface area of PGC packed in the column is ca. 30 m^2, based on BET measurements (120 m^2/g)[9] and amount of PGC loaded in the column (~0.25 g).

Instrumentation

Chromatographic experiments were performed using an Agilent 1200 Series module equipped with solvent cabinet, autosampler, quaternary pumping system, and UV/Vis diode array detector. The module was interfaced to a Pentium IV 600 MHz computer with ChemStation software. The software is used for the control of pump and injector parameters, set-up of sequences, and signal acquisition and data processing. The potential of the electrode was controlled using potentiostat/galvanostat model 263A (EG&G Princeton Applied Research, Oak Ridge, TN, USA).

Chemicals and Reagents

The analytes benzene (EMD, Gibbstown, NJ, USA), toluene (Sigma-Aldrich, St. Louis, MO, USA), ethylbenzene (Alfa Aesar, Ward Hill, MA, USA), *n*-propylbenzene (Alfa Aesar), *n*-butylbenzene (Alfa Aesar), 1,2-dimethylbenzene (Fluka, St. Louis, MO, USA), 1,3-dimethylbenzene (Alfa Aesar), 1,4-dimethylbenzene (Alfa Aesar), 1,3,5-trimethylbenzene (TCI America, Portland, OR, USA), 1,2,4-trimethylbenzene (Fluka), and 1,2,3-trimethylbenzene (TCI America) were used as received. Lithium perchlorate was purchased from Sigma-Aldrich. Water and acetonitrile were high purity solvents from EMD.

Mode of Operation

The mobile phase is a H_2O/ CH_3CN solution containing 0.10 M lithium perchlorate ($LiClO_4$) as the supporting electrolyte. The mobile phase flow rate was 0.40 mL/min.

The analytes were prepared at 0.100 mM concentration using acetonitrile as solvent which also served as the nonretained marker used for the determination of the dead time, t_0. Various mixtures of analytes were used, ensuring minimal overlapping of the component solute bands. The injection volume was 5.00 μL. The wavelength for detection is 214 nm. The separations were done in triplicate.

The mobile phase composition investigated ranged from 25/75 to 45/55 H_2O/CH_3CN, increasing the H_2O content by 5% and decreasing the CH_3CN content by 5%, with each set of runs. According to Cunningham and co-workers,[21] the dielectric constant, ε, of this mixed solvent decreases as the amount of CH_3CN increases [45/55 (*v/v*) H_2O/CH_3CN: 55.7; 40/60: 53.5; 35/65: 51.4; 30/70: 49.2; and 25/75: 47.0; all at 25 °C].

The potentiostat was set at a constant E_{app}. Again, the system was allowed to reach a steady state between changes in experimental conditions. This procedure was repeated at potentials from +0.350 to -0.250 V, in 0.100 V increments.

Data Analysis

To compensate for peak tailing, retention times, t_r, were determined from the first statistical moment analysis of all chromatographic peaks. The first moment, M_1, represents the centroid of the peak, and is defined as:

$$M_1 = \frac{\int_{-\infty}^{\infty} th(t)dt}{\int_{-\infty}^{\infty} h(t)dt}$$

where h(t) is the height at time t. The experimentally-determined retention factor, *k'*, is calculated according to the equation:

$$k' = (t_r - t_0)/t_0$$

The data from experiments that varied the mobile phase composition was analyzed based on the LSS model,[18, 19] which is given by the relationship:

$$\log k' = \log k_w - S\varphi$$

where φ is the volume fraction of the of the organic modifier, CH_3CN, in the mobile phase, k_w is the retention factor extrapolated to 100% water as mobile phase ($\varphi = 0$), and *S* is a constant for a given analyte and a given reversed phase LC system. *S* denotes the sensitivity of solute retention to changes in φ. Thus, log *k´* is plotted vs. φ, with the slope equal to *S* and the *y*-intercept equal to log k_w.

RESULTS AND DISCUSSION

The structures of the analytes, their designations, and log D_{ow} values[22] are shown in Figure 1. Abbreviations are used for benzene, toluene, and the rest of the alkylbenzenes. The positions of the methyl groups on the benzene ring are used for the di- and trimethylbenzenes. D_{ow} is defined as the quotient of the equilibrium concentration of a solute in the octanol-rich phase to that in the water-rich phase, thus log D_{ow} measures the hydrophobicity of the substance and can be related to solvophobic interactions. Five mobile phase compositions, ranging from 25/75 to 45/55 (*v/v*) H_2O/CH_3CN, were used in this work. Analyses were carried out at seven E_{app} values, ranging from -0.250 to +0.300V.

A few representative chromatograms are presented in Figure 2. At all the mobile phase composition studied, trends such as the order of elution and the shapes of ln *k'* vs. E_{app} plots are consistent with the findings of our earlier investigation of this set of 11 analytes.[23]

As shown in Figure 2, an increase in the CH_3CN content of the mobile phase decreases the retention time for all 11 analytes. At +0.350 V, for example, the most retained analyte, 1,2,3, elutes in 25, 14 and 8 min with 55, 65 and 75% (*v/v*) CH_3CN, respectively. The same analyte elutes at -0.250 V in 22, 12 and 7 min for the same respective mobile phase compositions.

This trend follows expectations for chromatographic retention based on solvophobicity considerations. The solubility of these solutes in the mobile phase increases with increasing CH_3CN content, resulting in enhanced solute affinity for the mobile phase. Moreover, increasing the CH_3CN concentration in the mobile phase increases the amount of organic modifier sorbed on the packing surface, and thus more competition by CH_3CN for adsorption sites with the solutes. Both organic modifier effects lead to decreased solute retention.

The data can be presented in more detail as plots of log *k'* vs. φ, based on the LSS model.[18, 19] This type of plot is presented in Figure 3A and B at +0.350 V and -0.250 V, respectively. The plots are linear for all solute-E_{app} combinations studied, with $R^2 \geq 0.99$. The *y*-intercept of the plot, log k_w, is a measure of solute hydrophobicity, much like the octanol-water partition coefficient, log D_{ow}. If D_{ow} is the octanol-water distribution coefficient, then k_w can be viewed as the PGC-water coefficient, which is then a measure

of the partitioning of the solute between PGC and water. The slope of the plot, *S*, is the sensitivity of solute retention to changes in the CH_3CN content of the mobile phase, and can be viewed as the integration of solubility effects in the mobile phase and at the mobile-stationary phase interface. Table 1 presents the *S* and log k_w values obtained from the retention data from each solute and each value of E_{app}.

An inspection of the data reveals three interesting points. First, the *S*-values of the three dimethylbenzenes are only marginally different. Second, the same can be concluded for the three trimethylbenzenes. Third, the log k_w- and *S*-values for the alkylbenzenes exhibit a dependence on the number of carbons in the alkyl chain. Moreover, and as expected, log k_w tracks with the hydrophobic nature of the solutes, and thus the log D_{ow} values in Figure 1.

To examine these trends further, plots for log k_w vs. the number of substituent carbons (i.e., the number of carbons on the alkyl chain for alkylbenzenes, the number of methyl groups for methylbenzenes, and zero for benzene) at +0.350 and -0.250 V are presented in Figure 4. Figure 5 shows a similar analysis of the *S* data. Since the log k_w values for isomeric methylbenzenes are similar, the results for methylbenzenes that are isomers are nearly indistinguishable, the data for 1,3 and 1,3,5 are used for di- and tri-methylbenzenes, respectively. Both sets of plots follow similar trends. That is, the values of log k_w increase as the number of methyl groups increases for the methylbenzenes, and as the length of the alkyl chain increases for the alkylbenzene series. The dependencies in moving from BZ to 1,2,3 are linear at +0.350 and -0.250 V, and have indistinguishable least-squares linear fitting equations. A careful comparison

also shows that the trends for the alkylbenzenes are nearly the same at the two different values of E_{app}; note that the observed departure from linearity is consistent with earlier liquid chromatographic studies using a PGC stationary phase.[24]

Figure 5 shows how *S* changes with the number of substituents carbons at +0.350 and -0.250 V vs. Ag/AgCl sat'd NaCl. Again, only 1,3 and 1,3,5 are used for di- and tri-methylbenzenes, respectively. The data for other values of E_{app} were also plotted and showed similar results. All plots are linear with $R^2 \geq 0.99$. The *S*-values are in the order: BZ < TO < EB < 1,3 < PB < 1,3,5 < BB, and, like the log k_w plots in Figure 4, are in accordance with increasing number of carbons. In contrast to log k_w, the position of the additional carbon substituent, regardless of whether it was added onto the alkyl chain or substituted onto the benzene ring, causes similar increases in sensitivity. Furthermore, the values of *S* are independent of E_{app}, as judged by the slope of the two plots. Not surprisingly, this set of data indicates that the hydrophobicity of the solute plays an important role in the sensitivity of retention to changes in mobile phase composition: the more hydrophobic the solute, the greater the impact of moving to a more hydrophobic mobile phase.

To investigate the effect of changing the mobile phase composition in EMLC, the values of log k_w and *S* were plotted against E_{app}, and the results are shown in Figure 6 and 7, respectively. All *y*-axis ranges are +0.400 to -0.300 V vs. Ag/AgCl sat'd NaCl. The *x*-axes in Figure 6 span 0.2 log k_w units, whereas that in Figure 7 span 1.1 *S* units. The absolute ranges of the plots are shown in Table 2.

The plots in Figure 6 are very similar to those we reported in an earlier EMLC study of these same analytes.[23] That study, however, did not take into account the role of CH_3CN in the mobile phase which is taken into consideration by a LSS analysis for the determination of log k_w. Thus, the apparent dependence of the trends in the degree of curvature found in plots of ln k' vs. E_{app} in that work, while correlating with solute hydrophobicity (i.e., log D_{ow} values), were shown to be defined primarily of the potential-dependent competition from supporting electrolyte anions and cations with the solute for adsorption sites on the PGC surface. The similarity of the plots in Figure 6 with those in our earlier work indicate that the possible contribution from the organic modifier (e.g., competition for adsorption sites and/or changes in the dielectric strength of the electrical double layer) can be reasonably assigned a minor role, further supporting our earlier interpretation.

Examination of Figure 7 shows the same trends apparent in Figure 6, but are more blurred by the scatter in the data. There is, however, one interesting point to examine, albeit highly speculative, in view of the scatter. From -0.250 to +0.150 V, the *S*-values for the more strongly retained compounds show small fluctuations with respect to E_{app}. From +0.150 to +0.350 V, the *S*-values for BZ and TO are too variable to define a trend. On the other hand, for the same potential range, the S-values for EB, the dimethylbenzenes, PB, the trimethylbenzenes and BB clearly decrease. These trends are consistent with a mechanism involving competition of the solutes with CH_3CN for adsorption sites on the stationary phase surface, especially when considering the high molar concentration of CH_3CN in comparison to all the other components in the system.

We note that more exacting studies are needed before such speculation can be substantiated.

CONCLUSIONS

In this work, the effect of mobile phase composition on the retention of alkylbenzenes and methylbenzenes on PGC stationary phase at varied E_{app} was investigated. The role of the CH_3CN organic modifier fits both the partition model where the organic modifier is a means to change the solubility of the solute in the mobile phase, and the adsorption model where the organic modifier and solute compete for adsorption sites on the stationary phase. The increase in the sensitivity of retention of the solute to changes in CH_3CN content with increasing number of carbons across both the alkylbenzene and methylbenzene series is attributed to changes in the strength of hydrophobic interactions that modulate the distribution of the solute between the stationary and mobile phases. The similarity in the potential-dependence of log k_w and ln k' implies that the organic modifier only plays a minor role in EMLC-based manipulation of retention of the solutes on PGC.

ACKNOWLEDGMENTS

This work was supported by the U.S. Department of Energy - Ames Laboratory and the Utah Science and Technology Research Initiative. The Ames Laboratory is operated for the U.S. Department of Energy by Iowa State University under Contract No. DE-AC0207CH11358.

REFERENCES

(1) Porter, M. D.; Takano, H. In *Encyclopedia of Separation Science*; Wilson, I. D., Adlar, E. R., Cooke, M., Poole, C. F., Eds.; Academic Press: London, 2000.

(2) Harnisch, J. A.; Porter, M. D. *Analyst* **2001**, *126*, 1841.

(3) Deinhammer, R. S.; Ting, E.-Y.; Porter, M. D. *J. Electroanal. Chem.* **1993**, *362*, 295.

(4) Deinhammer, R. S.; Ting, E.-Y.; Porter, M. D. *Anal. Chem.* **1995**, *67*, 237.

(5) Ting, E.-Y.; Porter, M. D. *J. Electroanal. Chem.* **1998**, *443*, 180.

(6) Ting, E.-Y.; Porter, M. D. *Anal. Chem.* **1997**, *69*, 675.

(7) Ting, E.-Y.; Porter, M. D. *J. Chromatogr. A*, **1998**, *793*, 204.

(8) Ponton, L. M.; Porter, M. D. *J. Chromatogr. A*, **2004**, *1059*, 103.

(9) Keller, D. W., Iowa State University, Ames, 2005.

(10) Keller, D. W.; Ponton, L. M.; Porter, M. D. *J. Chromatogr. A*, **2005**, *1089*, 72.

(11) Keller, D. W.; Porter, M. D. *Anal. Chem.* **2005**, *77*, 7399.

(12) Snyder, L. R. *Principles of Adsorption Chromatography*; Marcel Dekker Inc.: New York, 1968.

(13) Dill, K. A. *J. Phys. Chem.* **1987**, *91*, 1980.

(14) Nikitas, P.; Pappa-Louisi, A.; Agrafiotou, P. *J. Chromatogr. A*, **2002**, *946*, 9.

(15) Nikitas, P.; Pappa-Louisi, A.; Agrafiotou, P. *J. Chromatogr. A*, **2002**, *946*, 33.

(16) Gaudin, K.; Chaminade, P.; Baillet, A. *J. Chromatogr. A*, **2002**, *973*, 61.

(17) Jandera, P. *Chromatographia*, **1984**, *19*, 101.

(18) Snyder, L. R.; Dolan, J. W. *Adv. Chromatogr.* **1998**, *38*, 115.

(19) Baczek, T.; Markuszewski, M.; Kaliszan, R.; van Straten, M. A.; Claessens, H. A. *J. High Resol. Chromatogr.* **2000**, *23*, 667.

(20) Ting, E.-Y.; Porter, M. D. *Anal. Chem.* **1998**, *70*, 94.

(21) Cunningham, G. P.; Vidulich, G. A.; Kay, R. L. *J. Chem. Eng. Data*, **1967**, *12*, 336.

(22) *CRC Handbook of Chemistry and Physics*, 89 ed.; CRC Press: Boca Raton, 2009.

(23) Pimienta, G. F. M.; Porter, M. D. *in preparation*.

(24) Kriz, J.; Adamcova, E.; Knox, J. H.; Hora, J. *J. Chromatogr. A*, **1994**, *663*, 151.

FIGURES AND TABLES

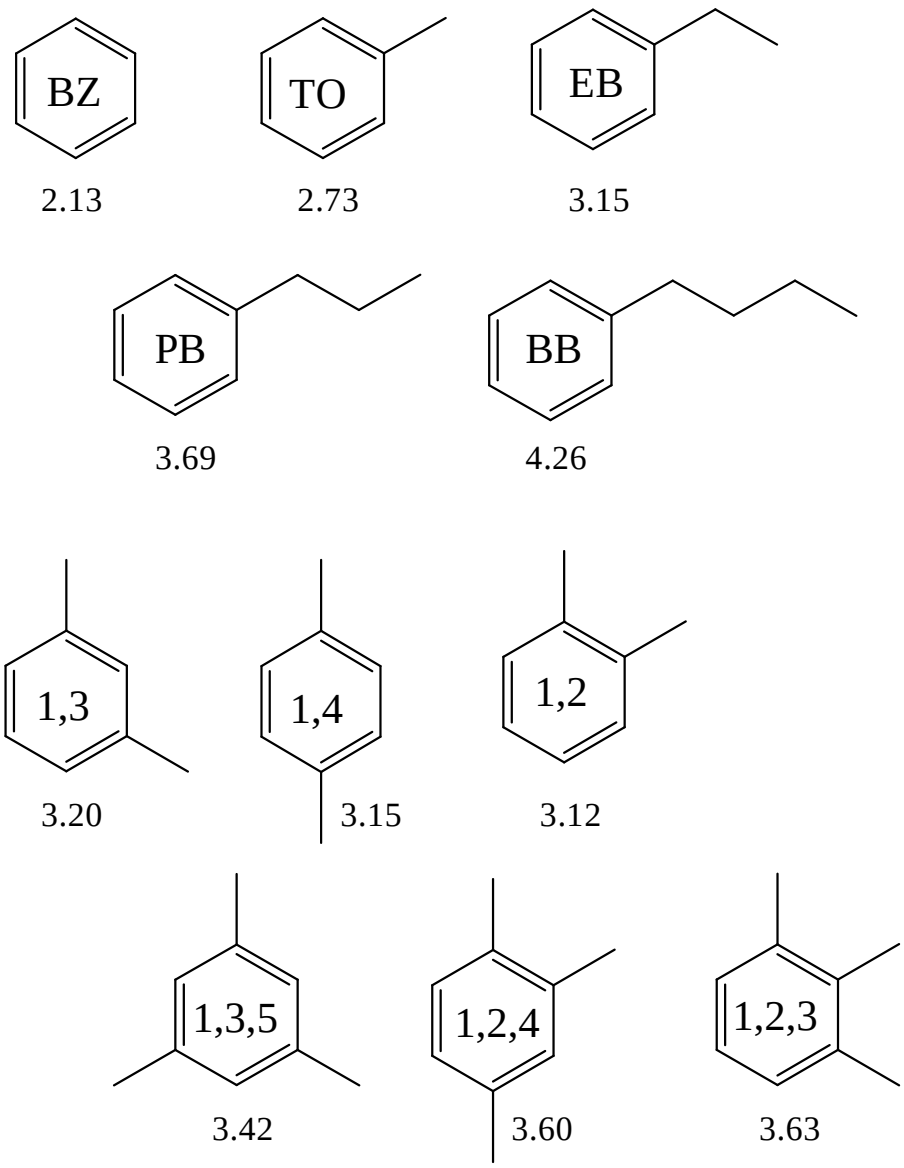

Figure 1. Structures and designations for the solutes used in this work: (BZ) benzene; (TO) toluene; (EB) ethylbenzene; (PB) propylbenzene; (BB) butylbenzene; (1,3), (1,4), and (1,2) dimethylbenzenes; and (1,3,5), (1,2,4), and (1,2,3) trimethylbenzenes. Values of the log D_{ow} are listed below each solute.

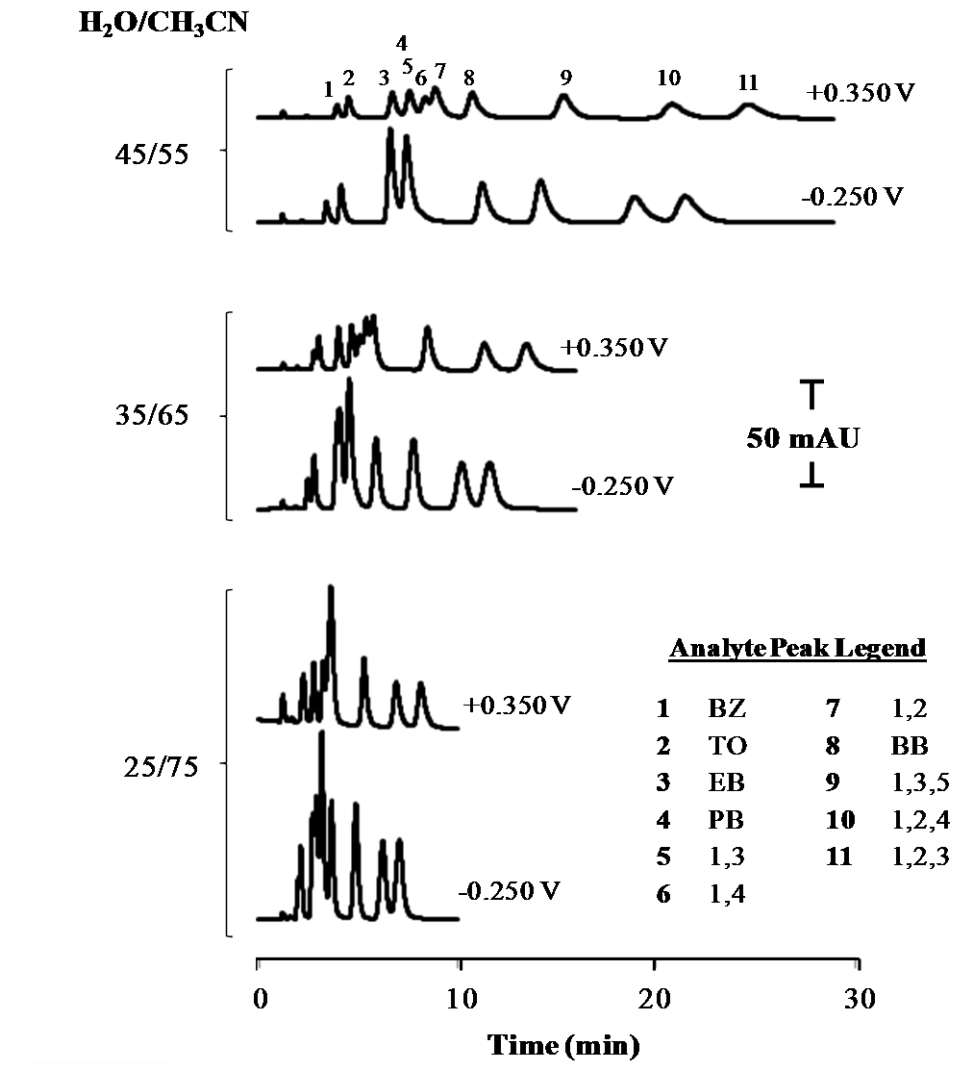

Figure 2. Chromatograms illustrating the effect of mobile phase composition on the retention of alkylbenzenes and methylbenzenes. The data shown are for two values of E_{app} (+0.350 and -0.250 V vs. Ag/AgCl sat'd NaCl), and three different H_2O/CH_3CN (*v/v*) compositions (45/55, 35/65, and 25/75). The mobile phase compositions each contained 0.100 M $LiClO_4$ as supporting electrolyte. The flow rate was 0.40 mL/min. The analytes were prepared in 0.10 mM concentration in CH_3CN. The injection volume was 5.00 μL. The wavelength of detection was 214 nm.

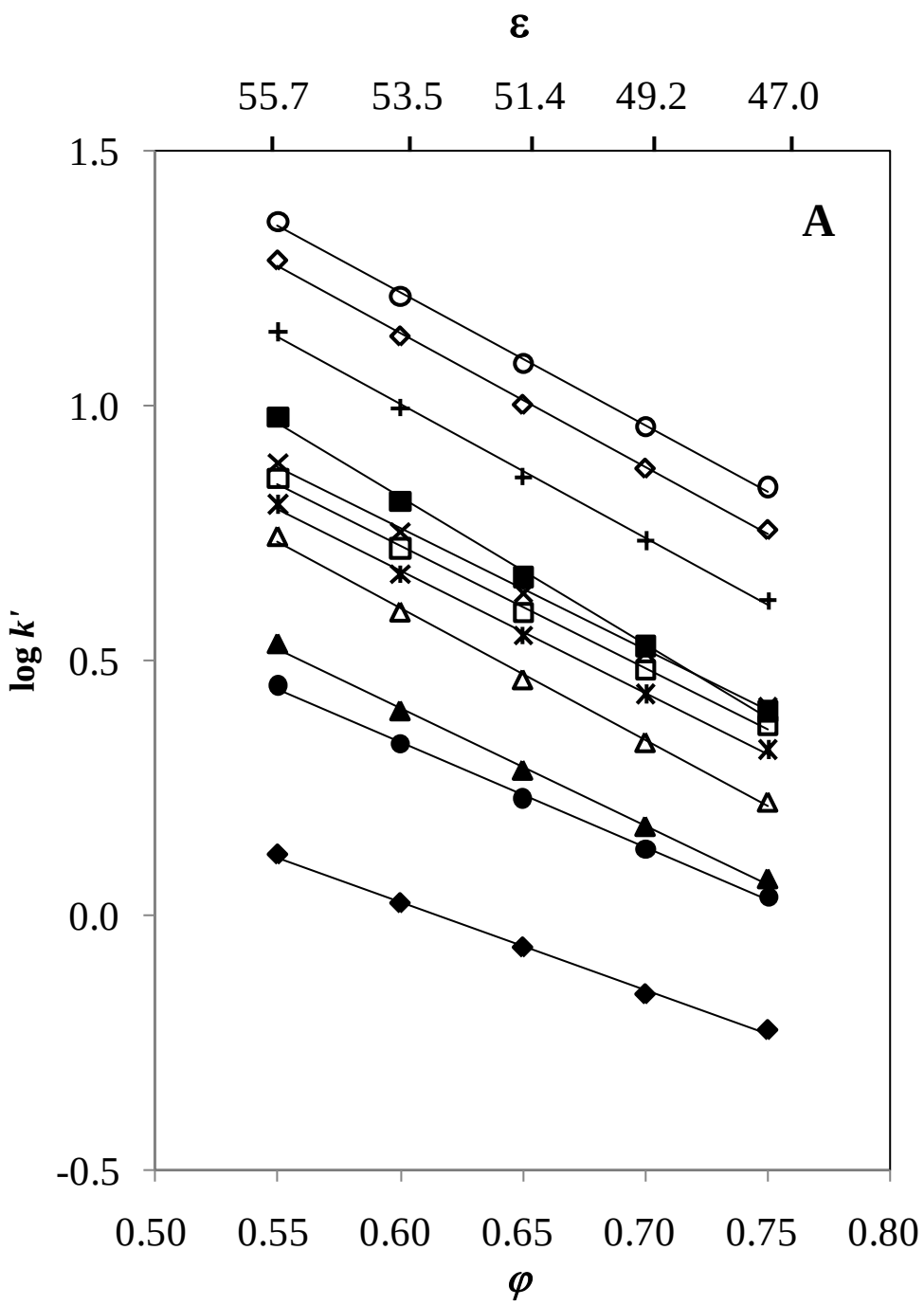

Figure 3A. Plots of log *k′* vs. φ at E_{app} of +0.350 V vs. Ag/AgCl sat'd NaCl. Legend: BZ (◆), TO (●), EB(▲), PB (△), 1,3 (✱), 1,4 (□), 1,2 (✖), BB (■), 1,3,5 (✚), 1,2,4 (◇), and 1,2,3 (○). N = 3, the error bars are about the size of the marker.

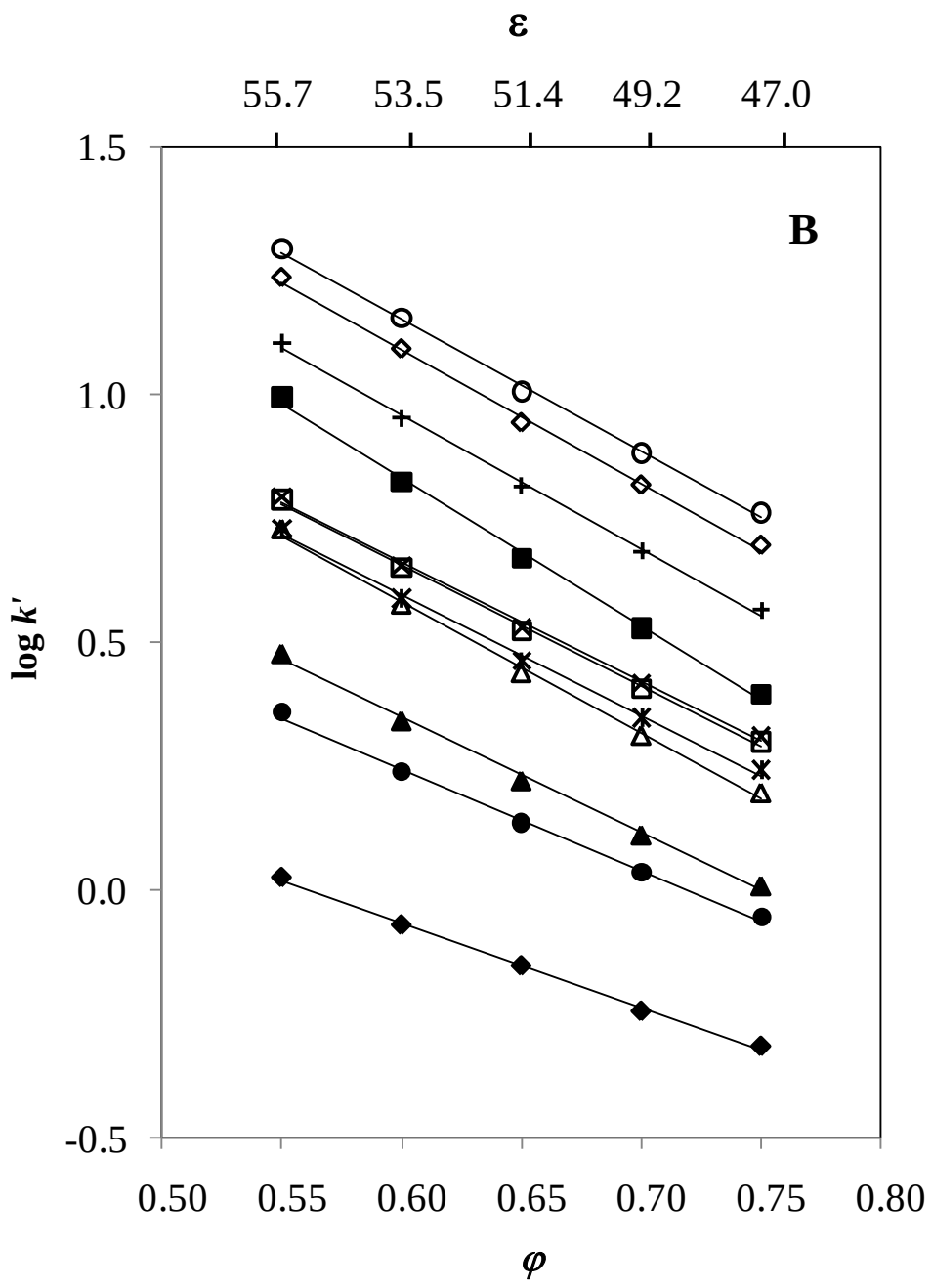

Figure 3B. Plots of log *k'* vs. φ at E_{app} of -0.250 V vs. Ag/AgCl sat'd NaCl. Legend: BZ (◆), TO (●), EB(▲), PB (△), 1,3 (✱), 1,4 (□), 1,2 (✖), BB (■), 1,3,5 (✚), 1,2,4 (◇), and 1,2,3 (○). N = 3, the error bars are about the size of the marker.

Table 1. The *y*-intercepts (log k_w) and the slopes (*S*) of the plots of log *k'* vs. φ.

Analytes	+0.350 V		+0.250 V		+0.150 V		+0.050 V		-0.050 V		-0.150 V		-0.250 V	
	log k_w	S	log k_w	S	log k_w	S	log k_w	S	log k_w	S	log k_w	S	log k_w	S
BZ	1.07	17.3	1.06	17.3	1.02	17.0	1.01	17.1	0.97	16.8	0.95	16.7	0.95	17.0
TO	1.58	20.7	1.57	20.7	1.57	20.9	1.55	20.9	1.51	20.5	1.50	20.6	1.48	20.5
EB	1.79	23.1	1.80	23.3	1.81	23.5	1.80	23.5	1.77	23.2	1.77	23.4	1.75	23.3
PB	2.16	26.0	2.18	26.2	2.22	26.8	2.22	26.7	2.20	26.6	2.19	26.5	2.17	26.5
BB	2.55	28.8	2.59	29.3	2.63	29.7	2.64	29.8	2.62	29.6	2.62	29.7	2.62	29.8
1,3	2.11	24.0	2.12	24.2	2.13	24.5	2.11	24.4	2.08	24.2	2.06	24.2	2.05	24.3
1,4	2.18	24.2	2.19	24.4	2.20	24.7	2.19	24.7	2.16	24.5	2.15	24.6	2.12	24.4
1,2	2.19	23.9	2.19	24.0	2.20	24.3	2.18	24.3	2.15	24.2	2.14	24.2	2.11	24.1
1,3,5	2.58	26.4	2.61	26.7	2.63	27.0	2.62	27.0	2.59	26.8	2.61	27.2	2.57	26.9
1,2,4	2.72	26.4	2.75	26.7	2.77	27.1	2.76	27.0	2.73	26.9	2.74	27.2	2.72	27.1
1,2,3	2.78	26.0	2.80	26.3	2.82	26.7	2.80	26.6	2.77	26.5	2.78	26.8	2.76	26.8

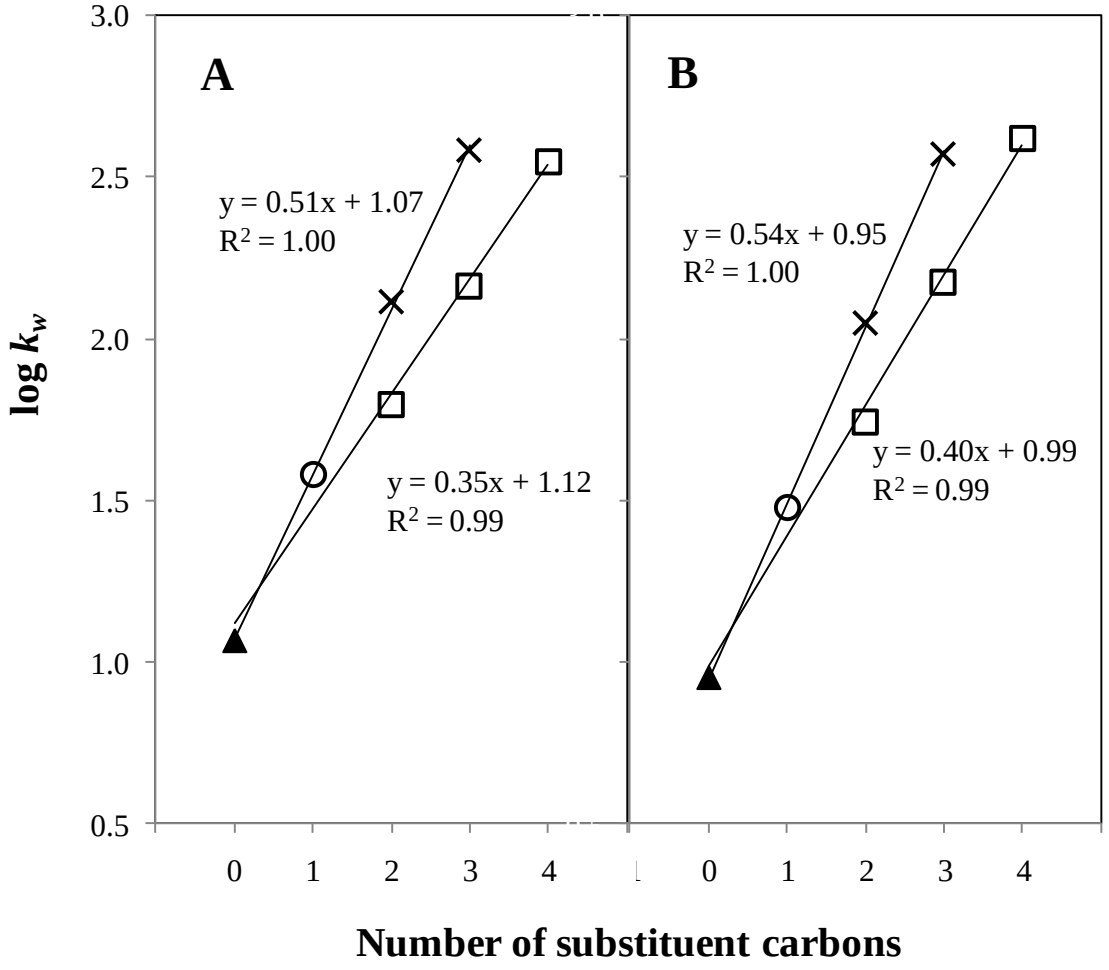

Figure 4. Plots of log k_w vs. number of substituent carbons at E_{app} of (A) +0.350 V and (B) -0.250 V vs. Ag/AgCl sat'd NaCl. Legend: BZ (▲); TO (○); rest of alkylbenzenes (□); di- and tri- methylbenzenes (×).

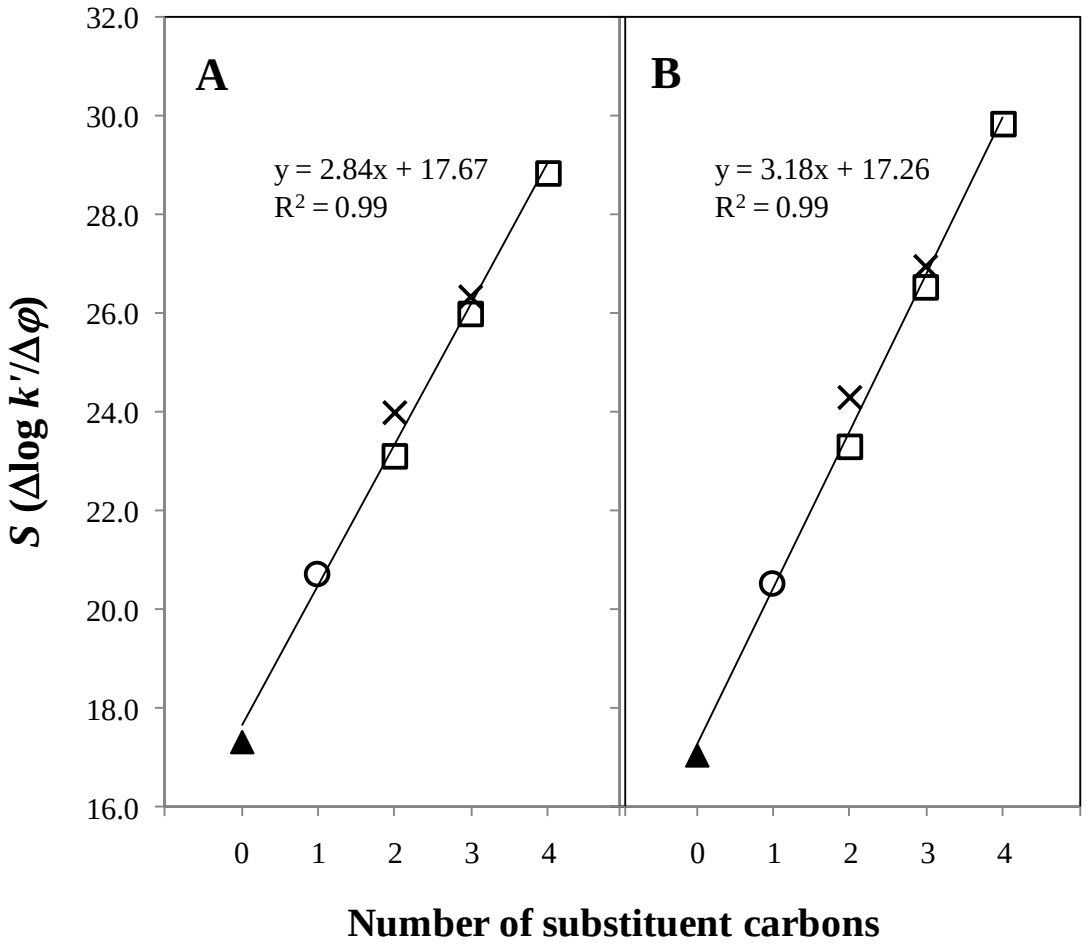

Figure 5. Plots of *S* vs. number of substituent carbons at E_{app} of (A) +0.350 V and (B) -0.250 V vs. Ag/AgCl sat'd NaCl. Legend: BZ (▲); TO (○); rest of alkylbenzenes (□); di- and tri- methylbenzenes (×).

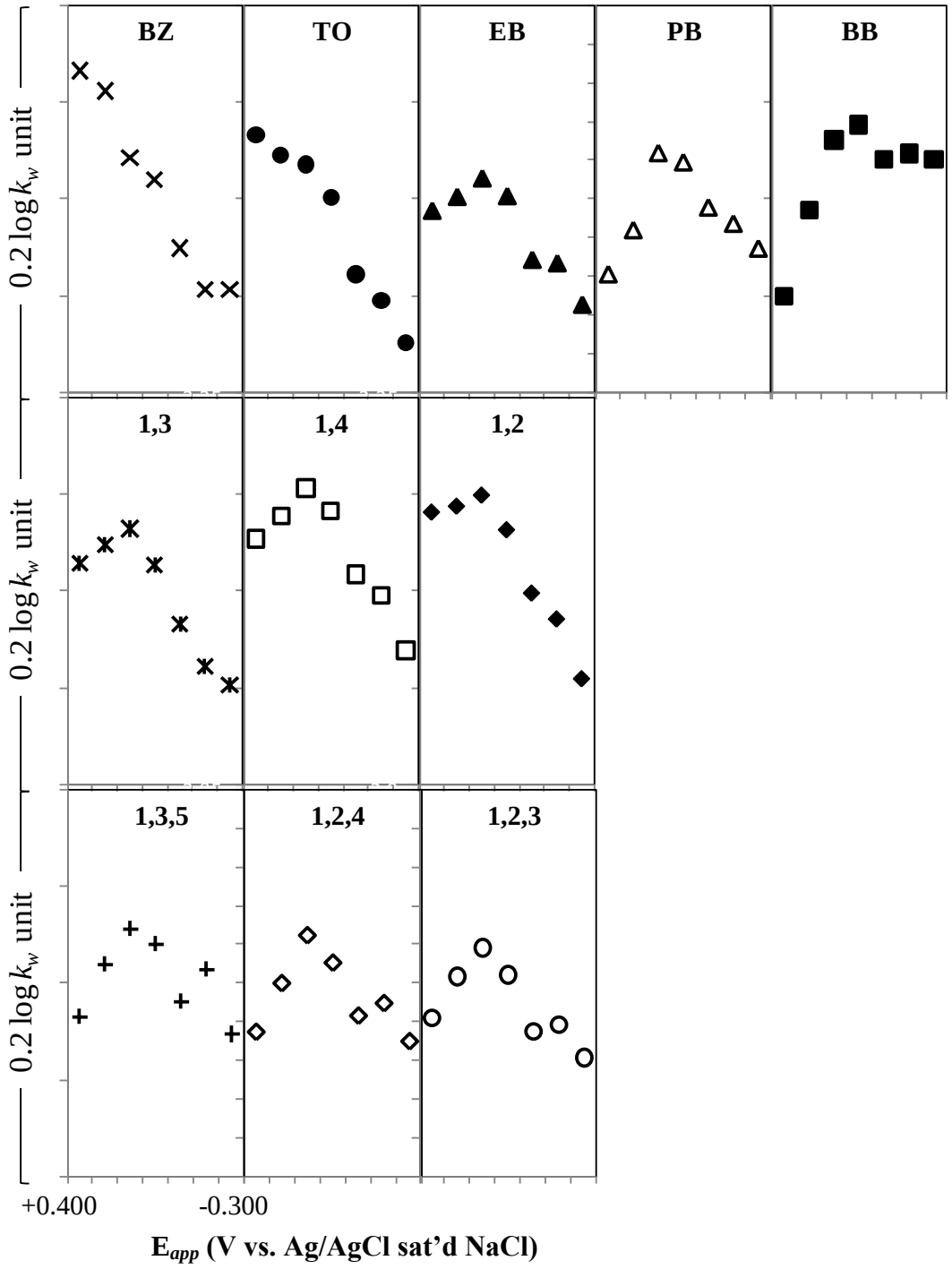

Figure 6. log k_w vs. E_{app}. All y-axis ranges span +0.400 to -0.300 V vs. Ag/AgCl sat'd NaCl. All x-axis span 0.2 log k_w unit, with absolute values listed in Table 2.

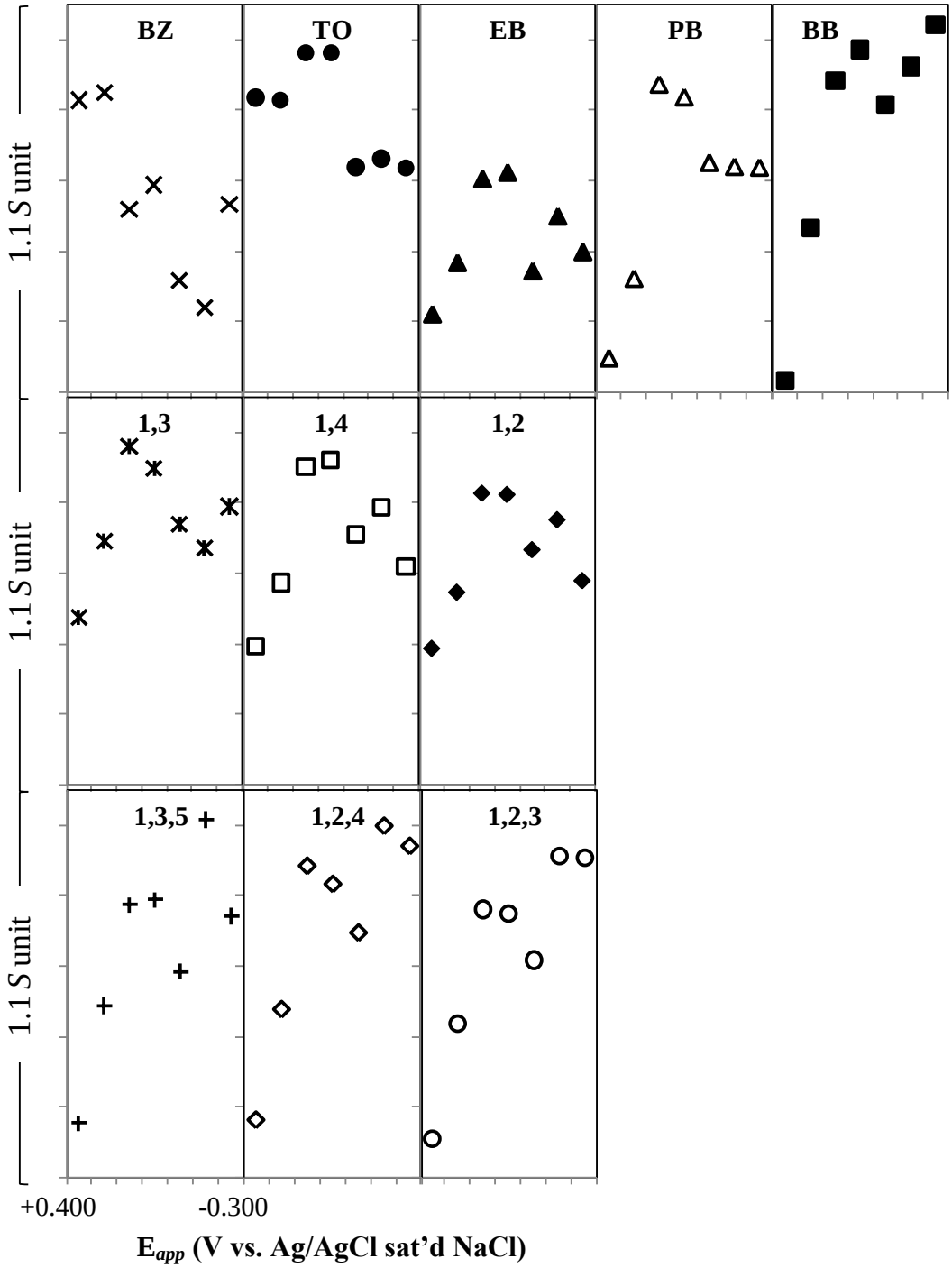

Figure 7. *S* vs. E_{app}. All y-axis ranges span +0.400 to -0.300 V vs. Ag/AgCl sat'd NaCl. All x-axis span 1.1 *S* unit, with absolute values listed in Table 2.

Table 2. The *y*-axis ranges for Figures 6 (log k_w vs. E_{app}) and 7 (S vs. E_{app}).

Analyte	log k_w vs. E_{app}	S vs. E_{app}
BZ	0.90 - 1.10	16.5 – 17.6
TO	1.45 - 1.65	19.9 – 21.0
EB	1.70 - 1.90	22.9 – 24.0
PB	2.10 - 2.30	25.9 – 27.0
BB	2.50 - 2.70	28.8 – 29.9
1,3	2.00 - 2.20	23.5 – 24.6
1,4	2.05 - 2.25	23.8 – 24.9
1,2	2.05 – 2.25	23.5 – 24.6
1,3,5	2.50 – 2.70	26.2 – 27.3
1,2,4	2.65 – 2.85	26.2 – 27.3
1,2,3	2.70 – 2.90	25.9 – 27.0

CHAPTER 5. THERMODYNAMIC STUDIES OF ALKYLBENZENE AND METHYLBENZENE ADSORPTION ON POROUS GRAPHITIC CARBON USING TEMPERATURE-CONTROLLED ELECTROCHEMICALLY MODULATED LIQUID CHROMATOGRAPHY

A paper to be submitted to *Langmuir*

Gloria Fe M. Pimienta[a,b] and Marc D. Porter[b,*]

[a]Department of Chemistry, Iowa State University

[b]Departments of Chemistry, Chemical Engineering, and Bioengineering, University of Utah, Salt Lake City, UT 84108

ABSTRACT

The temperature-dependence of retention of neutral solutes was studied using electrochemically modulated liquid chromatography (EMLC). EMLC couples liquid chromatography with electrochemistry such that solute retention is manipulated through changes in the potential applied (E_{app}) to a column packed with a conductive stationary phase. In this work, the effect of column temperature on the retention of benzene and several alkylbenzenes and di- and tri- methylbenzenes on porous graphitic carbon (PGC) was examined at several values of E_{app}. The van't Hoff relationship was used to determine the enthalpic and entropic contributions and Gibbs free energy for the transfer

---

*Corresponding author:

email: marc.porter@utah.edu

phone: 801-587-1505

of solute and other mobile phase components, including the supporting electrolyte, between the mobile and stationary phases. These results are employed as a means to develop a qualitative mechanistic model for the impact of E_{app} on retention.

INTRODUCTION

Electrochemically modulated liquid chromatography (EMLC) is a unique hybridization of HPLC and electrochemistry.[1] Retention is manipulated through changes in the potential applied (E_{app}) to a conductive stationary phase like porous graphitic carbon (PGC). The column is fashioned as an electrochemical cell, with the stationary phase also serving as working electrode. Variations in E_{app} alter the effective surface composition of the stationary phase, and thus its retention properties. EMLC has been utilized for the separation of a wide range of analytes, such as aromatic sulfonates,[2] monosubstituted benzenes,[3] corticosteroids,[4] and benzodiazepines.[5]

The advantages of carrying out HPLC analysis at elevated temperatures are well-documented.[6-12] Because of the decrease in solution viscosity and the reduction in back pressure, stationary phases with a smaller particle size can be employed for increased efficiency. It also allows higher flow rates to be used, increasing the diffusion rates within the stationary phase and the mobile phase. High temperature HPLC results to faster and more efficient separations. Marin and co-workers[12] evaluated a PGC column under temperature-programmed high temperature HPLC, and found no evidence of stationary phase collapse at high column temperatures of about 100 to 200 °C.

Moreover, elution profiles using temperature programming with an isocratic mobile phase were comparable to those obtained when using solvent gradient.

Temperature-controlled EMLC is currently utilized in our laboratory for improving separation efficiency and for studying retention mechanisms. The chromatographic and electrochemical performance of the EMLC column has been investigated previously,[13] and it was shown that the analysis time of a mixture of aromatic sulfonates in a mixed mobile phase is reduced by more than a factor of 20. That work also demonstrated that a higher temperature allows the separation of the mixture with an entirely aqueous mobile phase, eliminating hazards and waste disposal issues associated with organic modifiers.

The temperature dependence of retention in EMLC has been employed as a tool to measure electrosorption thermodynamics,[14] in particular using naphthalene disulfonates as analytes and glassy carbon (GC) as the stationary phase. The findings in this study were used to gain insights into the electrosorption mechanism.

Recently, the retention of alkylbenzenes and methylbenzenes in EMLC was investigated.[15] This paper presents work aimed at further understanding the mechanism of adsorption of this class of analytes on PGC by examining the temperature dependence of retention. The work detailed herein involves measuring retention at several values of E_{app} (-0.150 to +0.350 V) and several column temperatures (25.0 to 65.0°C). The results were used to examine the thermodynamic aspects of adsorption and develop a mechanism for the EMLC retention of alkyl-substituted benzenes on PGC.

EXPERIMENTAL SECTION

The EMLC Column

The design and construction of the EMLC column has been detailed elsewhere.[1, 16] Briefly, Nafion tubing (Perma Pure, Toms River, NJ, USA) is inserted into a porous stainless steel cylinder (Mott Metallurgical, Farmington, CT, USA). The column is then slurry packed with PGC (Thermo Scientific, Waltham, MA, USA) which serves as a stationary phase and working electrode. The Ag/AgCl (saturated NaCl) reference electrode (Bioanalytical Systems, West Lafayette, IN, USA) is placed inside the external electrolyte reservoir that surrounds the stainless steel cylinder. All values of E_{app} are reported with respect to this reference electrode.

The experiments employed 5-μm diameter PGC particles as the packing material. PGC is devoid of detectable oxygen-containing surface groups as revealed by x-ray photoelectron spectroscopy (detection limit ~0.2 atomic %).[17] The manufacturer specifies a nominal pore diameter of ~250 Å, and a porosity of ~80%. The surface area of PGC packed in the column is ca. 30 m^2, based on BET measurements (120 m^2/g) and amount of PGC loaded in the column (~0.25 g).

Instrumentation

Chromatographic experiments were performed using an Agilent 1200 Series module equipped with solvent cabinet, autosampler, quaternary pumping system, and UV/Vis diode array detector. The module was interfaced to Pentium IV 600 MHz computer with ChemStation software, which was used to control the pump, injector

parameters, and set-up of sequences, and to acquire signal and process data. The potential of the electrode was controlled using potentiostat/galvanostat model 263A (EG&G Princeton Applied Research, Oak Ridge, TN, USA).

The inclusion of temperature control in the EMLC experiment has been described previously,[13] and is shown in Figure 1. This setup was adapted from the design used by Carr and co-workers.[10, 18] The EMLC column and a 30-cm stainless steel tubing connected to the column inlet are placed inside a latex bag then immersed in a Polyscience model 9105 thermostated water bath (accuracy ±0.5 °C). The latex bag prevents direct contact of the column to water, and the stainless steel tubing minimizes band broadening by ensuring thermal equilibration of the mobile phase and sample prior to entering the column. A restrictor was placed in-line after the detector, providing an additional back pressure of 20 bar to avoid on-column boiling of the mobile phase.

Chemicals and Reagents

The analytes benzene (EMD, Gibbstown, NJ, USA), toluene (Sigma-Aldrich, St. Louis, MO, USA), ethylbenzene (Alfa Aesar, Ward Hill, MA, USA), *n*-propylbenzene (Alfa Aesar), *n*-butylbenzene (Alfa Aesar), 1,2-dimethylbenzene (Fluka, St. Louis, MO, USA), 1,3-dimethylbenzene (Alfa Aesar), 1,4-dimethylbenzene (Alfa Aesar), 1,3,5-trimethylbenzene (TCI America, Portland, OR, USA), 1,2,4-trimethylbenzene (Fluka), and 1,2,3-trimethylbenzene (TCI America) were used as received. Lithium perchlorate was purchased from Sigma-Aldrich. Water and acetonitrile were high purity solvents from EMD.

Mode of Operation

The mobile phase, which is a H_2O/CH_3CN mixture (40:60 *v:v*) contained 0.10 M $LiClO_4$ as the supporting electrolyte. The mobile phase flow rate was 0.40 mL/min. After the potentiostat was set at a given E_{app} and the water bath was fixed at the desired temperature, the system was allowed to reach a steady state for at least 30 min or after the baseline remained stable for 10 min, whichever took longer.

The analytes were prepared at 0.100 mM concentration using CH_3CN which also served as the nonretained marker used for the determination of the dead time, t_0. Various mixtures of analytes were used, ensuring minimal overlap of the component elution bands. The wavelength for detection is 214 nm. All separations were performed in triplicate at temperatures from 25 to 65˚C, in 10 ˚C increments, and values of E_{app} from +0.350 to -0.150 V, in 0.100 V increments.

Data Analysis

To compensate for band tailing, retention times, t_r, were determined from the first statistical moment analysis of all chromatographic peaks. The first moment, M_1, represents the centroid of the elution band, and is defined as:

$$M_1 = \frac{\int_{-\infty}^{\infty} th(t)dt}{\int_{-\infty}^{\infty} h(t)dt} \qquad [1]$$

where h(t) is the height at time t. The retention factor, *k'*, is calculated according to the equation:

$$k' = (t_r - t_0)/t_0 \quad [2]$$

Thermodynamic Relationships in HPLC. The retention mechanism in HPLC may be studied by examining the temperature dependence of retention. Retention is expressed as *k'*, which is the ratio of the number of moles of analyte in the stationary phase (n_{SP}) to the number of moles of analyte in the mobile phase:

$$k' = \frac{n_{SP}}{n_{MP}} \quad [3]$$

The equilibrium constant K for the interactions governing retention may be expressed as:

$$k' = K\phi \quad [4]$$

where ϕ is the phase ratio, i.e., the ratio of the volume of the stationary phase (V_{SP}) to the volume of the mobile phase (V_{MP}):

$$\phi = \frac{V_{SP}}{V_{MP}} \quad [5]$$

The Gibbs free energy for the transfer of the solute from mobile to stationary phase, $\Delta G°_{trans}$, is given by equations 6 and 7: [6]

$$\Delta G°_{trans} = \Delta H°_{trans} - T\Delta S°_{trans}$$

$$\Delta G°_{trans} = -RT \ln K \quad [7]$$

where $\Delta H°_{trans}$ is the change in standard enthalpy, $\Delta S°_{trans}$ is the change in standard entropy, R is the gas constant and T is the absolute temperature of the system.

Combination of Eqns. 4, 6 and 7 gives the van't Hoff relationship shown in Eqn. 8. This allows the determination of the thermodynamic quantities $\Delta H°_{trans}$ and $\Delta S°_{trans}$ for the transfer of the solute from the mobile phase to the stationary phase by examining the temperature dependence of retention.

$$\ln k' = \frac{-\Delta H°_{trans}}{RT} + \frac{\Delta S°_{trans}}{R} + \ln \phi \qquad [8]$$

$\Delta H°_{trans}$ can be determined from the slope of the plots of ln k' vs. 1/T, if $\Delta H°_{trans}$ is a constant over the temperature range studied. The *y*-intercept can be used to calculate the $\Delta S°$ of retention if the value of ϕ can be obtained. The definition and determination of ϕ is a long standing issue in chromatography. In this work, the value of V_{MP} is determined by the minor disturbance method using an "unretained" component of the mobile phase as a void marker. The pseudo-peak of water and the mobile phase flow rate are used to calculate a V_{MP} of 1.2 mL. V_{MP} is determined under the reasonable assumption that it is defined by the surface area of the packing material and the thickness of the compact component of the electrical double layer, which are both invariant with changes in E_{app}. The total surface area of the stationary phase is calculated using the mass of PGC loaded into the column (i.e., 0.25 g), the surface area of PGC as stated by the manufacturer (i.e., 120 m^2/g) and the thickness of the compact layer (i.e., 4.7 Å).[19, 20] Based on this model, the V_{SP} equals to 14 μL. The value of ϕ is thus calculated to be 0.029.

Molecular Area Calculations. The approximation of the molecular areas of the components of the system is based on the method used by O'Dea, *et al.*[21] The geometric

size of the molecule is calculated based on the bond lengths and van der Waals radii. It is assumed that each of the adsorbed solutes occupy a space equal to its molecular area, thus laying perfectly flat on the PGC surface when the plane of the aromatic ring is parallel to the surface.

The minimized-energy structure of the molecule is built using MOPAC (Molecular Orbital PACkage).[22] Chem3D is used to view the structure and obtain bond lengths (*l*) and bond angles (θ). These values, combined with atomic van der Waals radii (r), are used to approximate the length (L) and width (W) of the molecule. The molecular area (A) is calculated, assuming rectangular shape for simplicity (i.e., A = L*W), as shown in Figure 2 for 1,3-dimethylbenzene. For the hydrated lithium cation, the area is calculated using the radius of Li^+ ion, the radius of water, and a hydration number of 4.[23] The area of the solvents, H_2O and CH_3CN are based on how their dipoles are oriented with respect to the excess charge on the PGC surface.

RESULTS AND DISCUSSION

The solutes used in this work include benzene, a set of alkylbenzenes, and a series of di- and tri- methylbenzenes. Their structures and designations are shown in Figure 3. Abbreviations are used for benzene, toluene, and the rest of the alkylbenzenes; the positions of the methyl groups in the benzene ring are utilized for the di- and tri-methylbenzenes.

To gain insights into the thermodynamics associated with the electrosorption-based retention of these analytes, we investigated the effect of temperature (24, 35, 45, 55, and

65 °C) on the elution dependence at several values of E_{app} (+0.350, +0.250, +0.150, +0.050, -0.050, and -0.150 V vs. Ag/AgCl sat'd NaCl) using a PGC stationary phase. Two sets of chromatograms, which are representative of the collective results, are shown in Figure 4. The data presented were obtained at +0.250 (Figure 4A) and -0.150 (Figure 4B) V vs. Ag/AgCl sat'd NaCl at 25, 45 and 65 °C. At both values of E_{app}, the retention of all 11 analytes decreases as the column temperature increases. At +0.250 V, the retention time of PB decreased from 5.0 min to 3.4 min and that of 1,2,3 dropped from 17.0 to 8.6 as the temperature is increased from 25 °C to 65 °C; large changes are also evident at -0.150 in that the retention time over the same temperature span for PB changes from 5.3 to 3.4 min, and that for 1,2,3 from 15.5 to 8.3 min.

To examine these results in more detail, van't Hoff plots were constructed from the retention data for all solute-E_{app} combinations. Figure 5 presents the results of this analysis for the data at +0.250 (Figure 5A) and -0.150 (Figure 5B) V vs. Ag/AgCl sat'd NaCl. All the plots in Figure 5 indicate that ln *k'* follows a linear dependence with 1/T ($R^2 \geq 0.99$). The slopes of the plots can thus be used to deduce the enthalpic contribution to the retention process, and the *y*-intercept to determine the entropic component.

Table 1 and Figure 6 summarize the slopes of the plots for all six values of E_{app}, along with the calculated values of $\Delta H°_{trans}$. Table 2 and Figure 7 provide a comparable summary for the *y*-intercepts and calculated values of $T\Delta S°_{trans}$. All values of $\Delta H°_{trans}$ are positive, indicating an exothermic process for the retention of all the analytes.

Several interesting trends related to the molecular structure of the analytes emerge upon closer examination of the calculated $\Delta H°_{trans}$ values. First, when comparing the data

across the alkylbenzene series at each value of E_{app}, $\Delta H°_{trans}$ becomes 2-3 kJ more negative as the length of the alkyl chain increases. $\Delta H°_{trans}$ also becomes slightly more negative as the number of methyl groups increases across the methylbenzene series. Second, exothermicity increases more with methyl substitution than with methylene addition at all values of E_{app}. In other words, the differential change in enthalpy of transfer ($\Delta\Delta H°_{trans}$) vs. carbon number is larger for the methylbenzene series than for the alkylbenzene series. For example, at +0.050 V, $\Delta H°_{trans}$ of TO is 3.0 kJ/mol more positive than that of 1,4 and only 0.8 kJ/mol than that of EB. The difference in $\Delta H°_{trans}$ between PB and EB is 0.8 kJ/mol and that between 1,2,4 and 1,4 is 3.0 kJ/mol. Third, the retention of the methylbenzenes is more enthalpically favored than that of the alkylbenzene with the same molecular formula. That is, the values of $\Delta H°_{trans}$ for the dimethylbenzenes are all more negative than that of EB and those of the trimethylbenzenes are more negative than that of PB. At +0.050 V, $\Delta H°_{trans}$ for 1,4 and 1,2,4 are -11.4 and -13.8 kJ/mol, respectively, while those for EB and PB are -9.2 and -10.3 kJ/mol, respectively. Finally, methylbenzenes with the same number of methyl substituents have similar $\Delta H°_{trans}$ values at a given E_{app}.

The exothermicity of the retention process arises from the strong interactions of the solute as it adsorbs on the stationary phase. The stronger the solute-PGC interaction, the more negative the value of $\Delta H°_{trans}$. As discussed in a previous work,[24] the dispersion interactions are stronger with each additional methylene group on the alkyl chain for alkylbenzenes or each additional methyl substituent for methylbenzenes. The values of

$\Delta H°_{trans}$ become increasingly negative across both alkylbenzene and methylbenzene series.

In general, the values of $T\Delta S°_{trans}$ are positive, indicating that the disorder increases as the solutes transfer from the mobile phase to the stationary phase. The calculated $T\Delta S°_{trans}$ of 1,3,5 when the E_{app} is +0.350 is the only negative value, and this may just be a result of the uncertainty in the measurement and analysis (e.g., a discrepancy in the estimate of the phase ratio). Interestingly, the $T\Delta S°_{trans}$ shows maxima at +0.050 V (in a few cases at -0.050 V). For all plots, $T\Delta S°_{trans}$ increases from -0.150 V to +0.050 V then decreases as the E_{app} is poised at more positive values. Moreover, retention of alkylbenzenes is more entropically favored (more positive $\Delta S°$ values) than that of methylbenzenes. For example at +0.050 V, $T\Delta S°_{trans}$ of EB and PB are 1.8 and 2.0 kJ/mol, respectively, while those of 1,4 and 1,2,4 are both 1.3 kJ/mol. Furthermore, the values for $T\Delta S°_{trans}$ for the methylbenzenes do not seem to vary with the number and positioning of methyl substituents.

The trends in the $T\Delta S°_{trans}$ support an electrosorption process based on the displacement of ions and molecules adsorbed on the PGC surface by solute molecules in bulk solution. A depiction of the interfacial region and bulk solution is shown in Figure 8 as a means to illustrate the possible processes. In this model, changes in E_{app} alter the excess charge density, q^E, on the electrode, which induces a structural rearrangement of the electrical double layer.[19, 25] When E_{app} equals the potential of zero charge (PZC), q^E = 0, the inner Helmholtz plane is composed of H_2O, CH_3CN, ClO_4^-, and Li^+, at their bulk solution concentration. At E_{app} greater than the PZC, the H_2O dipoles orient such that the

oxygen atoms contact the PGC surface which has acquired $q^E > 0$. CH_3CN also orient accordingly, with the nitrogen end in contact with the PGC surface. The hydrated Li^+ cations are electrostatically repelled by the electrode and can thus be found only in the diffuse layer. An interfacial excess of ClO_4^- is adsorbed to maintain electroneutrality. When the E_{app} is less than the PZC, $q^E < 0$. The hydrogen atoms of H_2O are now in contact with the PGC surface, and CH_3CN is oriented with the nitrogen end away from the surface. Hydrated Li^+ cations, which maintain electroneutrality, can be found primarily in the outer Helmholtz plane.

The bulk solution consists of the mobile phase H_2O and CH_3CN, the supporting electrolyte ions, ClO_4^- and hydrated Li^+, and solute molecules. The illustration in Figure 8 also attempts to account for the hydrophobic effect,[26, 27] where organized water clusters form around the nonpolar solute. The hydrophobic effect is one contributing factor to the positive values of the $\Delta S°_{trans}$. When a solute like BZ transfers from mobile phase to stationary phase, these organized structures are broken, increasing the overall randomness in the system.

Some of the observed trends in $\Delta S°_{trans}$ can be qualitatively explained by an adsorption mechanism wherein the solute displaces species on the stationary phase upon retention. For example, when a BZ molecule transfers from the mobile phase to the stationary phase, it displaces some molecules and/or ions in the interfacial region in order to free up an area on the surface approximately equal to the molecular area of the solute. To examine this process, the calculated molecular areas of the molecules and ions involved in the retention process are presented in Table 3.

A solute molecule, BZ for example, needs to displace five H_2O molecules or three CH_3CN molecules, or any combination of the two molecules whose total area matches the area of a BZ molecule. If the solute displaces an ion, maintenance of electroneutrality must be considered, which would require movement of the same type of ion into the compact layer and therefore be enhalpically and entropically neutral. At E_{app} < PZC, when one ClO_4^- ion is displaced by the solute, a hydrated Li^+ must also be displaced. At E_{app} > PZC, the displacement of one ClO_4^- ion is accompanied by a transfer of ClO_4^- from the mobile phase to the stationary phase. Considering that the solutes have larger surface area compared to any of the species in the interfacial region, transfer of solute from the mobile phase to the stationary phase results to the transfer of a greater number of species from the stationary phase to the mobile phase, resulting to an increased entropy of the system during the retention process, resulting in a positive value for $\Delta S°_{trans}$. An alkylbenzene molecule occupies a larger surface area than a methylbenzene molecule of the same molecular formula, displacing more species from the surface, thus the more positive value of $T\Delta S°_{trans}$ that is observed for alkylbenzenes compared to methylbenzenes. Through the alkylbenzene series from BZ to BB, the molecular size increase generally translates to more positive $\Delta S°_{trans}$ values. For the methylbenzenes, the changes in the position of methyl groups and the further methyl substitution (di-substituted to tri-) do not detectably influence the $T\Delta S°_{trans}$ because the differences in molecular area are small. This simple displacement model roughly explains most of the observed trends.

In our study of the role of supporting electrolyte in EMLC,[15] we proposed another pathway to solute retention, in addition to displacement of species in the interface: the formation of a complex between the electrolyte anion ClO_4^- and the π-system of the aromatic ring. This interaction is related to the amount of adsorbed ClO_4^-, which increases with positive excursions from the PZC. How then would this interaction fit in the dependence of $\Delta H°_{trans}$ and $T\Delta S°_{trans}$ on E_{app}? For $\Delta H°_{trans}$, a conclusion can not be rigorously made because of a lack of information regarding the binding energies between PGC and Li^+, PGC and ClO_4^-, PGC and solute, and ClO_4^- and solute. For $T\Delta S°_{trans}$, it can be roughly said that such complexation has a much smaller contribution to the system disorder because it does not involve displacement of adsorbed species. Hence, the observed decreases in the values of $T\Delta S°_{trans}$ at E_{app} > PZC, which, based on this reasoning is at about +0.050 V, consistent with the rest of the results in this series of retention studies.

The values of $\Delta H°_{trans}$ and $T\Delta S°_{trans}$ determined from the van't Hoff plots were used to calculate the $\Delta G°_{trans}$. The results are shown in tabular form in Table 4, and in graphical form in Figure 9. All values of $\Delta G°_{trans}$ are negative, indicating that the retention process is spontaneous. The values of $\Delta G°_{trans}$ are in agreement with retention data. For comparison, plots of ln k' vs. E_{app} obtained from data at 25 °C is presented in Figure 10. Analytes that are more retained have more negative $\Delta G°_{trans}$ values. Moreover, for a given analyte, the trend in $\Delta G°_{trans}$ values at varied potentials is consistent with the dependence of ln k' on E_{app}.

CONCLUSIONS

EMLC is used as a technique to study the thermodynamics of retention. In this work, a mechanism for the retention of alkylbenzenes and methylbenzenes on PGC is proposed. The process exhibits a complex mixing of exothermic and enthalpic processes. The transfer of solute from mobile phase to stationary phase increases the overall entropy of the system. The findings are consistent with an adsorption mechanism.

ACKNOWLEDGMENTS

The authors would like to thank Drs. Ian Pimienta and Julio Facelli of University of Utah's Center for High Performance Computing for the MOPAC calculations. This work was supported by the U.S. Department of Energy - Ames Laboratory and the Utah Science and Technology Research Initiative. The Ames Laboratory is operated for the U.S. Department of Energy by Iowa State University under Contract No. DE-AC0207CH11358.

REFERENCES

(1) Harnisch, J. A.; Porter, M. D. *Analyst*, **2001**, *126*, 1841.

(2) Deinhammer, R. S.; Ting, E.-Y.; Porter, M. D. *Anal. Chem.* **1995**, *67*, 237.

(3) Ting, E.-Y.; Porter, M. D. *J. Electroanal. Chem.* **1998**, *443*, 180.

(4) Ting, E.-Y.; Porter, M. D. *Anal. Chem.* **1997**, *69*, 675.

(5) Ting, E.-Y.; Porter, M. D. *J. Chromatogr. A*, **1998**, *793*, 204.

(6) Antia, F.; Knox, J. H. *J. Chromatogr.* **1988**, *435*.

(7) Bowermaster, J.; McNair, J. *J. Chromatogr.* **1984**, *22*, 165.

(8) Dolan, J. *J. Chromatogr.* **2002**, *965*, 195.

(9) Greibrokk, T.; Anderson, A. *J. Sep. Sci.* **2001**, *24*, 899.

(10) Yan, B.; Zhao, J.; Brown, J.; Blackwell, J.; Carr, P. *Anal. Chem.* **2000**, *72*, 1253.

(11) Guillarme, D.; Heinisch, S.; Rocca, J. L. *J. Chromatogr. A*, **2004**, *1052*, 39.

(12) Marin, S. J.; Jones, B. A.; Felix, W. D.; Clark, J. *J. Chromatogr. A*, **2004**, *1030*, 255.

(13) Ponton, L. M.; Porter, M. D. *Anal. Chem.* **2004**, *76*, 5823.

(14) Ponton, L. M.; Keller, D. W.; Porter, M. D. *in preparation*.

(15) Pimienta, G. F. M.; Porter, M. D. *in preparation*.

(16) Ting, E.-Y.; Porter, M. D. *Anal. Chem.* **1998**, *70*, 94.

(17) Knox, J. H.; Ross, P. In *Advances in Chromatography*; Brown, P. R., Grushka, E., Eds.; Marcel Dekker Inc: New York, 1997; Vol. 37.

(18) Li, J.; Hu, Y.; Carr, P. W. *Anal. Chem.* **1997**, *69*, 3884.

(19) Bard, A. J.; Faulkner, L. R. *Electrochemical Methods: Fundamentals and Applications*; John Wiley & Sons, Inc.: New York, 2001.

(20) Mingos, D. M. P.; Rohl, A. L. *Inorg. Chem.* **1991**, *30*, 3769.

(21) O'Dea, A. R.; Smart, R. S. C.; Gerson, A. R. *Carbon*, **1999**, *37*, 1133.

(22) Stewart, J. J. P. In *http://OpenMOPAC.net*: Colorado Springs, 2008; Vol. 2010.

(23) An, H.-L.; Liu, Y.-Z.; Zhang, S.-H.; Zhan, Y.; Zhang, H.-L. *Chin. Phys. Lett.* **2008**, *25*, 3165.

(24) Pimienta, G. F. M.; Porter, M. D. *in preparation* **2010**.

(25) Stojek, Z. *Electroanalytical Methods: Guide to Experiments and Applications* 2nd ed.; Springer: New York, 2010.

(26) Ben-Naim, A. *Hydrophobic Interactions*; Plenum Press: New York, 1980.

(27) Boyd, G. E.; Vaslow, F.; Shchwarz, A.; Chase, J. W. *J. Phys. Chem.* **1967**, *71*, 3879.

FIGURES AND TABLES

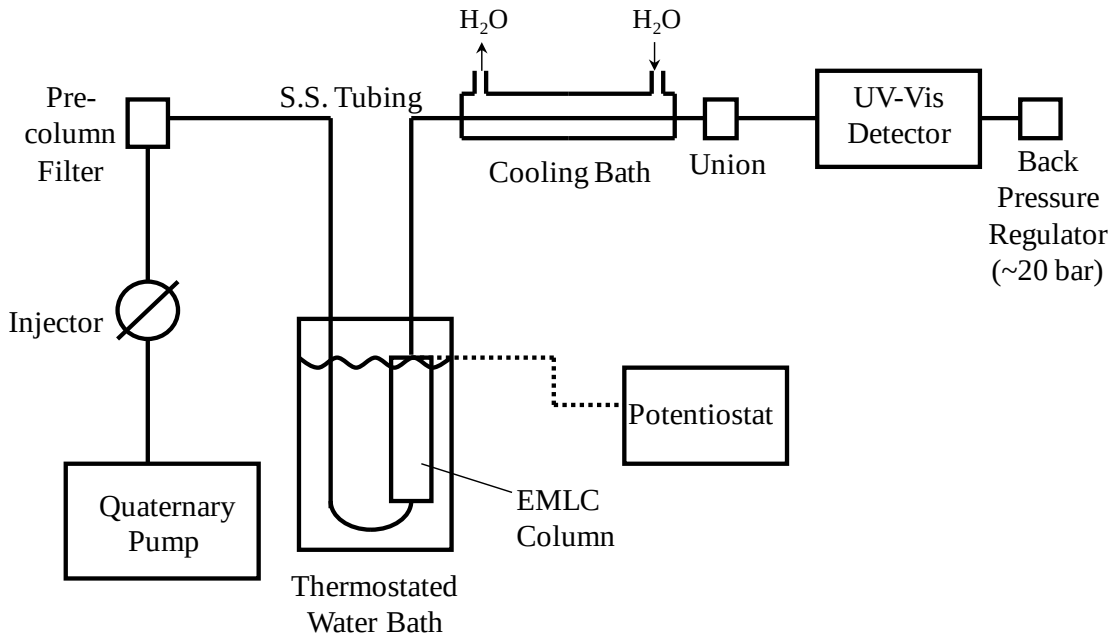

Figure 1. Schematic of the instrument for temperature-controlled EMLC.

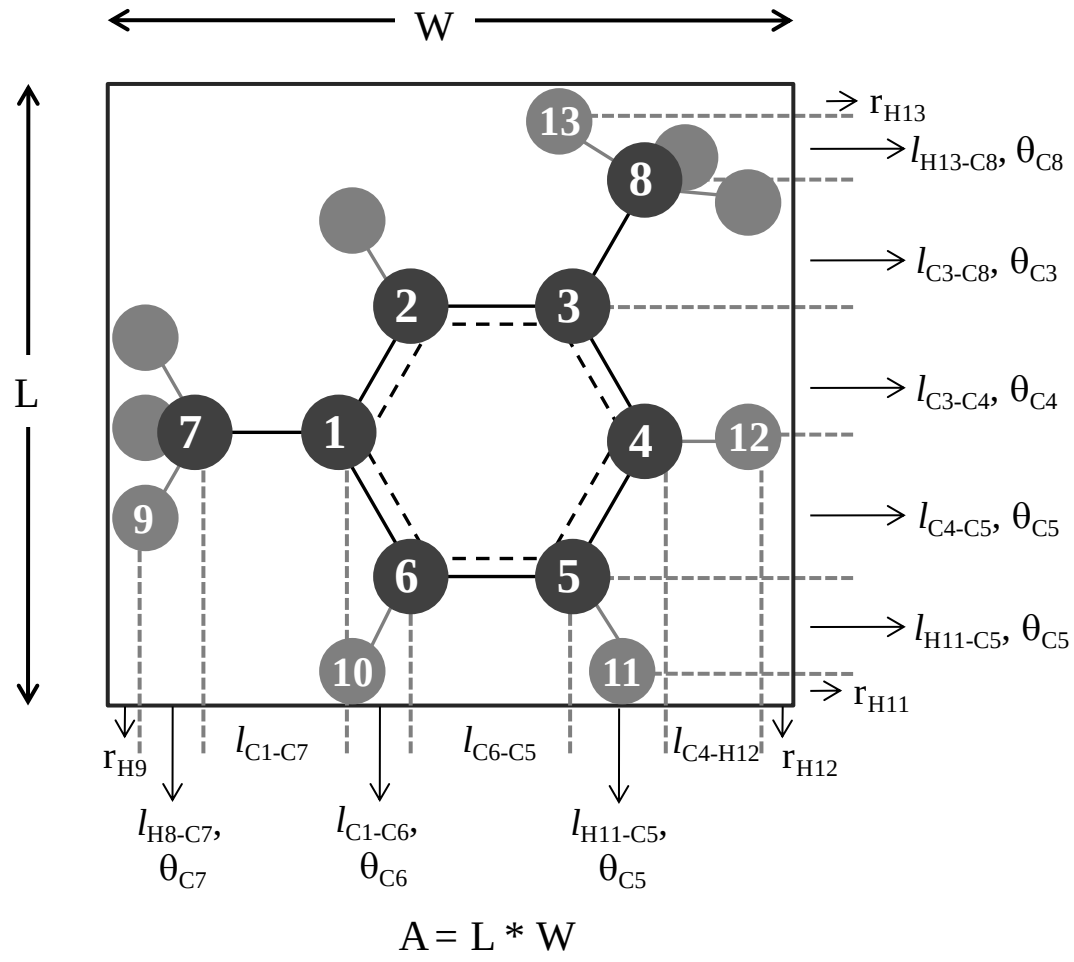

Figure 2. Illustration of molecular area calculation for 1,3-dimethylbenzene.

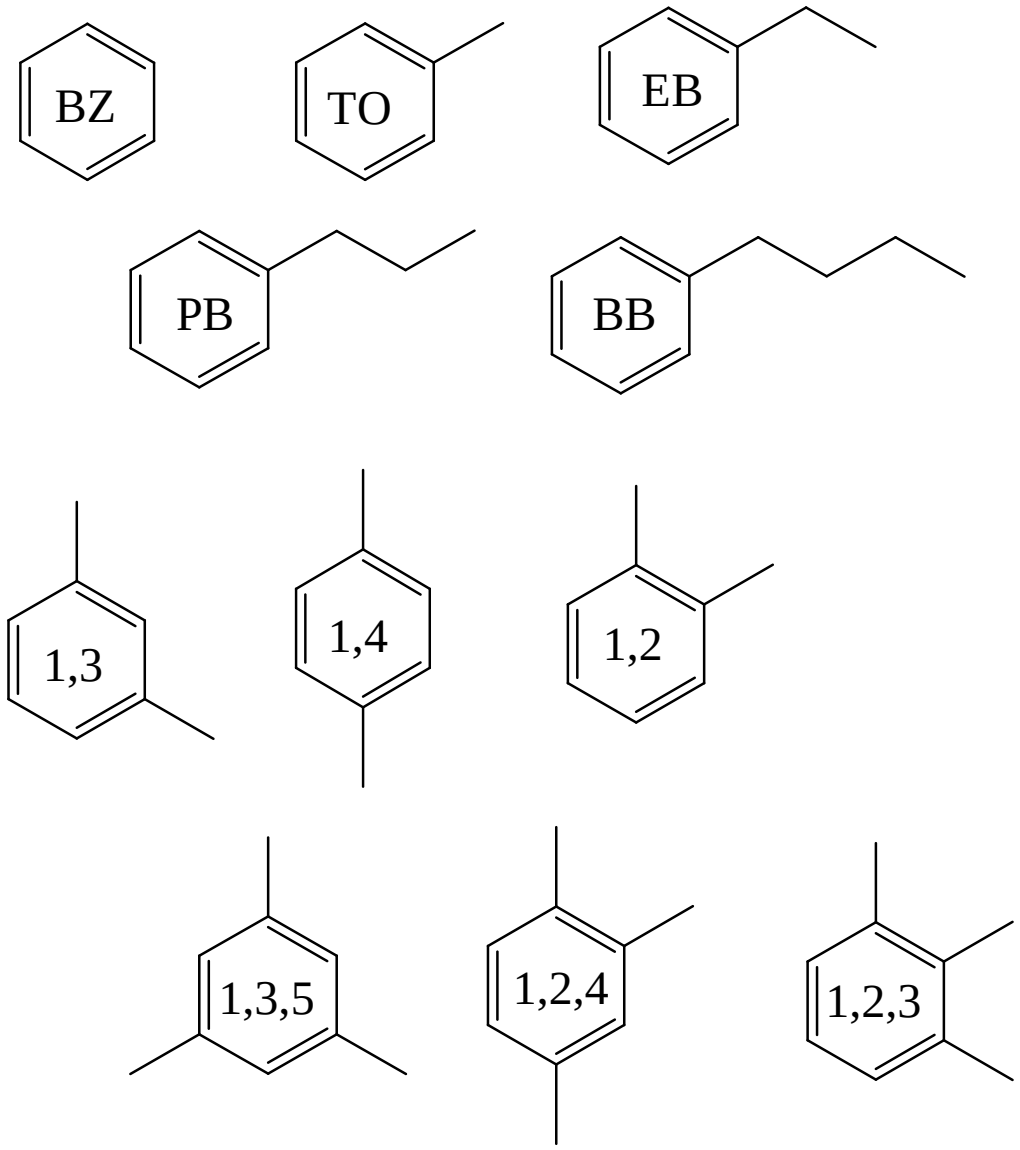

Figure 3. Structures and designations for the analytes used in this work: (BZ) benzene; (TO) toluene; (EB) ethylbenzene; (PB) propylbenzene; (BB) butylbenzene; (1,3), (1,4), and (1,2) dimethylbenzenes; and (1,3,5), (1,2,4), and (1,2,3) trimethylbenzenes.

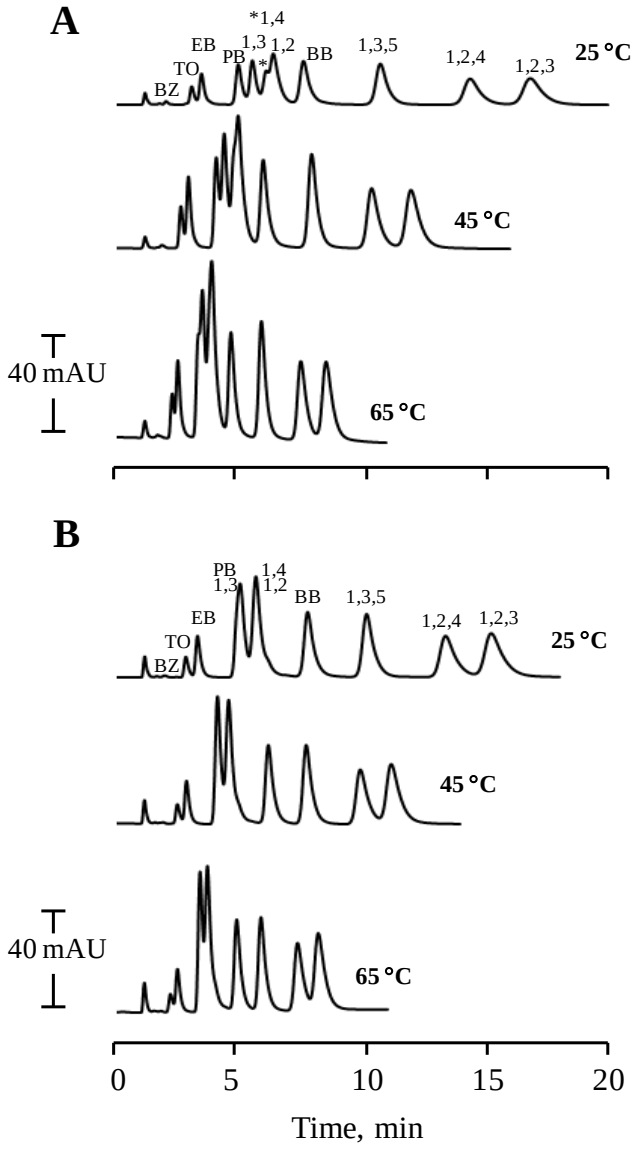

Figure 4. Chromatograms illustrating the effect of temperature (25, 45, and 65° C) and E_{app} (+0.250 and -0.150 V vs. Ag/AgCl sat'd NaCl) on the retention of alkylbenzenes and methylbenzenes. The mobile phase was 40/60 H_2O/CH_3CN with 0.100 M $LiClO_4$, flowing at 0.40 mL/min. The analytes were prepared in 0.10 mM concentration in CH_3CN. The injection volume was 5.00 μL. The stationary phase was poised at E_{app} of (A) +0.250 V and (B) -0.150 V vs. Ag/AgCl sat'd NaCl.

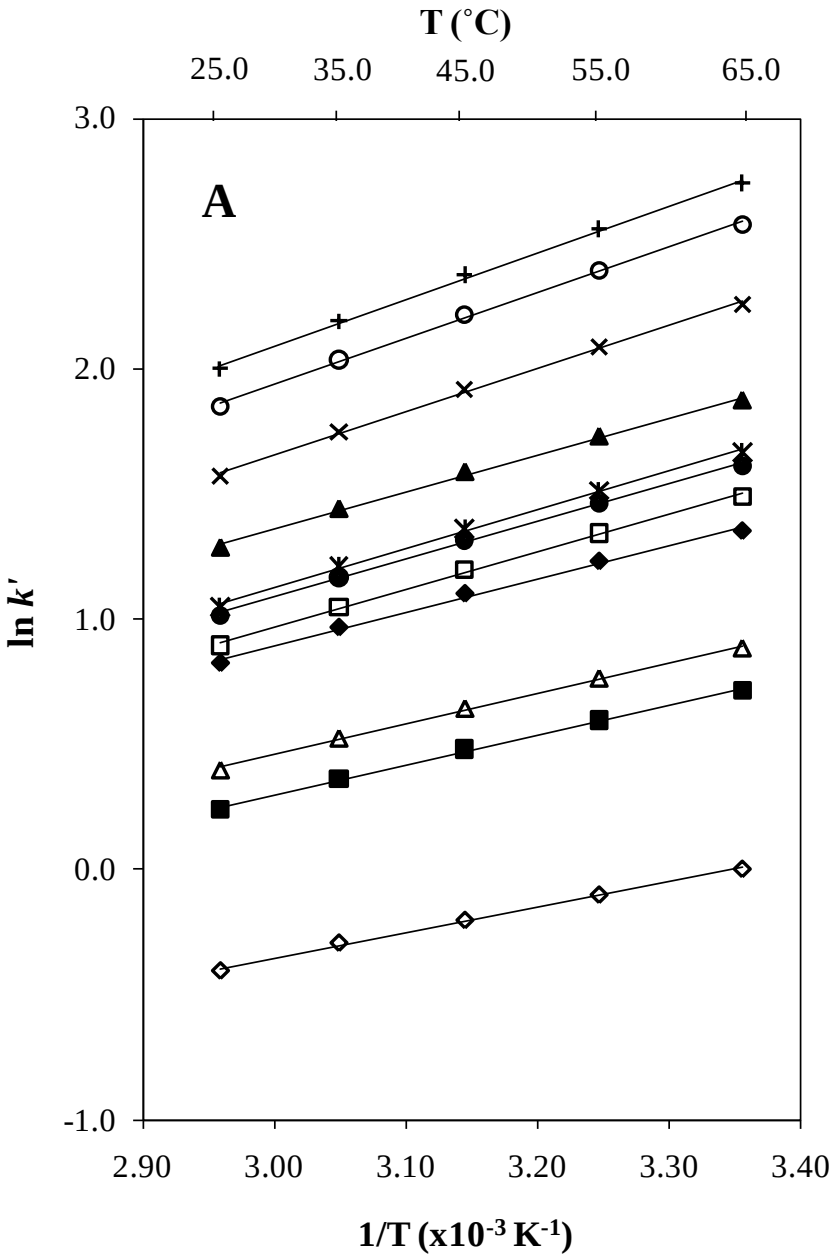

Figure 5A. van't Hoff plots (ln *k'* vs. 1/T) at E_{app} of +0.250 V vs Ag/AgCl sat'd NaCl. Legend: BZ (◇); TO (■); EB (△); PB (◆); 1,3 (□); 1,4 (●); 1,2 (∗); BB (▲); 1,3,5 (×); 1,2,4 (○); and 1,2,3 (+). N = 3, error bars are about the size of the marker. All the linear least squares fits to the data have R^2 values ≥ 0.99.

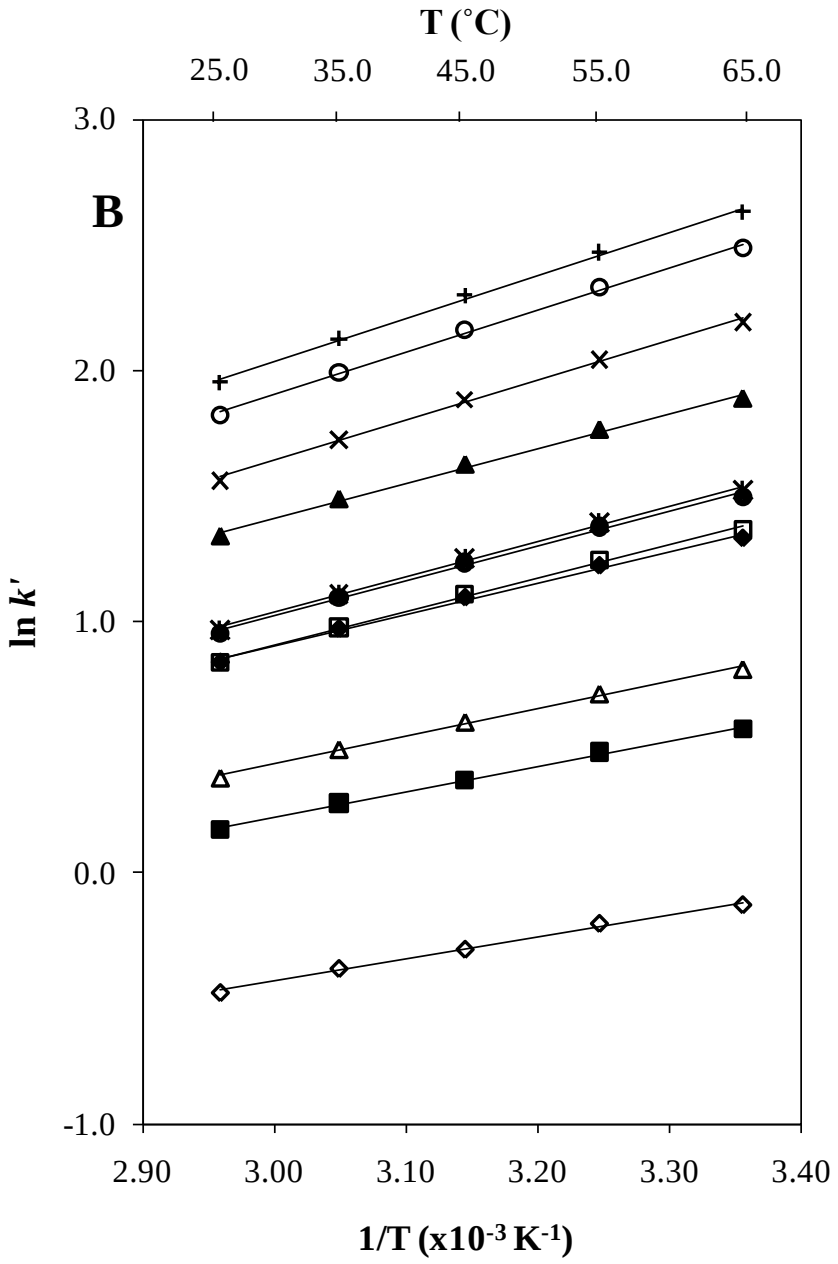

Figure 5B. van't Hoff plots (ln *k'* vs. 1/T) at E_{app} of -0.150 V vs Ag/AgCl sat'd NaCl. Legend: BZ (◇); TO (■); EB (△); PB (◆); 1,3 (□); 1,4 (●); 1,2 (∗); BB (▲); 1,3,5 (×); 1,2,4 (○); and 1,2,3 (+). N = 3, error bars are about the size of the marker. All the linear least squares fits to the data have R^2 values ≥ 0.99.

Table 1. Slopes (K^{-1}) of the van't Hoff plots and calculated $\Delta H°_{trans}$ (kJ/mol) of the solutes at PGC as a function of E_{app} (V vs. Ag/AgCl sat'd NaCl). Error bars for $\Delta H°_{trans}$ = ± 0.1 kJ/mol.

Analytes	+0.350 V		+0.250 V		+0.150 V		+0.050 V		-0.050 V		-0.150 V	
	Slope	$\Delta H°_{trans}$	Slope	$\Delta H°_{trans}$	Slope	$\Delta H°_{trans}$	Slope	$\Delta H°_{trans}$	Slope	$\Delta H°_{trans}$	Slope	$\Delta H°_{trans}$
BZ	1.04	-8.7	1.02	-8.5	0.92	-7.7	0.90	-7.5	0.86	-7.2	0.87	-7.3
TO	1.21	-10.1	1.19	-9.9	1.08	-9.0	1.01	-8.4	1.01	-8.4	1.01	-8.4
EB	1.25	-10.4	1.23	-10.2	1.17	-9.7	1.10	-9.2	1.10	-9.1	1.09	-9.1
PB	1.34	-11.1	1.33	-11.1	1.31	-10.9	1.23	-10.3	1.25	-10.4	1.26	-10.5
BB	1.47	-12.2	1.47	-12.3	1.45	-12.0	1.34	-11.1	1.38	-11.4	1.39	-11.5
1,3	1.50	-12.5	1.50	-12.4	1.43	-11.9	1.36	-11.3	1.34	-11.2	1.33	-11.1
1,4	1.50	-12.5	1.51	-12.5	1.45	-12.0	1.38	-11.4	1.38	-11.5	1.38	-11.4
1,2	1.55	-12.9	1.55	-12.9	1.47	-12.3	1.41	-11.7	1.40	-11.6	1.40	-11.6
1,3,5	1.74	-14.5	1.72	-14.3	1.65	-13.7	1.58	-13.1	1.59	-13.2	1.59	-13.2
1,2,4	1.81	-15.1	1.82	-15.1	1.75	-14.5	1.66	-13.8	1.68	-14.0	1.68	-14.0
1,2,3	1.86	-15.5	1.87	-15.5	1.78	-14.8	1.70	-14.2	1.72	-14.3	1.71	-14.2

Table 2. *y*-intercepts of the van't Hoff plots and calculated $T\Delta S°_{trans}$ (kJ/mol) of the solutes at PGC as a function of E_{app} (V vs. Ag/AgCl sat'd NaCl). Error bars for $T\Delta S°_{trans}$ = ± 0.1 kJ/mol.

Analytes	+0.350 V		+0.250 V		+0.150 V		+0.050 V		-0.050 V		-0.150 V	
	***y*-Int**	**$T\Delta S°_{trans}$**	***y*-Int**	**$T\Delta S°_{trans}$**	***y*-Int**	**$T\Delta S°_{trans}$**	***y*-Int**	**$T\Delta S°_{trans}$**	***y*-Int**	**$T\Delta S°_{trans}$**	***y*-Int**	**$T\Delta S°_{trans}$**
BZ	-3.46	0.2	-3.42	0.3	-3.14	1.0	-3.07	1.2	-2.99	1.4	-3.05	1.2
TO	-3.33	0.6	-3.27	0.7	-2.94	1.5	-2.75	2.0	-2.77	1.9	-2.81	1.8
EB	-3.29	0.7	-3.23	0.8	-3.04	1.3	-2.84	1.8	-2.84	1.8	-2.85	1.7
PB	-3.14	1.0	-3.11	1.1	-3.02	1.3	-2.76	2.0	-2.84	1.7	-2.87	1.7
BB	-3.10	1.1	-3.06	1.2	-2.95	1.5	-2.58	2.4	-2.71	2.1	-2.75	2.0
1,3	-3.52	0.1	-3.52	0.1	-3.31	0.6	-3.12	1.1	-3.10	1.1	-3.09	1.1
1,4	-3.43	0.3	-3.44	0.3	-3.25	0.7	-3.03	1.3	-3.10	1.1	-3.10	1.1
1,2	-3.52	0.1	-3.52	0.1	-3.30	0.6	-3.12	1.1	-3.13	1.1	-3.16	1.0
1,3,5	-3.59	-0.1	-3.50	0.1	-3.28	0.7	-3.05	1.2	-3.11	1.1	-3.12	1.1
1,2,4	-3.52	0.1	-3.51	0.1	-3.30	0.6	-3.02	1.3	-3.11	1.1	-3.14	1.0
1,2,3	-3.51	0.1	-3.51	0.1	-3.25	0.7	-3.00	1.4	-3.08	1.2	-3.10	1.1

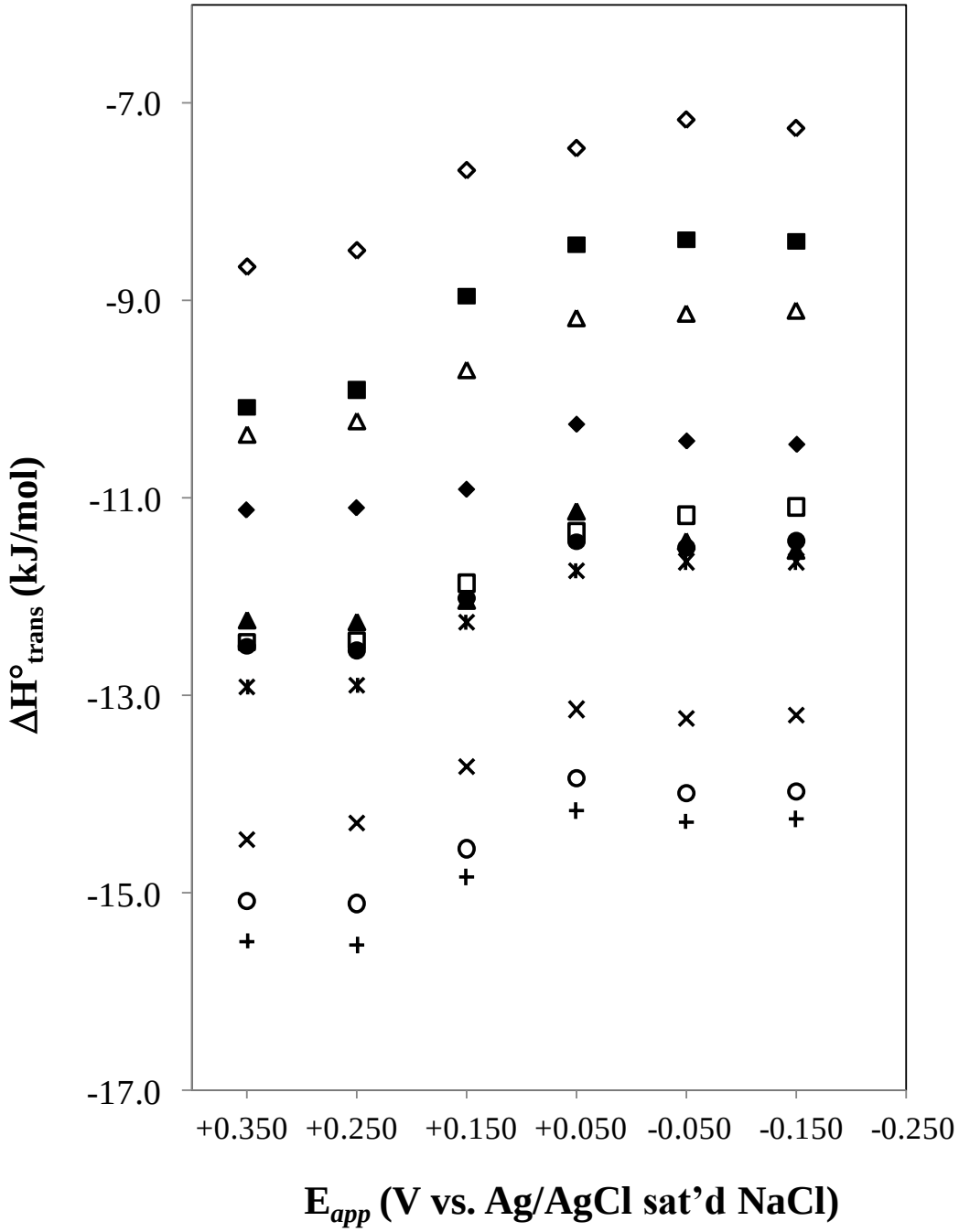

Figure 6. ΔH°_{trans} vs. E_{app} plots. Legend: BZ (◇); TO (■); EB (△); PB (◆); 1,3 (□); 1,4 (●); 1,2 (✳); BB (▲); 1,3,5 (×); 1,2,4 (○); and 1,2,3 (+). Error bars = ± 0.1 kJ/mol.

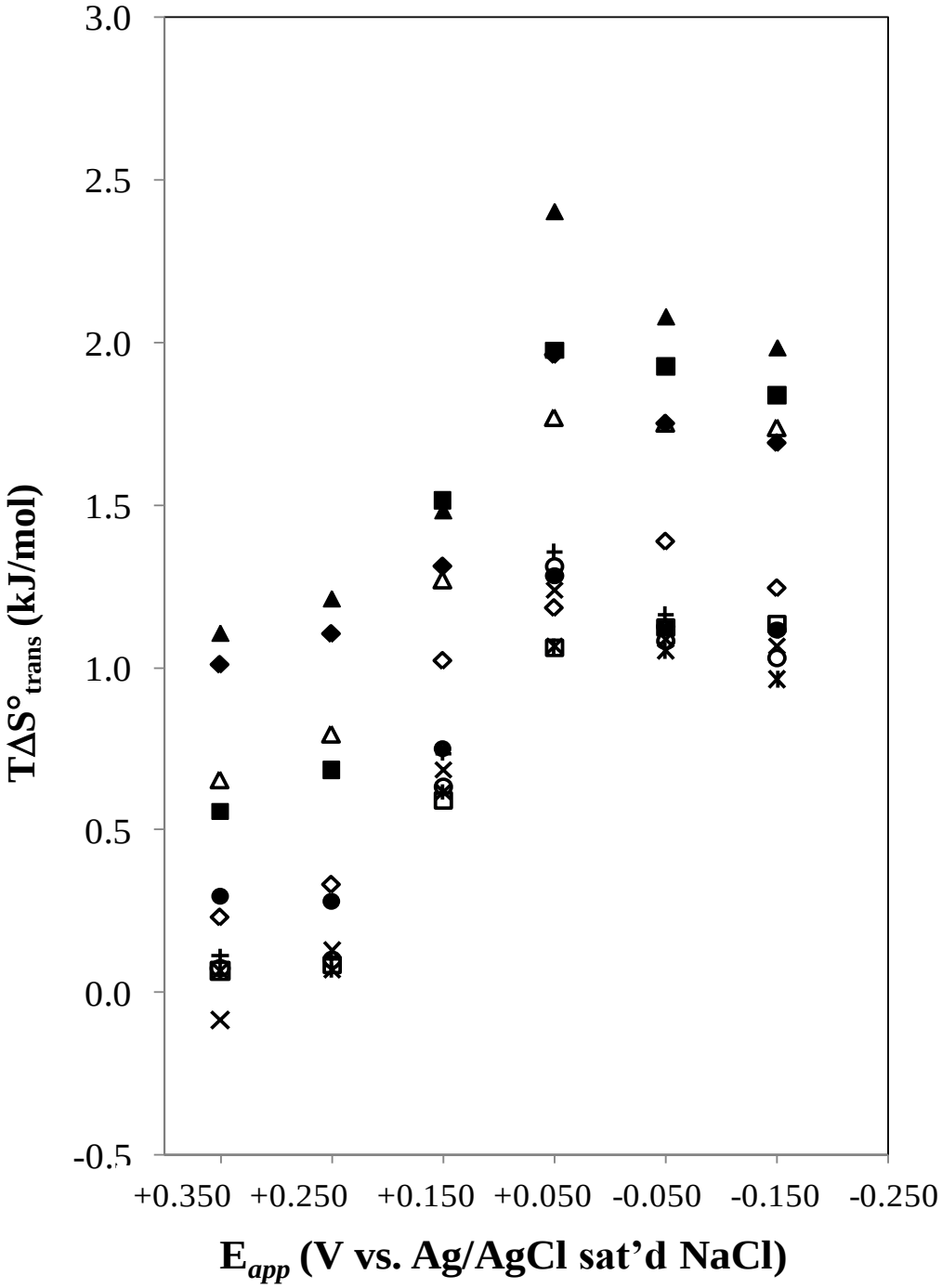

Figure 7. $T\Delta S^{\circ}_{trans}$ vs. E_{app} plots. Legend: BZ (◇); TO (■); EB (△); PB (◆); 1,3 (□); 1,4 (●); 1,2 (✳); BB (▲); 1,3,5 (×); 1,2,4 (○); and 1,2,3 (+). Error bars = ± 0.1 kJ/mol.

Table 3. Molecular areas ($Å^2$)* for the solutes and mobile phase components.

Solute	A ($Å^2$)	Solute	A ($Å^2$)	Mobile Phase	A ($Å^2$)
BZ	49.1	1,3	67.0	H_2O	11.8
TO	55.6	1,4	60.8	CH_3CN	17.4
EB	64.0	1,2	67.0	ClO_4^-	28.9
PB	69.4	1,3,5	78.4	Li^+	47.88
BB	77.4	1,2,4	72.6	(hydrated)	
		1,2,3	67.0		

*Calculated using MOPAC models (see experimental section for details).

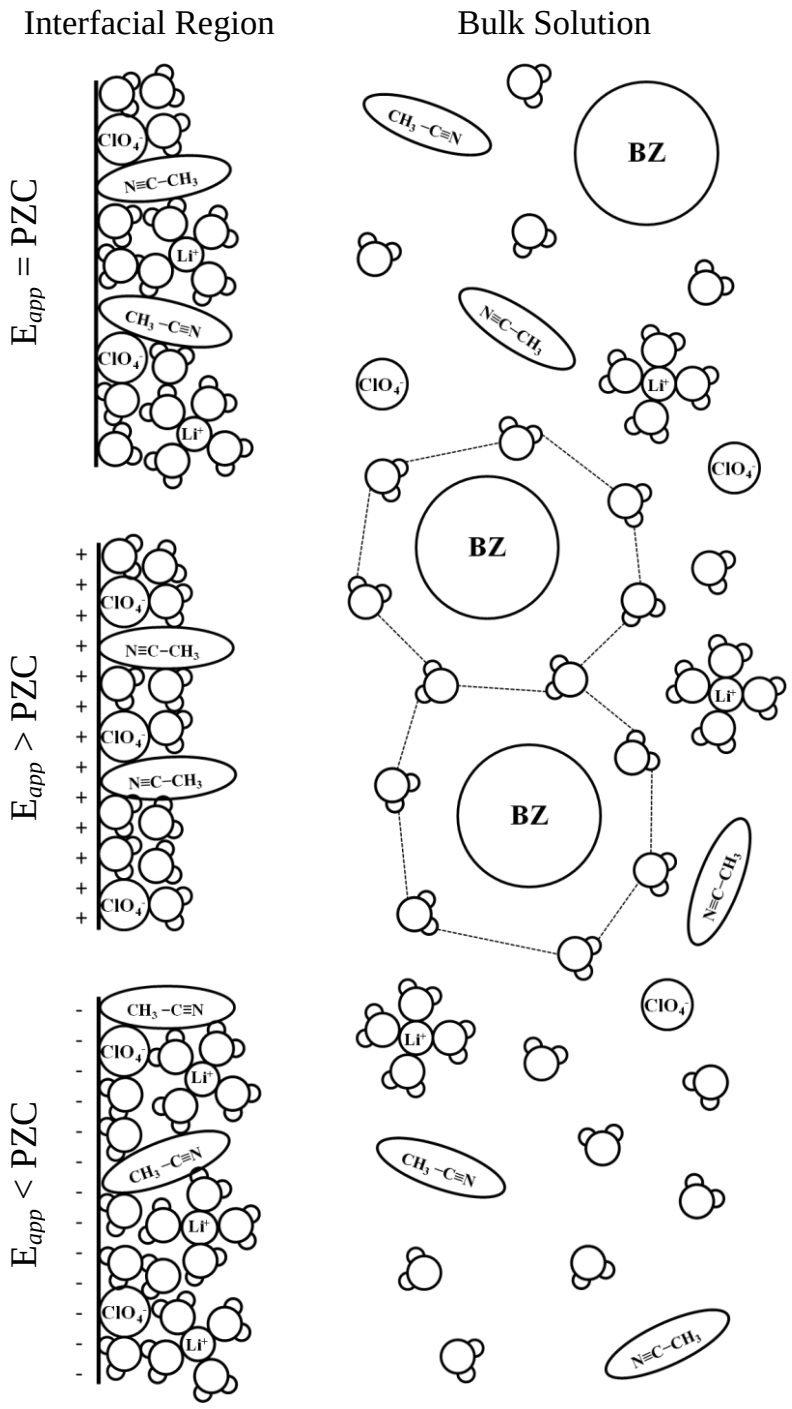

Figure 8. Illustration of the interfacial region and the bulk solution during EMLC when E_{app} is equal to the PZC (top), greater than the PZC (middle) and less than the PZC (bottom).

Table 4. ΔG°_{trans} (kJ/mol) values for the retention of the analytes on PGC.

Analytes	E_{app} (V vs. Ag/AgCl sat'd NaCl)					
	+0.350	**+0.250**	**+0.150**	**+0.050**	**-0.050**	**-0.150**
BZ	-8.9	-8.8	-8.7	-8.6	-8.6	-8.5
TO	-10.6	-10.6	-10.5	-10.4	-10.3	-10.2
EB	-11.0	-11.0	-11.0	-10.9	-10.9	-10.8
PB	-12.1	-12.2	-12.2	-12.2	-12.2	-12.1
BB	-12.5	-12.5	-12.5	-12.4	-12.3	-12.2
1,3	-12.8	-12.8	-12.8	-12.7	-12.6	-12.6
1,4	-13.0	-13.0	-12.9	-12.8	-12.7	-12.6
1,2	-13.3	-13.5	-13.5	-13.5	-13.5	-13.5
1,3,5	-14.4	-14.4	-14.4	-14.4	-14.3	-14.3
1,2,4	-15.2	-15.2	-15.2	-15.1	-15.1	-15.0
1,2,3	-15.6	-15.6	-15.6	-15.5	-15.4	-15.4

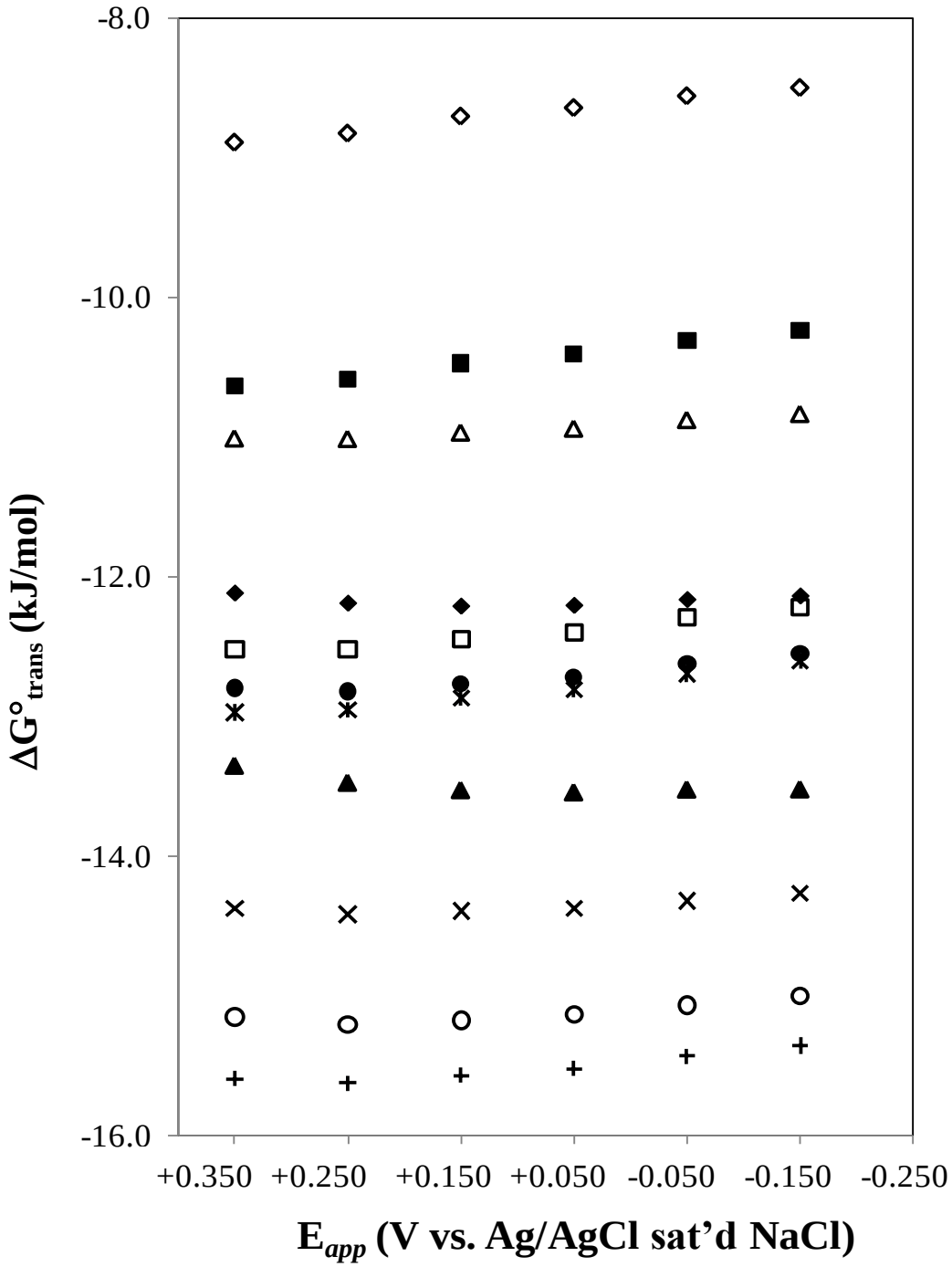

Figure 9. ΔG°_{trans} vs. E_{app} plots. Legend: BZ (◇); TO (■); EB (△); PB (◆); 1,3 (□); 1,4 (●); 1,2 (∗); BB (▲); 1,3,5 (×); 1,2,4 (○); and 1,2,3 (+). Error bars = ± 0.1 kJ/mol.

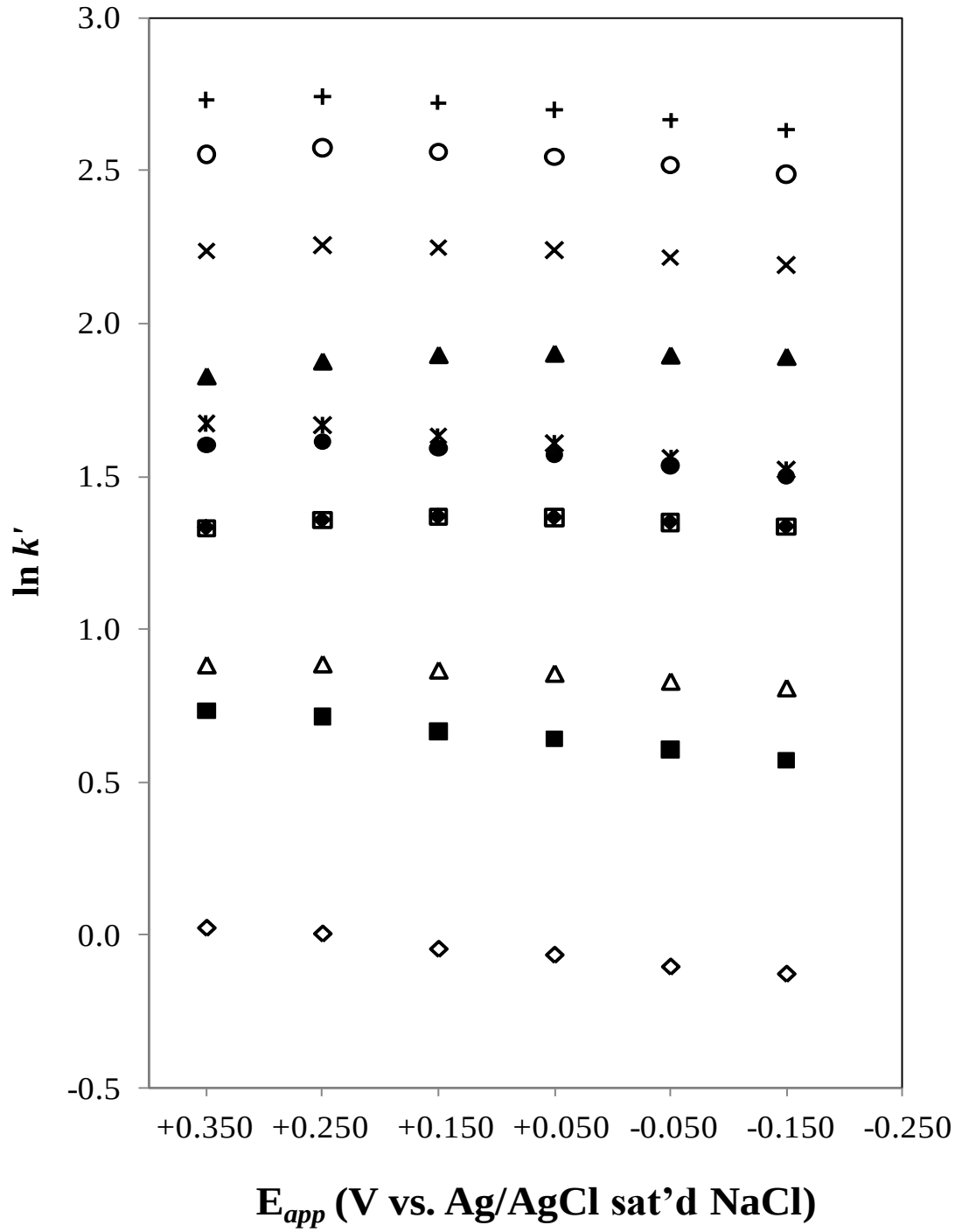

Figure 10. ln *k′* vs. E_{app} plots. Legend: BZ (◇); TO (■); EB (△); PB (◆); 1,3 (□); 1,4 (●); 1,2 (✳); BB (▲); 1,3,5 (×); 1,2,4 (○); and 1,2,3 (+).

CHAPTER 6. SUMMARY AND GENERAL CONCLUSIONS

The main goal of this dissertation was to develop and refine the mechanism of electrochemically modulated liquid chromatography (EMLC). Investigations focused on understanding how retention is manipulated through changes in the potential applied (E_{app}) to the porous graphitic carbon (PGC) stationary phase. The influence of other factors, in particular, the supporting electrolyte and the organic modifier in the mobile phase, in retention, were also investigated. In addition, the thermodynamics of the transfer of solute from mobile to stationary phase was studied by varying column temperature.

Chapter 2 presented the retention behavior of benzene and a series of alkylbenzenes, and di- and tri- methylbenzenes on PGC at varying E_{app} values. Retention showed interesting dependence on E_{app}, as evident in the evolution of the shapes of $\ln k'$ vs. E_{app} plots. The retention maximum of such plots was ascribed to the potential of zero charge (PZC) for a given system. EMLC-based manipulation in retention was attributed to alterations in the strength of solute-stationary phase interactions, i.e., electron donor-acceptor interactions and solvophobic interactions. Competition of the supporting electrolyte with the solutes for adsorption sites on the stationary phase also come into play.

In Chapter 3, the role of the supporting electrolyte in EMLC was examined. The supporting electrolyte, which is an electrochemical requirement, exerts a strong impact on retention, revealing an aspect in the EMLC mechanism that has not yet been explored.

Previous works with charged analytes showed the influence of the supporting electrolyte arise from changes in electrical double layer structure and competition for adsorption sites. In the present work, for these neutral, nonpolar solutes, increased supporting electrolyte concentration enhanced retention. This result is consistent with the interaction of the supporting electrolyte anion with the solute through complexation with its aromatic π-system. A two-site adsorption mechanism was thus proposed, wherein solute retention arises not only from direct interaction with PGC, but also from the adsorption of the solute as an anion-π complex. This model predicts a linear relationship between k' and the supporting electrolyte concentration, which fit well with the results.

Retention was examined as a function of mobile phase composition in Chapter 4. The Linear Solvent Strength (LSS) model was employed for data analysis by plotting log k' vs. volume fraction of CH_3CN in a water/CH_3CN mobile phase. The linear dependency was used for the determination of values of log k_w (i.e., distribution coefficient between PGC and the purely aqueous mobile phase) and S (i.e., sensitivity to changes in CH_3CN content). This study allowed us to reasonably conclude that the organic modifier plays a minor role on potential-induced changes in retention.

In Chapter 5, the temperature dependence of retention was used to study the thermodynamics of EMLC-based retention. The van't Hoff relationship was used to examine enthalpic ($\Delta H°_{trans}$) and entropic ($T\Delta S°_{trans}$) contributions and determine the Gibbs free energy ($\Delta G°_{trans}$) for the transfer of solutes and other components during the retention process. The values of $\Delta H°_{trans}$ were correlated with the strength of solute-stationary phase interactions. The trends in the values of $T\Delta S°_{trans}$ with respect to E_{app}

were used to examine the retention mechanism as adsorption involving displacement of species in the stationary-mobile phase interface by solute molecules. The calculated values of ΔG°_{trans} were in agreement with retention data, i.e., stronger retention translates to more negative ΔG°_{trans} value.

This research is of fundamental and technical significance. The results of this work demonstrated the potential utility of EMLC as a technique in studying electrosorption processes. This work, more broadly, has implications to electrosorption phenomena in other areas, e.g., the use of carbon electrodes in energy production and storage such as in fuels and batteries. Moreover, the advancement of knowledge of the mechanism of EMLC serves as a tool for chromatographers when designing solutions to separation problems.